The Function of Anaplastic Lymphoma Kinase Receptor and the Activities of Its Inhibitors in Neuroendocrine Prostate Cancer

By

FRED ERICK ARREOLA HERNANDEZ

DISSERTATION

Submitted in partial satisfaction of the requirements for the degree of

DOCTOR OF PHILOSOPHY

in

Biochemistry, Molecular, Cellular and Developmental Biology

in the

OFFICE OF GRADUATE STUDIES

of the

UNIVERSITY OF CALIFORNIA

DAVIS

Approved:

_____

Hongwu Chen, Chair

_____

Kermit Carraway

_____

Chengfei Liu

Committee in Charge

2024

Table of Contents

The functional role of anaplastic lymphoma kinase receptor in neuroendocrine prostate cancer

Neuroendocrine prostate cancer (NEPC) represents an aggressive subtype of prostate cancer, which may either manifest de novo or emerge because of anti-androgen receptor (AR) drug treatment. Unfortunately, there is currently no established effective treatment for NEPC. Alectinib and entrectinib are FDA-approved receptor tyrosine kinase inhibitors designed to target the anaplastic lymphoma kinase receptor (ALK) initially developed for NSCLC patients who developed resistance to the receptor tyrosine kinase (RTK) inhibitor crizotinib. In this study, we sought to assess the potential of alectinib and entrectinib as therapeutic agents for NEPC. We conducted experiments using various NEPC cell lines and castration-resistant prostate cancer (CRPC) cells, subjecting them to treatment with alectinib and entrectinib. Notably, treatment with these drugs, particularly in cell lines 42D, NCI-H660, C42B-entry, and LuCaP, significantly inhibited cell growth and proliferation. Further investigation revealed that alectinib and entrectinib exerted their effects by impacting the ALK signaling pathway. Specifically, downstream targets of ALK signaling, such as STAT3 and AKT phosphorylation, exhibited reductions in treated cells. Additionally, the expression of NEPC cellular markers, including enolase2, BRN2, and ASCL1, decreased upon alectinib treatment. Notably, NEPC tumors treated with alectinib or entrectinib in combination with CM 272, a G9a/DMNT1 inhibitor, exhibited a notable decrease in tumor volume. Both alectinib and entrectinib demonstrated their efficacy in inhibiting various cellular pathways, including the Neuroactive ligand-receptor and cytokine-to-

cytokine receptor interaction pathways. The findings of our current study provide compelling evidence that alectinib and entrectinib have the potential to effectively inhibit NEPC cell and tumor growth. Consequently, these drugs hold promise as therapeutics for patients grappling with NEPC, offering a potential avenue for improved treatment outcomes.

Acknowledgements

I am writing to express my gratitude to those who have significantly contributed to the successful completion of my thesis project. First and foremost, I would like to extend my heartfelt appreciation to my mentor, Dr. Hong-Wu Chen. His invaluable guidance and insightful interpretations of my experimental results played a pivotal role in enabling me to accomplish this project. Dr. Chen's unwavering support and willingness to assist me in planning future experiments were instrumental in my progress. Moreover, I am grateful for the conducive laboratory environment he fostered, which greatly facilitated the advancement of our experiments.

Next, I would like to acknowledge the contributions of Xiong Zhang. Xiong has played a crucial role in several key aspects of this thesis project. Serving as my secondary mentor and advisor within the lab, he provided essential training and assisted with analyzing data from some of the experiments presented herein. Since I joined the lab, Xiong has consistently been a wellspring of knowledge, offering guidance in experiment design, data analysis, and future research planning. Whenever I encountered challenges in my experiments, Xiong was invariably available with solutions. I extend my heartfelt gratitude to Xiong Zhang for his invaluable assistance and mentorship.

Finally, I would like to express my appreciation to Dr. Joanne Engebrecht, my advisor, and the members of the BMCDB graduate group. Joanne has always been receptive to my concerns and has provided invaluable guidance to steer me in the right direction. I also commend her for

her patience and courtesy throughout my journey toward a Ph.D. degree. Additionally, I am thankful to the BMCDB graduate group for providing all the necessary tools and resources to successfully complete a Ph.D.

Chapter 1: Prostate cancer and its major tumorigenic factors

Chapter 1.1 Overview of prostate cancer and prostate cancer treatments

In 1853, J. Adams was the first to characterize prostate cancer as a "very rare disease" (Adams, 1853). Prostate cancer is the second most frequent disease in men worldwide, which is mostly caused by an aging population and the adoption of Western lifestyles (Baade et al., 2009). Prostate cancer contributed to almost 33,000 fatalities in the US in 2020 and shows an increase in incidence and mortality globally (Siegel et al., 2020). Treatment for prostate cancer, which is primarily an androgen-dependent condition, involves endocrine medications that either directly inhibit the androgen receptor (AR) or target androgen depletion (Sartor and de Bono, 2018; Wilding, 1992). Androgens bind to AR, a ligand-dependent receptor that acts as a transcription factor. Androgens like testosterone and dihydrotestosterone (DHT) are essential for the expression of the masculine phenotype (Richmond and Rogol, 2007). Normal prostate cell physiology depends on AR signaling, whereas prostate cancer amplifies AR signaling, which encourages uncontrolled cellular migration and proliferation (Culig and Santer, 2014).

For advanced prostate cancer, the mainstay of care has been ADT, which is essentially castration either surgically or medically. 20-30 percent of cases develop resistance advance to CRPC despite being initially successful (Harris et al., 2009). Although AR signaling is not necessary for CRPC, new research has made it clear that AR is essential for the growth of CRPC tumors. Abiraterone and enzalutamide are two novel AR signaling inhibitors that were developed in response to this resistance (Sartor and de Bono, 2018). Although treatment

options have improved, patients develop resistance and transition to tumors with a neuroendocrine phenotype. Unlike other advanced prostate cancers, NEPC still poses a challenge. Treatment options for NEPC are fleeting, and life expectancy decreases to a year (Yamada and Beltran, 2021). This highlights the need to understand and develop novel therapeutics to treat primary and advanced prostate cancers.

Chapter 1.2 Targeting the androgen receptor cellular signaling axis for treatment of prostate cancer

In the 1960s there were major discoveries related to androgen receptor structure and ligand binding. Understanding the structure of AR paved the way, for developing first generation antiandrogens that work by binding to AR countering the effects of testosterone and DHT to halt the progression of prostate cancer driven by androgens (Anderson and Liao, 1968; Bruchovsky and Wilson, 1968; Mainwaring, 1969). Our enhanced comprehension of ARs role in prostate cancer has led to the development of targeted therapies for treating this type of cancer.

Several methods have been developed to treat prostate cancer by targeting AR. As mentioned, prostate cancer cell growth at early stages is dependent on AR signaling. As the disease progresses researchers have found that AR expression increases. Furthermore, several point mutations in the ligand binding domain of AR change the activation properties of the receptor. Furthermore, even variants of AR have been reported. Several treatments have been developed that target AR which include inhibitors that target the N-terminal domain, initiate

degradation, and splice variants of AR.

Cyproterone was among the first antiandrogens developed. However, due to its side effects, research began on creating nonsteroidal anti-androgens as alternatives (Pavone-Macaluso et al., 1986). Flutamide became the first nonsteroidal anti-androgen approved by the US Food and Drug Administration (FDA) in 1989. Flutamide inhibits AR signaling and decreased prostate cancer tumor growth. Nonsteroidal anti-androgens showed promising antitumor properties, but combination therapies were not as successful (Seidenfeld et al., 2000).

To treat prostate cancer researchers targeted androgen receptor. Ketoconazole, currently used as an antifungal, inhibits androgen receptor and glucocorticoid receptor. Treatment with ketoconazole decreases serum testosterone levels, but these levels elevate after 24 hours. Interestingly, patients treated with ketoconazole showed decreased tumor growth, but ketoconazole treatment did not extend survival (Alva and Hussain, 2013).

Newer technologies have led to the improvement of prostate cancer therapies that target AR. For instance, several inhibitors have been developed that target the AR-V7 splice variant. Niclosamide is an FDA-approved drug used to treat parasitic infections. Interestingly, researchers have shown that Niclosamide decreased AR-V7 activity by promoting protein degradation of both AR and AR-V7 (Liu et al., 2014). Thailstatins have been shown to target the pre-mRNA of AR-V7. Thailastatins function by targeting the U2AF65/SAP155 spicing complex that helps assemble the mRNA of the AR-V7 variant (Wang et al., 2017). Other drugs that have been shown to target the AR-V7 variant include Rutaecarpine, Indisulam, and Nobiletin.

Through genetic sequencing, researchers revealed that mutations in the N-terminal domain (NTD) of AR rarely occur, making it a prime target for therapeutic drug targets. One of

the first drugs developed targeting the NTD domain of AR was EPI-001. EPI-001 was effective at inhibiting prostate tumor growth without altering AR expression (Hirayama et al., 2020). Newer versions of EPI-001 have been shown to be effective at decreasing the expression of AR. Currently, EPI-7386 is undergoing clinical trials (Morris et al., 2023).

Interestingly, there are several other drugs that target AR folding and synthesis. Heat shock protein 90, a critical protein for AR structure, has had promising results. Interestingly, inhibition of Hsp90 by Herceptin decreased breast cancer tumor growth, but no benefits were seen in prostate cancer (Modi et al., 2007). Solubility with the compound remains an issue. Interestingly, targeting histone acetyltransferases (HAT) and histone deacetylases (HDACs) also has positive effects on prostate cancer treatment. Interestingly, the targeting of HDACs stops the expression of AR in both mCRPC and mCSPC. In addition, targeting HDACs decreased tumor growth in tumor models (Rokhlin et al., 2006).

Enzalutamide, a second-generation AR inhibitor, disrupts stages of the AR signaling cascade by hindering AR binding to DNA and impeding AR translocation to the nucleus (Tran et al., 2009). Various trials such as PREVAIL, AFFIRM, ENZAMET, ARCHES, and PROSPER have indicated improvements in overall survival, prostate specific antigen PFS, and radiographic survival in prostate cancer scenarios including mCRPC and mCSPC (Armstrong et al., 2019b; Beer et al., 2014; Davis et al., 2019; Scher et al., 2012). Apalutamide is another nonsteroidal second-generation AR antagonist that inhibits transcription, DNA binding, and nuclear translocation of AR (Chong et al., 2018). Following the SPARTAN and TITAN studies, it gained FDA approval for nmCRPC and mCSPC, presenting a treatment option in prostate cancer care evolution.

Apalutamide is another nonsteroidal second generation AR antagonist that inhibits transcription, DNA binding, and nuclear translocation of AR (Chong et al., 2018). Following the SPARTAN and TITAN studies apalutamide gained FDA approval for nmCRPC and mCSPC, presenting a treatment option for prostate cancer. Compared to the placebo plus ADT group, in the SPARTAN study, administering 240 mg of apalutamide alongside ADT enhanced patients' OS and metastasis-free survival (MFS) in mCRPC patients (Small et al., 2019). In the TITAN study, individuals with mCSPC experienced notably better OS and PFS when treated with the same amount of apalutamide alongside ADT compared to receiving a placebo alongside ADT (Chi et al., 2021). Enzalutamide and apalutamide have documented side effects that individuals should consider before initiating therapy.

Darolutamide, an AR antagonist, consists of a 1;1 mixture of two diastereomers that exhibit activity. Both darolutamide and its primary active metabolite effectively inhibit testosterone induced AR translocation to the nucleus reducing AR gene activation (Fizazi et al., 2018). The FDA has approved a dosage of 600 twice daily in combination with ADT for metastatic castration resistant prostate cancer based on positive findings from the phase 3 ARAMIS study, which demonstrated significant enhancements in MFS and OS (Fizazi et al., 2020). Notably, darolutamide had non-negative side effects on the central nervous system (CNS) when compared to enzalutamide and apulatimide (Crawford et al., 2020).

Therapeutic resistance can develop when anti-androgens bind with low affinity to AR. Overactivity of the androgen receptor or changes in its ligand binding domain can lead to drug resistance. Even more concerning is that current studies suggest these alterations may convert these drugs into agonists (Chen et al., 2004). As a result, newer drugs were developed to

address this issue and are now widely used in the treatment of prostate cancer and are the first line of defense.

Chapter 1.3 Common treatments in Androgen deprivation therapy

Currently the first line of defense to treat prostate cancer is ADT. ADT's goal patients receiving treatment is to suppress androgen hormones either with drugs or surgical castration. To get to this point researchers had to make to major break throughs. The first break through that ADT might be used to treat prostate cancer goes back a couple of centuries to the research done in 1786 by John Hunter on the effects of castration on animals (JF, 1837). J.W. White noted decreased prostate weight in dogs after castration in 1893(White, 1893). Charles Huggins and associates made another important discovery in 1941 when they proved that ADT was beneficial for metastatic prostate cancer (Huggins and Hodges, 1972). Huggins was awarded the Nobel Prize in 1966 for this work. Even though ADT was initially successful, it soon became apparent that more potent treatments were required. The effects of ADT are lessened by the adrenal glands' continued secretion of androgens (Huggins and Scott, 1945).

The second important breakthrough against prostate cancer came in 1971 when Andrew Schally described how the hypothalamus regulates pituitary activity (Matsuo et al., 1971). Andrew Schally developed synthetic luteinizing hormone-releasing hormone (LHRH) agonists and provided an explanation of the structure LHRH. LHRH agonists cause a spike in serum testosterone levels at first, a phenomenon called testosterone flare (Matsuo et al., 1971; Schally et al., 2000). However, prolonged use of these agonists inhibits pituitary gonadotropin release by downregulating the LHRH receptor. This finding provided a fresh approach to the

treatment of prostate cancer by influencing the hypothalamic-pituitary axis.

Follicle-stimulating hormone (FSH) was one of these initial targets. Serum testosterone decreased because of FSH suppression, which was consistent with the outcomes of surgical castration (Sandow et al., 1978; Schally et al., 2000). While gonadotropin-releasing hormone analogs are preferred due to their non-surgical, reversible, and convenient nature, surgical castration remains a feasible and cost-effective option (Sun et al., 2016). The understanding of how androgens are produced, and that androgen suppression inhibits prostate cancer growth led to the development of drugs effective at inhibiting prostate cancer growth.

Cyproterone was among the first antiandrogens developed, with its efficacy compared to DES castration in medical practice. However, due to its effects, research began on creating nonsteroidal anti-androgens as alternatives (Pavone-Macaluso et al., 1986). Flutamide became the first nonsteroidal anti-androgen approved by the US Food and Drug Administration (FDA) in 1989. Flutamide inhibits AR signaling and decreased prostate cancer tumor growth. Nonsteroidal anti-androgens showed promising antitumor properties, but combination therapies were not as successful (Seidenfeld et al., 2000). In prostate cancer cases nonsteroidal anti-androgens demonstrated reduced survival compared to castration methods like LHRH agonists or orchiectomy. Combining castration with a first-generation nonsteroidal anti-androgen slightly improved overall survival, but studies indicate potential for more negative side effects, such as androgen surge at the beginning of treatment (Akaza et al., 2009; Schmitt et al., 2000).

Another drug developed to target androgen production was abiraterone. Abiraterone has emerged as a therapy for prostate cancer due to its potent inhibition of CYP17A1 (Rehman

and Rosenberg, 2012). 10% of testosterone in the bloodstream is generated by an enzyme known as 17α /C17,20 lyase found in the adrenal glands Studies have shown that abiraterone and its byproducts act as antagonists to the AR. Initially, most men with prostate cancer respond well to ADT. In some cases, men develop resistance and progress to metastatic castration resistant prostate cancer (mCRPC). Abiraterone leads to an increase in hormone (ACTH) production, necessitating supplementation. It also diminishes androgen synthesis along with serum levels of testosterone and other androgens (Rehman and Rosenberg, 2012). Various studies have shown the benefits of abiraterone in advanced prostate cancer scenarios. For instance, in patients newly diagnosed with metastatic Castration Sensitive Prostate Cancer (mCSPC) the LATITUDE phase 3 study revealed that combining abiraterone and prednisone with ADT significantly prolonged Overall Survival (OS) and median radiographic progression free survival (PFS) (Fizazi et al., 2019). Similar positive outcomes were observed in the STAMPEDE trial where combining prednisolone and abiraterone with ADT extended OS at three years for patients with mCSPC or risk advanced CSPC (Hoyle et al., 2019; James et al., 2017). The trials COU AA 301 and COU AA 302 revealed that abiraterone notably boosts survival in patients who have previously undergone docetaxel therapy and those who have not received chemotherapy after ADT failure (Fizazi et al., 2012; Ryan et al., 2015). In a series of studies, other drugs like Enzalutamide and Apalutamide showed similar benefits.

Patients undergoing ADT suffer from the secondary effects of drug treatments. Relugolix is a medication designed to mitigate the effects associated with ADT. Common side effects of ADT include diabetes, metabolic issues, increased cardiovascular risks, cognitive impairments, and sexual dysfunction (Grossmann and Zajac, 2011). To minimize these effects, researchers

developed relugolix, an administered nonpeptide LHRH antagonist. It competes with the LHRH receptor, inhibiting LH secretion and reducing testosterone production (Kunath et al., 2015; van Poppel and Nilsson, 2008). In the HERO phase 3 trial relugolix showed testosterone suppression compared to leuprolide and significantly lowered the risk of cardiovascular issues (Shore et al., 2020).

Chapter 1.4 Resistance Mechanisms in Prostate Cancer

Resistance, both primary and secondary, continues to be prevalent despite advancements and the introduction of medications that focus on the AR signaling pathway, which have improved outcomes for individuals with advanced prostate cancer. To effectively address the nature of prostate cancer, it is essential to develop innovative treatment strategies based on an understanding of the biological mechanisms that drive resistance. Several theories have been proposed in prostate cancer to elucidate the processes underlying primary and secondary resistance to therapies targeting the androgen receptor signaling pathway. These theories can be broadly categorized into those promoting AR independence, those triggering AR signaling reactivation, and those involving pathways that bypass AR.

Therapies directed at the AR signaling pathway often face challenges in combating prostate cancer as they reignite AR activity through various mechanisms. These include boosting ligands that activate AR, mutations in AR heightened expression of AR, and alternative splicing of AR. The development of resistance is an issue with drugs focusing on the AR signaling pathway; overexpression of the androgen receptor frequently plays a significant role in this

phenomenon. Studies utilizing tissue samples have revealed a strong association between elevated levels of AR expression and castration resistant prostate cancer (CRPC). Amplification of the AR gene has been linked to increased levels of AR expression. The standard genetic change in CRPC tissues is found in about half of all cases (Robinson et al., 2015). It is believed that an increase in AR expression might be triggered by the body's response to castration (Cai et al., 2011; Shan et al., 1990). Androgens typically stop AR genes from being activated in prostate cells through a feedback mechanism. Studies have shown that high levels of AR allow prostate cancer cells to grow when androgen levels are low, leading to resistance against treatments targeting AR (Waltering et al., 2009). Increased AR levels or gains in cell DNA from CRPC patients have been linked to resistance against enzalutamide and abiraterone, supporting these findings (Romanel et al., 2015; Wyatt et al., 2016).

Another way resistance can develop is through mutations in the androgen receptor. Mutations in the androgen receptor occur in 10% to 30% of cases of castration prostate cancer, with most changes happening later in the disease within the ligand binding domain (LBD) of the AR (Wallén et al., 1999). Initially, prostate cancer does not show any mutations in the AR, but the mutation rate increases to 21% in advanced prostate cancer (Marcelli et al., 2000). Only a small number of over a thousand identified AR mutations linked to prostate cancer are considered significant. Key mutations, like F877L, W742C, H875Y have been identified as pathogenic. The T878A mutation, often found in CRPC alters the residue in the AR ligand binding pocket to alanine. This change enlarges the pocket, allowing it to bind ligands like estrogen (Steketee et al., 2002). On the other hand, the H875Y mutation modifies a vital section of the receptor structure (helix 12) by replacing histidine with tyrosine. Consequently, this

alteration makes it easier for conventional ligands such as progesterone and estradiol to activate the receptor (Duff and McEwan, 2005). Moreover, by enhancing ARs interaction with coactivators, this mutation boosts ARs activity. In the presence of antiandrogens like enzalutamide, the F877L mutation triggers a conformational shift that activates AR through substitution of leucine for phenylalanine. The W742C mutation brings helix 12 to its active position. While this decreases AR LBD's affinity for androgens, it paradoxically triggers a response to antiandrogens like belicutamide. The clinical significance of W742C remains a topic of debate due to its rarity (Robinson et al., 2015). These mutations typically induce alterations in AR that allow a broader range of ligands to activate it. Mutations in the androgen receptor have been associated with responses to treatments like abiraterone or enzalutamide, particularly in patients with detectable mutations in circulating free DNA (cfDNA), although they are less common than AR gene amplification (Conteduca et al., 2017). Additionally, androgen receptor splice variants (AR SVs) can develop and lead to resistance in prostate cancer.

Various forms of AR have been identified in tissues of patients with prostate cancer and in preclinical models due to alternative splicing mechanisms (Antonarakis et al., 2014; Efstathiou et al., 2015). These AR splice variants often produce versions of the receptor by lacking the LBD while retaining the N terminal domain (NTD) and DNA binding domain (DBD). Many of these variations exhibit activity that is not dependent on androgens, enabling prostate cancer cells to survive and resist treatments targeting the androgen receptor (Watson et al., 2010). Among these variants, AR V7 has received attention as it is frequently present in advanced prostate cancer cases. Resistance to therapies targeting AR has been associated with the presence of AR V7 protein and mRNA in circulating tumor cells (Antonarakis et al., 2017; Armstrong et al.,

2019a; Scher et al., 2018). However, not all patients negative for AR V7 mRNA or protein respond well to treatments like enzalutamide or abiraterone, indicating that lack of AR V7 expression may not reliably predict treatment success (Armstrong et al., 2019a; Dirix, 2019; Sharp et al., 2019). This suggests the presence of resistance mechanisms like mutations and amplification of AR. The creation of AR V7 has been associated with several enzymes, notably JMJD1A/KDM3A, KDM4B, and JMJD6, three members of the 2 oxoglutarate dependent JmjC domain containing oxygenase family (Duan et al., 2019; Fan et al., 2018; Paschalis et al., 2021). These enzymes could potentially serve as targets to combat the effects of AR V7 in advanced prostate cancer.

Another way resistance may occur in prostate cancer is through increased availability of AR ligands, which could lead to restoration of AR signaling and subsequent resistance. Despite reductions in serum testosterone levels following surgical or medical castration, there remains a notable amount of androgen present (Titus et al., 2005). This ongoing presence of androgen is partly due to the glands' production of precursors like androstenedione (AD) and dehydroepiandrosterone (DHEA), which are then converted into active AR ligands—testosterone and dihydrotestosterone (DHT)—in the prostate. Even after abiraterone therapy, residual androgens persist in the form of sulfated DHEA—a commonly circulating form capable of replacing DHEA and countering abiraterone effects (Tamae et al., 2015). Moreover, changes in enzymes involved in synthesizing androgens may further contribute to resistance, for instance, a gain of function mutation in 3β hydroxysteroid dehydrogenase type 1. A change in this enzyme has been associated with increased conversion rates within the prostate and reduced

effectiveness of treatments like abiraterone and enzalutamide (Chang et al., 2013; Lu et al., 2020). This enzyme plays a role in the initial stages of converting DHEA to DHT.

In instances of prostate cancer, an AR bypass has been linked to AR independence, indicating a detachment from the AR signaling system. This differs from bypass signaling, which typically refers to the reactivation of downstream signaling pathways by an unregulated protein kinase in various cancer types. However, recent advancements in sequencing technologies suggest that bypass signaling may also play a role in prostate cancer, potentially suggesting a mechanism for AR resistance (Arora et al., 2013).

Significant overlap has been noted between the DNA segments regulated by the AR and those affected by the glucocorticoid receptor (GR) based on chromatin immunoprecipitation and sequencing (ChIP-seq) studies (Li et al., 2017a). Studies showing an increase in GR expression following enzalutamide treatment provide insight into its importance as elevated GR levels may continue to activate genes promoting cell growth even when AR is blocked, thus worsening enzalutamide resistance in CRPC (Li et al., 2017a). Recent research suggests that treatment with enzalutamide could impact levels of 11β hydroxysteroid dehydrogenase 2. 11β HSD2 is an enzyme that typically deactivates cortisol, leading to a decrease in its levels. This suggests that by maintaining cortisol levels within tumors, enzalutamide might indirectly boost the transcription of AR target genes mediated by GR (Li et al., 2017a). Furthermore, research has found that restoring 11β HSD2 in animal studies can reverse enzalutamide resistance. Apart from GR, resistance to AR targeted therapy has also been associated with AR bypass mechanisms involving nuclear receptors like the progesterone receptor (PR) and the mineralocorticoid receptor, which are steroid hormones. These receptors may influence a

subset of AR target genes due to their similarities with the AR (Lu et al., 2006). While there is a link between PR expression in primary prostate cancer and increased clinical recurrence, the evidence supporting this connection is not as robust as it is for GR (Grindstad et al., 2015).

The exploration of steroid hormone nuclear receptors in prostate cancer remains an ongoing area of investigation. RAR related orphan receptor gamma (RORγ) represents another nuclear receptor that that may aid in AR bypass signaling. RORs are nuclear receptors with varying tissue expression patterns, and ROR is found in the prostate among tissues (Stone, 2016). An isoform of RORγ known as RORγt plays a role in T cell maturation (He et al., 2000). Upon investigation, researchers discovered that ROR was highly expressed in prostate cancer that had metastasized to other areas of the body. Inhibiting RORα resulted in cell death, reduced cell multiplication, and halted tumor growth (Wang et al., 2016a).

Another critical factor contributing to treatment resistance is AR independence. AR negative tumors display a range of characteristics, including carcinomas, mixed prostatic adenocarcinomas with neuroendocrine traits, neuroendocrine prostate cancer, and small cell carcinomas (SCCs) (Beltran et al., 2014). These types do not rely on AR signaling for survival. They are thought to play a significant role in therapy resistance. Studies have shown that patients with CRPC mainly exhibit adenocarcinoma features with minimal neuroendocrine differentiation and a higher occurrence of SCC. There is debate about the origin of AR-negative phenotypes – whether they arise from the transformation of AR-positive adenocarcinomas or from pre-existing neuroendocrine cells within the prostate gland, especially after prolonged androgen deprivation therapy (Parimi et al., 2014). Understanding these subgroups is crucial as they are associated with more aggressive disease progression and poorer outcomes.

An interesting discovery is that prostate cancer undergoes genetic changes as it progresses to CRPC. Mutations occurring simultaneously in p53 and retinoblastoma protein 1 (RB1) are rare in tumors but are frequently observed in advanced CRPC, particularly in cases displaying neuroendocrine-like characteristics (Mu et al., 2017). The development of resistance to antiandrogen therapies like enzalutamide and the growth of cancer cells of androgen receptor activity have been linked to the loss of p53 and RB1 (Mu et al., 2017). These alterations also trigger lineage flexibility, prompting basal cells to proliferate over luminal cells that are dependent on androgen receptors. In addition, gene knockdown of p53 and RB1 increased neuroendocrine marker expression. From these results, it can be concluded that p53 and RB1 loss contribute to ADT resistance. Understanding these complexities is crucial for advancing markers and novel treatment strategies to combat resistance to therapies targeting the androgen receptor in deadly prostate cancer. A detailed exploration of neuroendocrine prostate cancer will be addressed subsequently.

Chapter 1.5 Neuroendocrine prostate cancer and tumor cell lineage plasticity

The expression of certain genes essential for neuronal and neuroendocrine differentiation, the epithelial-mesenchymal transition, and pathways linked to stem-like traits and cell cycle progression characterize neuroendocrine prostate cancer (Abida et al., 2019). A decrease in the expression of a cellular marker linked to the prostate cell lineage and suppression of androgen receptor activity indicate the change from adenocarcinoma to NEPC. Cellular plasticity and the maintenance of the neuroendocrine phenotype are largely

dependent on the dysregulation of important oncogenic drivers and transcription factors, including SOX2, ASCL1, BRN2, MYCN, and ONECUT2 (Lee et al., 2006; Metz et al., 2020; Rotinen et al., 2018; Yamada and Beltran, 2021; Zhang et al., 2018).

Transcription factor N-Myc is known to be an oncogenic driver in several different neuroendocrine tumors and is elevated in NEPC. It supports lineage plasticity and acts as an inhibitor of AR signaling (Dardenne et al., 2016). In NEPC and several subtypes of castration-resistant prostate cancer with adenocarcinoma, N-Myc is overexpressed (Beltran et al., 2011). Patients with CRPC-Adeno and NEPC have a worse overall survival rate when their N-Myc levels are high. Epigenetic modifications are known to be induced by N-Myc's interaction with AR, Enhancer of zeste homolog 2 (EZH2), and other members of the Polycomb Repressive Complex 2 (PRC2) (Dardenne et al., 2016). Mitotic protein Aurora kinase A (AURKA) further stabilizes N-Myc and stops it from degrading (Beltran et al., 2011). Alisertib, an AURKA inhibitor, has been investigated as a means of disabling the N-Myc-AURKA complex and preventing NEPC tumor growth (Beltran et al., 2019).

In addition to being a primary neuronal transcription factor, BRN2 is a lineage-specific transcription factor and NEPC driver (Bishop et al., 2017). AR inhibits BRN2 expression, which in turn regulates the expression of the stem cell transcription factor SOX2. One possible role for SOX2, which is regulated by TP53 and RB1, is to restore cells to a more pluripotent or stem-like state, which is a prerequisite for neuroendocrine development (Metz et al., 2020). Histone H3 hypomethylation has been linked to the suppression of SOX2, and lysine-specific demethylase 1 is the step that starts it (Li et al., 2020). The neuroendocrine phenotype is supported by SPINK1

activation, which is another effect of elevated SOX2 expression (Tiwari et al., 2020).

Several other biological variables are connected to the pathophysiology of NEPC. These include the increased expression of the RNA-splicing factor SRRM4, the decreased expression of REST, a crucial regulator of neural differentiation, and PEG10, which promotes cell cycle progression and plasticity (Akamatsu et al., 2015; Li et al., 2019b; Ooi and Wood, 2007). REST is partially controlled by SRRM4 and binds to gene regions necessary for a neuronal phenotype, blocking their transcription. MUC-1, which is highly expressed in NEPC, can also enhance lineage plasticity pathways (Yasumizu et al., 2020). It has been demonstrated that MUC-1 inhibition suppresses BRN2 and cellular self-renewal in vivo.

Additionally, NEPC has been linked to metabolic susceptibilities. It is discovered that NEPC has downregulated protein kinase C (PKC) λ/ι, a tumor suppressor that increases serine production through the mTORC1/ATF4 pathway (Reina-Campos et al., 2019). Increased intracellular S-adenosyl methionine (SAM) levels brought on by this metabolic change affect DNA methylation and may play a role in the formation of NEPCs (Reina-Campos et al., 2019). The transcription factor ONECUT2, which activates SMAD3, influences hypoxia signaling and promotes a neuroendocrine phenotype, is one of the factors that govern hypoxia inside NEPC tumors. As a master regulator in prostate cancer, ONECUT2 inhibits the AR network and activates genes involved in neural differentiation. It has been demonstrated that blocking ONECUT2 slows the growth and spread of tumors (Rotinen et al., 2018).

Chapter 1.6 Emergence of neuroendocrine prostate cancer

The understanding of the complex biology of NEPC has advanced significantly, yet there remains a need for a more refined comprehension of the emergence and cooperative action of these factors in the context of resistance to AR-targeted therapies. As mentioned earlier, drug resistance is a problem in the treatment of advanced prostate cancer. Advanced prostate cancers change and adopt alternative growth and survival strategies to overcome therapeutics. Currently, 20-30 percent of prostate-resistant tumors morph into AR-independent tumors with neuroendocrine features, which leads to the formation of highly aggressive and fatal neuroendocrine prostate cancer. How NEPC arises is still under debate.

Lineage switching refers to the ability of cancer cells to evolve into different cell types after treatment. Like other cancer cells, prostate cancer has this capacity. Continued treatment with therapeutics like enzalutamide can lead to resistance. Prostate cancer to NEPC is supported by lab research showing an epithelial-mesenchymal transition (EMT) and neuroendocrine differentiation. In prostate cancer, this phenomenon is known as treatment-induced lineage crisis. NEPC Tumors have low AR expression, stem cell-like properties, and enhanced cell cycle activity, which results in a more aggressive cancer. How NEPCs arise is still under investigation, but evidence suggests cellular linear plasticity of prostate cancer cells.

EMT involves epithelial cells transitioning from differentiated to a de-differentiated state and abandoning characteristics, such as cell-cell adhesion and apical-basal polarity, and reactivating mesenchymal cell features, like increased invasive and migratory capabilities and enhanced resistance to apoptosis. Prostate cancer cells exploit the EMT program to acquire

malignant traits like motility, invasiveness, and drug resistance. Clinically, EMT induction and mesenchymal trait acquisition correlate with more severe disease indicators.

Cellluar markers such as N-cadherin, a mesenchymal marker whose expression increases during EMT, are prevalent in CRPC cells and tumors, particularly those exhibiting low AR pathway activity (Tanaka et al., 2010). This expression is associated with enhanced invasion, metastasis capabilities, and castration resistance. Evidence linking cell plasticity with neuroendocrine differentiation includes the induction of EMT, cancer stem cell (CSC) population enrichment, and neuroendocrine differentiation following AR pathway inhibition in prostate cancer cell lines and clinical samples (Wang et al., 2016b). Further, there's a significant overlap between the molecular markers defining epithelial plasticity and a neuroendocrine phenotype. For instance, small-cell neuroendocrine prostate tumors share transcriptional programs with normal adult prostate basal stem cells, and forced expression of the EMT transcription factor SNAI1 in certain cell lines leads to the emergence of neuroendocrine characteristics (McKeithen et al., 2010). Preclinical data suggest that adenocarcinoma cells might undergo an incomplete EMT-like process to transdifferentiate into NEPC. The transcription factor SOX11, which is linked to both EMT and MET, has been identified as a driver of neuroendocrine differentiation in NEPC models (Ji et al., 2022).

In prostate cancer, the IL-6–signal transducer and activator of transcription 3 (STAT3) signaling pathway is a crucial nexus connecting the epithelial-mesenchymal transition program, the cancer stem-like cell phenotype, and neuroendocrine differentiation. Studies using in vitro prostate cancer cell line models have demonstrated that IL-6 activation of STAT3 signaling, after inhibition of AR, imparts cells with stem-like features, EMT characteristics, and neuroendocrine

differentiation markers (Culig, 2014). Inhibition of IL-6–STAT3 signaling, such as through an IL-6 cytokine trap, has been shown to reduce the CSC population in these models (Malinowska et al., 2009). To support these results is the expression of STAT3, EMT transcription factor TWIST1, as well as stemness markers SOX2 and NANOG detected in human prostate tumors. Clinically, elevated IL-6 levels in the blood serum of patients with aggressive metastatic prostate cancer have been associated with poorer survival outcomes, aligning with the observed in vitro and in vivo links between IL-6–STAT3 signaling, EMT, CSC properties, and neuroendocrine differentiation in prostate cancer (Nakashima et al., 2000).

The WNT–β-catenin signaling pathway is active in castration-resistant prostate cancer, leading to increased resistance to androgen deprivation therapy and the development of a neuroendocrine phenotype (Chen et al., 2019; Yu et al., 2011). For instance, neuroendocrine differentiation has been observed in the prostates of transgenic mice expressing stabilized β-catenin. The inhibition of β-catenin using a small-molecule inhibitor (C3) has been shown to reduce prostate tumor growth in vivo and prevent the rise of CSCs following antiandrogen therapy (Lee et al., 2013). In addition, studies in both mouse embryonic stem cells and prostate cancer mouse models have revealed interactions between the WNT–β-catenin and STAT3 pathways, with β-catenin enhancing STAT3 transcription and WNT5A activation of the Frizzled receptor leading to STAT3 phosphorylation (Fragoso et al., 2012).

The role of cell surface markers like CD44 in lineage plasticity and neuroendocrine differentiation also underscores the complexity of these transitions. CD44 is a well-established marker for prostate CSCs and is associated with EMT and neuroendocrine differentiation traits (Shang et al., 2015). CD44 Silences the EMT transcription factor ZEB1 and interacts with CDH1,

which encodes E-cadherin and affects CD44 expression (Marín-Aguilera et al., 2014). CD44 is predominantly expressed in cells positive for the neuroendocrine marker Neuron-specific enolase (NSE), and the transplantation of CD44+ CD24- CSCs into mice leads to the development of tumors with mesenchymal and neuroendocrine characteristics (Li et al., 2016c). Clinical evidence further supports these connections, with immunohistochemical analysis of prostate tumors showing a high prevalence of CD44+ cells among neuroendocrine cells.

The molecular processes driving neuroendocrine transdifferentiation remain largely elusive. Despite extensive next-generation sequencing efforts, only a few genetic variances have been identified between prostate adenocarcinoma and neuroendocrine prostate cancer. These primarily involve alterations in pathways related to NMYC proto-oncogene protein (MYCN), RB1, and cellular tumor antigen p53 (TP53). These findings imply that neuroendocrine transdifferentiation may be predominantly governed by epigenetic modifications that dictate cellular identity — such as alterations in DNA methylation and dysregulation of the histone lysine methyltransferase EZH2 — rather than by a straightforward mutation and selection process. Furthermore, the tumor microenvironment may play a role in fostering and maintaining the neuroendocrine phenotype through signals from stroma cells and immune cells associated with the tumor.

Chapter 1.7 An overview of epigenetics and prostate cancer

Epigenetic regulation is a crucial process for the normal development of a cell. Epigenetic regulation is the process that alters gene expression without altering DNA sequence and is inherited through cell division. Altering gene expression could lead to genes being on or off, affecting cell protein production. Epigenetic regulation involves several key processes, including DNA methylation, hormone modification, chromatin remodeling, non-coding RNA, and not strictly epigenetics RNA splicing. DNA methylation is the addition of a methyl group to DNA, usually in cytosine bases in CpG dinucleotides, which can prevent transcription factor binding or by recruiting proteins that condense chromatin, making DNA less accessible. Histones are proteins that wrap DNA, which can be methylated, acetylated, phosphorylated, or ubiquitinated, and can either condense(heterochromatin) or relax(euchromatin) chromatin structure affecting gene expression. Chromatin remodeling involves changing proteins involved in chromatin structure, which changes accessibility to DNA, hence changing gene expression. Non-coding RNA involves the expression of microRNA or long non-coding RNAs that can lead to gene silencing or activation. RNA splicing refers to changing how premature RNA is spliced, leading to different protein products and altering gene expression.

Epigenetic changes are critical for normal development and differentiation. This process allows cells with the same DNA to develop into different cell types such as muscle, skeletal, and neurons. However, changes in epigenetic regulation have been found to contribute to the development and onset of several diseases (Jia et al., 2015). Altered H3K4, a histone that promotes gene activation, methylation has been associated with neurodegenerative diseases. DNA hypomethylation, and hyperacetylation also contribute to other diseases like rheumatoid arthritis (Greer and McCombe, 2012). Even asthma seems to be passed on from mother to

offspring through epigenetic modifications. Several changes in epigenetic regulation have been reported in cancer, such as Gastric, colorectal, melanoma, breast, lung, pancreatic, adenocarcinoma, and prostate cancer. Reported epigenetic changes include increased promoter methylation, histone modifications, and changes in miRNA expression.

DNA methylation and histone modifications are observed and reported to be critical in the progression of prostate cancer. Both hypermethylation and hypomethylation of genes contribute to tumor growth and metastasis. Several proteins have been reported to alter DNA methylation, such as the GSTP1 promoter and the promoter of the Androgen receptor. Hypermethylation of the GSTP1 promoter leads to gene silencing (Mahon et al., 2014). Androgen Receptor has been reported to be hypermethylated in castration-resistant prostate cancer, which leads to the loss of AR expression (Suzuki et al., 2003). Additionally, AR promoter hypermethylation often silences the PTEN and p16 tumor suppressor genes, contributing to carcinogenesis and disease progression (Jarrard et al., 1997; Li et al., 2017b). Hypomethylation of genes like heparanase and urokinase plasminogen activator (uPA) increases tumor invasion and metastasis (Pakneshan et al., 2003).

Lysine methyltransferases (KMTs) and demethylases (KDMs), histone modifiers, have also been implicated in prostate cancer. KMTs like SUV39H1 and SETDB1 are upregulated in prostate cancer, enhancing cell migration and invasion, and are proposed as therapeutic targets (Yu et al., 2017). SET and MYND domain-containing protein 3 (SMYD3) is also upregulated lysine methyltransferase that promotes cell proliferation and migration in prostate cancer (Huang and Xu, 2017). Arginine methyltransferase 5 (PRMT5) has been shown to drive tumor growth by silencing tumor suppressor genes and activating AR target genes (Stopa et al., 2015).

Demethylases like lysine-specific demethylase 1 (LSD1/KDM1A) are histone modifiers that have been associated with the progression of diseases, including cancer. LSD1/KDM1A are implicated as oncogenes in prostate and other cancers, promoting carcinogenesis through various mechanisms. One of these mechanisms includes the overexpression of LSD1, which correlates with prostate cancer recurrence and poor survival. LSD1 binds with AR, which changes the expression of AR target genes. LSD1's coactivator function is typically associated with demethylation of H3K9me1,2, leading to the transcriptional de-repression of AR target genes. The histone demethylase family, which includes KDM3A, KDM4A, KDM4B, KDM4C, KDM5B and KDM5C, have been reported to contribute to prostate cancer (Komura et al., 2016). KDM3A activation occurs in the presence of androgens, influencing AR activity and activating genes involved in the androgen response (Wilson et al., 2017). KDM4A and KDM4C have been shown to modulate AR transcriptional activity and contribute to prostate cancer pathogenesis (Shin and Janknecht, 2007). KDM4B acts as a coactivator for AR, regulating AR transcriptional activity by demethylation, preventing ubiquitination, and improving AR stability (Xiang et al., 2007). KDM5B and KDM5C are upregulated in prostate cancer, while KDM5D is downregulated. Other lysine demethylases have been found to suppress tumor growth in prostate cancer, specifically KDM5D (Li et al., 2016b).

NSD2, a member of the histone methyltransferase NSD family, is overexpressed in prostate cancer. NSD2 contributes in several ways to the pathogenicity of prostate cancer. One of the ways that NSD2 contributes to prostate cancer pathogenicity is through the activation of the NF-kB signaling pathway. Activation of the NF-kB signaling pathway has been shown to contribute to the growth and survival of prostate cancer cells (Yang et al., 2012). Another

mechanism that NSD2 exploits is the activation of the AKT pathway. Activation of the AKT pathway by NSD2 activates downstream cellular pathways associated with survival and metastasis (Li et al., 2017b). It has been reported that NSD2 binds with the AR DNA-binding domain, specifically the PSA gene, enhancing AR transcriptional activity (Nalla et al., 2016). Lastly, NSD2 can potentially promote androgen receptor independence.

Another epigenetic regulator involved in prostate cancer is EZH2. EZH2 is a member of the Polycomb Repressive Complex 2, which regulates histone methylation(Di Croce and Helin, 2013). Methylation of H3K27 is associated with gene silencing, specifically in silencing genes associated with cell lineage-specifying factors. The upregulation of EZH2 promotes cell stemness, epithelial-to-mesenchymal transition, and metastatic progression. EZH2 expression is upregulated in prostate cancer. As discussed earlier, EZH2 and SOX2 drive neuroendocrine differentiation, plus EZH2 functions with E2F1 in castration-resistant prostate cancer (Xu et al., 2016).

Bromodomain-containing proteins are chromatin readers that are implicated in prostate cancer. BRDs function by recognizing mono-acetylated lysine histone residues and facilitate chromatin remodeling by opening chromatin structure and facilitating gene transcription. Currently, there are 42 known bromodomain proteins. Alterations in proteins with bromodomains are frequently observed in various cancers. Specifically, over half of primary and metastatic prostate cancers show genetic changes in these proteins. The prevalence of these alterations is even higher in neuroendocrine prostate cancers, where more than 70% of cases involve genomic changes in at least one of the bromodomain proteins. (Urbanucci and Mills, 2018). Bromodomain-containing proteins act as transcription factors, cofactors,

methyltransferases, histone acetyltransferases (HATs), helicases, and ATP-dependent chromatin remodelers. The BET subgroup of bromodomain proteins, especially BRD4, has been extensively studied in prostate cancer. BETs work as enhancers/super-enhancers and recruit factors to initiate gene transcription (Jang et al., 2005). Specific single nucleotide polymorphisms (SNPs) in super-enhancer regions of DNA bound by BRD4 are significantly associated with increased prostate cancer risk. BRD4 interacts with the AR, promoting its nuclear translocation, recruitment to target loci, and overall activity, particularly in castration-resistant prostate cancer (Asangani et al., 2014). The BET inhibition has been shown to disrupt BRD4 recruitment to AR enhancer regions (Faivre et al., 2017). BET proteins also play a role in resistance to antiandrogens. BRD4 can also bind the TMPRSS2-ERG fusion, which stimulates cell growth and invasion (Blee et al., 2016). Furthermore, BRD4 has been linked to the oxidative stress response in prostate cancer (Hussong et al., 2014). The Bromodomain-containing proteins TRIM24 and CHD1 have been associated with prostate cancer progression and aggressiveness. TRIM24, overexpressed in CRPC and linked to disease recurrence, enhances AR signaling and promotes tumor growth. CHD1, an H3K4me2-3 epigenetic reader, is frequently mutated in aggressive prostate cancers (Grasso et al., 2012; Rodrigues et al., 2015).

FOXA1 is a well-documented DNA binding protein implicated in prostate cancer. It interacts with and recruits the androgen receptor to chromatin sites, thereby defining and controlling the AR cistrome and resulting in context-dependent regulation of gene expression (Wang et al., 2007). FOXA1 increases DNA accessibility and AR binding, which leads to high FOXA1 expression (Zhao et al., 2016). This, in turn, leads to the upregulation of AR target genes, increasing tumor metastasis.

GATA genes, especially GATA2, play a crucial role in prostate cancer. GATA 2 has been shown to contribute to prostate cancer cell growth by altering androgen receptor dynamics. It has been reported that GATA2 expression decreased AR expression without changing DNA AR accessibility, hence implying that these two proteins have a cofactor capacity. Interestingly, the activity of GATA2 in human prostate cancer is closely associated with androgen receptor levels. FOXA1, an androgen receptor recruiter, has been reported to alter the function of GATA2. FOXA1 binds to both AR and GATA2 in prostate cancer. This suggests that FOXA1 and GATA2 play a crucial role in regulating AR gene expression in prostate cancer (Zhao et al., 2016).

Lineage plasticity in prostate cancer stem cells is a crucial element of carcinogenesis. Several changes in the expression of Yamanaka factors (OCT4, SOX2, KLF4, and c-MYC), NANOG, and LIN28 have been reported to occur and contribute to the pathogenicity of prostate cancer. The elements are necessary for the triggering pluripotency but are also associated malignancies, including cancer.

SOX2 overexpression is linked to tumorigenesis in various cancers, including prostate cancer, with its expression correlating with tumor grade (Wong et al., 2010). SOX2, as an epigenetic reprogramming factor and oncogene. Altered SOX2 expression has been reported in advanced CRPC. SOX2 has been shown to promote androgen independence, evasion of apoptosis, and tumor metastasis (Li et al., 2013). It has been reported that SOX2 may interact with EGFR to promote cancer stem cell transition (Rybak and Tang, 2013). SOX2 has also been associated with neuroendocrine trans-differentiation (Esposito et al., 2015). SOX2 is transcriptionally regulated by the neural transcription factor BRN2, which is, in turn, suppressed by AR, revealing an AR-dependent suppression of cell differentiation toward a neuroendocrine,

AR-independent phenotype (Bishop et al., 2017).

Several different members of the MYC family of proteins have been associated with prostate cancer progression. The MYC family of proteins are oncogenes with several functions, including the regulation of the cell cycle, cell death, and DNA damage response. c-MYC is a well-established oncogene associated with prostate cancer progression, recurrence, and poor prognosis. C-Myc functions with the loss of PTEN to drive cancer progression and metastasis in prostate cancer (Hubbard et al., 2016; Kim et al., 2012). MYCN upregulates the expression of EZH2 in prostate cancer, which activates NEPC trans differentiation (Dardenne et al., 2016). MYC also regulates the expression of histone modifiers such as PHF8. Histone demethylases PHF8 and KDMA3 is regulated by MYC in NEPC and CRPC (Maina et al., 2016). Normally, AR signaling represses MYC expression in normal prostate, but recent reports suggest that MYC overexpression deregulates the AR signaling of prostate cancer.

Several pathways have been reported to be altered in the prostate. Interestingly, several oncogenic pathways are altered in prostate cancer. The RB, PI3K/AKT, and Ras/Raf are pivotal due to mutations in several members and reported to be altered in prostate cancer (Taylor et al., 2010). The Ras/Raf pathway contributes to cancer aggressiveness by activating epithelial-mesenchymal transition transcriptional programs. One model suggests that secreted extracellular protein Hsp90 initiates ERK signaling, leading to the recruitment of EZH2 to the E-cadherin promoter, driving EMT and invasion (Nolan et al., 2015). DAB2IP, a tumor suppressor Ras-GAP, modulates various pathways. In prostate cancer DABP2IP, this leads to the activation of programs associated with tumor aggressiveness such as the Ras and NF-kappa B pathways (Chen et al., 2005). Activation of bothPI3K and MAPK pathways results in aggressive and fully

metastatic tumors resistant to castration (Aytes et al., 2013).

Retinoblastoma is a tumor suppressor gene that has been implicated in several cancers. The loss of RB1 is common in advanced prostate cancers such as mCRPC and NEPC. RB1 loss leads to increased EZH2 and SOX2 expression, which, in turn, changes several epigenetic programs. As mentioned earlier, EZH2 and SOX2 changes are reported with transitions to a stem cell-like state, facilitating metastasis, neuroendocrine trans-differentiation, and acquisition of ADT resistance (Ku et al., 2017). TP53 and RB1 mutations can promote a cellular plasticity state mediated by increased SOX2 expression, leading to resistance through lineage switching when combined with antiandrogen therapy (Mu et al., 2017).

The PTEN/PI3K/AKT pathway alterations are hallmarks of prostate cancer. Loss of PTEN and activation of this pathway contribute to a switch from global H3K27 acetylation to trimethylation, increasing EZH2 expression and decreasing tumor suppressor genes. A downstream target of AKT phosphorylation is NSD2. Phosphorylation of NSD2 prevents its degradation, which in turn enhances AKT signaling. Loss of PTEN functions with c-MYC to contribute to cancer pathogenicity.

The tumor TGF-β signaling activation is a recognized mechanism for inducing EMT and metastasis. TGF-β1-induced EMT is mediated by histone methyltransferase RbBP5, modulated by SMAD2/3 binding to the Snail promoter (Li et al., 2016a). Snail activates EMT by inhibiting E-cadherin transcription through the recruitment of repressive histone modification enzymes. ERG signaling regulation of SOX4 suggests cooperation in TGF-β1-induced EMT in prostate cancer cells. SOX4, a key component of the PI3K/AKT pathway, regulates EZH2 expression and chromatin remodeling. Inhibition of SOX4 reduces AKT and β-catenin pathways activation,

decreasing cancer invasiveness (Bilir et al., 2016).

Ack1 is a tyrosine kinase involved in cellular proliferation and survival. Interestingly, there is a link between ACK1 oncogenic signaling and epigenetic regulation. ACK1 has been found to be upregulated in primary and advanced prostate cancers. It has been reported that ACK1 interacts with AR to promote the onset of ARI resistance and CRPC growth (Mahajan et al., 2007). ACK1 phosphorylates histone H4, recruiting the WRD5/MLL2 complex, mediating H3K4 trimethylation and AR transcriptional activation. Inhibition of ACK1 confirms that this epigenetic activity maintains AR transcription and CRPC tumor growth.

Chapter 1.8 An overview Receptor Tyrosine Kinases (RTKs)

Receptor tyrosine kinases are a group of tyrosine kinases that play a role in cell communication and the regulation of various complex biological processes such as cell growth, movement, differentiation, and metabolism. There are two categories of tyrosine kinases: receptor tyrosine kinases and non-receptor tyrosine kinases (non-RTKs). Out of the 90 identified tyrosine kinases, 58 fall under RTKs across 20 subfamilies, while 32 are classified as non-RTKs within ten subfamilies. There is an extracellular domain at the amino terminus that binds ligands, a single transmembrane α helix, an intracellular domain that acts as a tyrosine kinase, and areas that are high in tyrosine at the carboxy terminus and juxtamembrane regions (Lemmon and Schlessinger, 2010).

Receptor tyrosine kinase activation typically involves four ways of dimerization that affect the tyrosine kinase domain. The first method is set off by the ligand, which makes two

receptors join together without any interaction between their parts, as seen in TrkA (Wehrman et al., 2007). The second method uses receptor interactions to drive dimerization in which the ligands do not physically interact, as seen in members of the ErbB family (EGFR, HER2/ErbB2, HER3/ErbB3, and HER4/ErbB4) (Zhang et al., 2006). This method forms dimers when homodimers of ligands bind to two receptor units and interact at the dimer interface. This is similar to what happens in the KIT receptor (Manning et al., 2002). The fourth method combines ligand attachment with interactions between receptors and additional molecules like heparin or heparan sulfate to assist in dimerization within the FGFR family of RTKs (Yayon et al., 1991).

Upon activation and autophosphorylation, RTKs act as points for gathering downstream signaling molecules. Most of these autophosphorylation sites serve as points for signaling proteins containing SH2 or PTB domains. Proteins with SH2 domains can be directly recruited to the receptor or through docking proteins connected to RTKs via their PTB domains. These docking proteins function as "assembly platforms," facilitating the recruitment of molecules with SH2 or other functional domains (Brummer et al., 2010). Docking proteins enable activated RTKs to interact with and regulate a variety of signaling pathways, which include the PI3K/AKT and JAK/STAT pathways. As a result, RTKs play roles in interpreting external signals related to cell growth and movement.

Among RTKs, EGFR/HER receptors like EGFR, HER3, and HER4 have been extensively studied. All the RTKs mentioned bind to multiple ligands. In contrast, HER2 doesn't have a known ligand. EGFR interacts with ligands such as EGF and TGFα; these ligands are believed to be monomeric in solution and engage with receptors through their slightly diverse EGF-like

domains. These ligands can trigger EGFR signaling in ways leading to a range of cellular reactions, such as growth, division, and movement. For example, TGFα and heparin-binding EGF are more efficient at stimulating DNA replication in rat liver cells compared to EGF despite having binding strengths. Additionally, amphiregulin promotes increased mobility. Invasiveness in breast cells compared to EGF (Herbst, 2004).

The rise of technology has underscored the significance of RTKs in cancer research. Several studies using next-generation sequencing (NGS) have revealed alterations in genes for receptor tyrosine kinases. The recurring presence of these changes in RTKs raises questions about their impact on cancer development and the effective treatment approaches for tumors with specific RTK mutations.

Under physiological conditions, the activity of RTKs is carefully controlled by protein kinases and tyrosine phosphatases. Through several mechanisms, RTKs can acquire oncogenic properties that disrupt the balance between cell growth, proliferation, and cell death. The deregulation of RTK signaling in terms of timing and location adds a layer of complexity to understanding how these processes work. Prolonged RTK activation transforms cells and gives them oncogenic properties. These changes in RTK activation contribute to the pathogenicity of the cancer and lead to increased survival and proliferation.

Four distinct mechanisms of RTK activation have been described in cancer: gain-of-function mutations, amplification at the genetic level, rearrangements within chromosomes, and self-stimulation through autocrine pathways.

The Epidermal Growth Factor Receptor (EGFR) stands out as an RTK studied extensively within the context of lung cancer research. Researched changes often focus on EGFR-activating

mutations, which in NSCLC are typically found in exons 18–21 of the TKD gene. Most of these mutations consist of exon 19 deletions and the L858R point mutation, which trigger EGFR activation of ligand binding (Shigematsu and Gazdar, 2006). This process boosts kinase activity by shifting the balance between the inactive states of the receptor. Additionally, cancers such as lung, brain, and colon tumors display mutations in the domain (ECD) of EGFR. Some of these mutations lead to activation without ligands of EGFR and hinder the binding of EGFR monoclonal antibodies (Gazdar, 2009).

EGFR amplification is another outcome of these mutations. EGFR mutations are observed across various cancer types like breast, lung, ovarian, and prostate cancers (Sudhesh Dev et al., 2021). This amplification increases receptor abundance on cell surfaces, promoting receptor dimerization and subsequent kinase activation. In lung cancer cases, common EGFR gene fusions like EGFR RAD51 involve interactions between EGFR TKD and the DNA damage response protein RAD51. These interactions activate pathways such as MAPK and PI3K/Akt, encouraging cell proliferation of cytokines (Konduri et al., 2016). Various EGFR fusions can occur in NSCLC, such as those involving PURB, SEPTIN14, and KIF5B (Konduri et al., 2016; Zhu et al., 2019). Activation of EGFR can also happen through kinase domain duplications (KDDs), which involve tandem duplications of EGFR exons 18–25, leading to increased signaling via intramolecular dimers. The first reported case of an EGFR KDD was in a patient with cell carcinoma potentially associated with aggressive disease progression (Wang et al., 2020). Furthermore, EGFR activation can occur in an autocrine manner, supporting cancer stem cells and activating EGFR in tumor cells.

Vascular Endothelial Growth Factor Receptor (VEGFR) VEGFR1, VEGFR2, and VEGFR3, along with five VEGF ligands (VEGFA VEGFB, VEGFC, VEGFD, and PIGF) and neuropilin coreceptors play roles in regulating angiogenesis and lymphangiogenesis processes (Rapisarda and Melillo, 2012). These receptors and ligands are expressed in cancers like lung, breast, and colorectal prostate cancers, among others. Increased levels of VEGFR1 and VEGF expression in cancer cells activate the MAPK pathway to enhance cell growth (Itakura et al., 2000). In cancer cases, levels of VEGFR2 expression have been linked to poor overall survival rates along with increased cellular proliferation and invasiveness. Additionally, overexpression of Vascular Endothelial Growth Factor Receptor 2 (VEGFR2) has been associated with the epithelial-mesenchymal transition in breast cancer as with other types of cancer; however, varying roles for this receptor have been observed across different types of cancer based on findings from a human carcinoid cell line. (Longatto Filho et al., 2005; Tanno et al., 2004). The levels of VEGFR expression can differ depending on the stage of cancer, with VEGFR3 being more pronounced in stages. In liver and gastric cancer, autocrine VEGF signaling influences the effectiveness of molecule inhibitors, where higher levels of VEGFR1/2 in the autocrine circuit lead to inhibition of cell growth from drug treatment and slower tumor development (Peng et al., 2014).

Fibroblast Growth Factor Receptor (FGFR) genes FGFR1, FGFR2, FGFR3, and FGFR4 play roles in both development and adult functions. Among these genes, FGFR1 shows the frequency of mutations in cancer, followed by FGFR3, FGFR2, and then FGFR4 (Liu et al., 2021). Amplifications of FGFRs have been associated with increased signaling through MAPK and PI3K pathways, as well as elevated stem cell marker expression in lung, breast, and gastric cancers. Various cancers show around 200 mutations across all four FGFRs. The fusion gene FGGR3-

TACC3 is the first known FGFR fusion associated with a gene found in glioblastoma and other cancers; this fusion promotes cell proliferation and activates MAPK and ERK signaling pathways. Other fusion genes involving domains that promote receptor activation without ligands have also been identified (Nelson et al., 2016; Singh et al., 2012).

Platelet-derived growth factor receptors (PDGFRs), including PDGFAα and PDGFBβ, are activated by five PDFG ligands. Changes in genes within the PDGF family are frequently observed in lung, colon, and glioblastoma (Farooqi and Siddik, 2015). Mutations in PDGFRA in stromal tumors (GISTs) are commonly associated with heightened phosphorylation of ERK and STAT5, leading to continuous activation of the receptor (Velghe et al., 2014).

Chapter 1.9 Anaplastic Lymphoma Kinase receptor (ALK)

The anaplastic lymphoma kinase receptor was initially discovered in 1994. Researchers recorded a chromosomal rearrangement, which resulted in an NPM1-ALK (Shiota et al., 1994). Further research led to the discovery of the full wild-type receptor in 1997 (Iwahara et al., 1997). ALK is a highly conserved receptor tyrosine kinase part of the insulin receptor superfamily. In adult humans, ALK expression is localized to the central nervous system, testes, and small intestine (Vernersson et al., 2006). ALK activation requires ligand binding of either Augmentor a or b (FAM150), which triggers receptor dimerization and autophosphorylation. Unfortunately, there is limited information on the function of ALK in humans (Guan et al., 2015). Humans do express two variants of ALK, which differ in size: the 220 kDa full-size variant and the 140 kDa variant.

Potential functions of ALK have been discovered using fruit flies and mice. In *Drosophila melanogaster,* ALK is activated by the ligand Jelly Belly (Jeb). The binding of ALK to Jeb initiates several signaling cascades that help regulate the development of the gut musculature and visual nervous system (Vernersson et al., 2006). In mice, ALK is expressed in the nervous system during the embryonic and neonatal stages. In adult mice, the expression of ALK is significantly decreased. It has been reported that ALK knockout in mice is not lethal but knock mice do exhibit abnormalities (Lasek et al., 2011; Witek et al., 2015).

ALK possesses structure features typical of all RTKs, but it also possesses unique features. Like all RTKs, ALK possesses a ligand binding domain, a transmembrane domain, and an intracellular domain. In the extracellular domain, ALK has a low-density lipoprotein class A domain (LDL) surrounded by two mephrin/A5 protein/PTPmu domains (MAM)(Alexander et al., 2011). In addition, the extracellular domain contains an N-terminal signal peptide and a glycine-rich region. Having two extracellular MAM domains is unique to ALK; even more interesting, having two MAM domains connected to a low-density lipoprotein is also unique to ALK receptors. The biological function of the LDL in ALK is not fully understood, but recent evidence suggests that the MAM domains serve for cell-to-cell interactions through homophilic binding (Alexander et al., 2011).

The whole structure of ALK has yet to be fully elucidated, and most research has focused on the ALK kinase domain. The ALK kinase domain contains an amino-terminal lobe and a carboxy-terminal lobe. The amino-terminal lobe is composed of several beta-strands that form antiparallel strands, loop regions including a glycine-rich loop, and one helix (aC helix). The carboxy-terminal contains a-helices, two b-strands, and multiple loop regions (Bossi et al., 2010).

The catalytic activity of the kinase domain is affected by several regions that include a catalytic loop, an activation loop, an aC-helix, and a glycine-rich loop. Crucial residues of the catalytic loop include K1150, H1247, R1248, D1249, K1150, and K1267(Huang, 2018). Crucial residues of the aC-helix include E1167, D1270, F1271, and G1272 (Knighton et al., 1991).

The activation of ALK has yet to be fully understood, but it is believed that it follows the canonical RTK activation mechanism. The canonical RTK activation mechanism is ligand-induced activation. Once the ligand is bound to the extracellular region of the receptor, this triggers receptor homodimerization or heterodimerization. Receptor dimerization triggers trans-phosphorylation of specific tyrosine residues, which may lead to the phosphorylation of more tyrosine residues. Phosphorylation of the tyrosine residues leads to the activation of the catalytic activity of the RTK. The activated RTK can phosphorylate neighboring proteins, allowing for signal transduction of the RTK. Several mechanisms exist to inhibit RTK signaling, including either dephosphorylation through tyrosine phosphatases or degradation after endocytosis.

Numerous possible human ALK ligands have been identified, but further research is needed to understand the details of human ALK ligands fully. Recent studies have confirmed that anaplastic lymphoma kinase and leukocyte tyrosine kinase activating ligands (ALKALs) serve as ALK ligands. These findings indicate that ALKALs (FAM150A and FAM150B), or ALKAL1 and ALKAL2, which also bind to the leukocyte tyrosine kinase receptor (LTK), interact with the ALK extracellular domain (ECD) to activate it (Guan et al., 2015). Laboratory experiments demonstrate that ALKALs stimulate ALK's kinase activity. Moreover, mediums containing ALKALs have activated ALK in various ALK-expressing cell lines.

In other model organisms, introducing ALKALs has had a similar effect. ALKALs triggered the activation of normal ALK in a Drosophila model. In addition, in vivo research using zebrafish has further validated ALKALs as ligands for the ALK/LTK receptor family. Another study identified heparin as a potential ligand for mammalian ALK. A specific heparin-binding motif was located in the N-terminal region of the ALK ECD (Murray et al., 2015). Furthermore, a study on canine ALK revealed that the normal ALK ECD, but not a mutant version, could be isolated using heparin-sepharose chromatography. Longer-chain heparins can physically bind and activate ALK. In Drosophila melanogaster, jelly belly (Jeb) has been established as a biological ligand of ALK. ALK and Jeb are also vital in the development of the visual system. Without a functional AlLK gene, the gut development in the fruit fly is impaired (Lorén et al., 2003).

A pivotal attribute of ALK is its classification as a dependence receptor. In the absence of ligand-mediated kinase activation, ALK undergoes caspase-3-mediated cleavage during apoptosis (Mourali et al., 2006). Specifically, a caspase-3 cleavage site is located within the juxtamembrane region of ALK (amino acids 1160–1163: DELD), where increased caspase-3 activity facilitates the release of an intracellular ALK fragment (~60 kDa) into the cytoplasm. This process accentuates apoptosis via the revelation of a pro-apoptotic segment within the same region of ALK (Mourali et al., 2006). Notably, the ALK D1160N mutation impedes caspase-3 cleavage at this site, thereby mitigating the receptor's pro-apoptotic function. Additionally, synthesized peptides that emulate the pro-apoptotic domain of ALK have been observed to induce cytotoxicity through caspase-dependent apoptosis in ALK-positive anaplastic large cell lymphoma (ALCL) and neuroblastoma cell lines (Aubry et al., 2015).

N-glycosylation represents a pivotal post-translational modification of ALK, with 16 distinct N-glycosylation sites identified within its extracellular domain (ECD). This modification substantially augments the molecular mass of the full-length wild-type ALK: unglycosylated, it stands at approximately 180 kDa, whereas post-glycosylation, it manifests as roughly 220 kDa when analyzed via SDS-PAGE. Generally, N-glycosylation plays a crucial role in the folding, quality control, and membrane trafficking of membrane glycoproteins. Specifically, for ALK, N-glycosylation may be instrumental in its protein folding, quality control processes, and membrane anchoring. Empirical evidence suggests that the inhibition of ALK's N-glycosylation adversely impacts its phosphorylation and consequent downstream signaling, underscoring the significance of this modification in ALK's functional regulation (Del Grosso et al., 2011).

Chapter 1.9 ALK and Cancer

Several types of cancer have been found to have different changes in ALK expression. These changes in expression have been reported either through ALK amplification, ALK gain-of-function mutations, or ALK fusion mutations.

ALK fusion proteins are important oncogenic drivers in cancer. Several ALK fusions have been described in distinct cancers such as ALC, and NSCLC (Choi et al., 2008; Soda et al., 2007). These fusions involve an ALK fragment, through chromosomal translocation, joined with a fusion partner. The most well studied ALK fusions include NPM–ALK in ALCL and EML4–ALK in NSCLC. In ALCL alone, nine distinct fusions have been documented. The most prevalent ALCL is the NPM–ALK fusion (Roskoski, 2013). It is known that these fusion proteins stimulate

downstream signaling pathways that play a role in the development of cancer. The current understanding of ALK activation was elucidated by studying ALK activation in cancer. Constitutive activation of ALK is achieved by having ALK fusion proteins that are active even though ligand binding is absent. ALK fusion proteins induce dimerization (or oligomerization) irrespective of ligand contact. Furthermore, the fusion partner affects the resulting ALK fusion protein's subcellular location. Since the fusion protein's N-terminal domain is generated from the ALK fusion partner, the promoter of the partner protein usually regulates the fusion protein's transcription. Breakpoints for translocations of the ALK gene are typically located in exons 19–20 or 20–21 (Huang, 2018). The ALK kinase domain, whose activation triggers downstream signaling cascades, most notably the RAS/MAPK and JAK/STAT pathways, is typically included in these fusion proteins.

In neuroblastoma, ALK activation mutations and amplifications were identified years ago (Carén et al., 2008). Multiple ALK activation mutations, including hotspot residues in the kinase domain like R1275, F1174, and F1245, have been reported. Both germline and somatic activating mutations contribute to oncogenesis (Carén et al., 2008; Chen et al., 2008; Janoueix-Lerosey et al., 2008). Additionally, truncated activated ALK mutants, including various deletions, have been found in cell lines and tumor samples. These truncations result from genomic rearrangements and play a significant role in driving neuroblastoma pathogenesis, often synergizing with other proteins like MYCN. Using transgenic mice, researchers have shown that MYCN and ALK signaling lead to the onset of neuroblastoma (Berry et al., 2012). Beyond neuroblastoma, ALK amplifications and copy number gains have been observed in other cancers, including rhabdomyosarcomas (Corao et al., 2009). Since the discovery of ALK fusions in 1994,

several other fusions of ALK have been discovered. In 2008, discoveries of ALK mutations in pediatric neuroblastoma introduced another pathway for oncogenic activation of ALK, predominantly through point mutations in the intact receptor tyrosine kinase. While ALK overexpression has been observed in various human tumors and cell lines its role in initiating or progressing tumors remains largely unverified.

There are 30 different partners identified in ALK fusion proteins. Although several fusion proteins have been studied experimentally, only a handful have been studied, including NPM-ALK in ALCL and EML4-ALK in NSCLC. It is noteworthy that transgenic models driven by NPM-ALK in ALCL and EML4-ALK in NSCLC have been created. ALK fusions are found in only approximately 5% of NSCLC cases, but the sheer number of patients with NSCLC makes EML4-ALK the most common type of ALK gene rearrangement, accounting for 40,000 new cases annually (Huang, 2018).

Studies on ALK fusion proteins have highlighted several fundamental ideas, one of which is the importance of oligomerization, which is made possible by ALK's fusion partners. Different ALK fusion proteins react differently to ALK tyrosine kinase inhibitors (TKIs), exhibiting different stabilities and sensitivities. The finding of several variants for certain ALK fusions (e.g., over 15 variants have been documented for EML4-ALK in NSCLC adds to the complexity. Different ALK fusions can occur; however, within tumor subtypes, some fusions might be more common than others. Adenocarcinoma-type NSCLC patients who are younger and do not smoke have higher levels of ALK fusion proteins. Most ALK-positive cases in NSCLC are caused by the primary fusion EML4-ALK, while other fusions like KIF5B-ALK, TFG-ALK, and others have also been

documented. On the other hand, NPM-ALK is the major characteristic of ALCL in more than 50% of cases, however, other variations have also been reported (Huang, 2018).

Chapter 1.10 ALK inhibitors

In 2007, Soda et al. discovered the EML4-ALK fusion oncogene in a non-small-cell lung cancer patient. This fusion of EML4-ALK promotes the growth and survival of cancer cells. The fusion protein locks ALK in an activated state and upregulates its kinase activity. Several forms of abnormal ALK activity have been observed in different cancers. ALK inhibitors were developed to treat patients with abnormal ALK activity and ALK fusions.

One of the first ALK inhibitors to be developed was crizotinib. Crizotinib was initially developed as a c-Met inhibitor, but it also targets ALK, ROS1, and MET. It was fast-tracked by the FDA in 2011 based on promising early trial results, showing substantial response rates and median progression-free survival improvements in ALK-positive patients. Subsequent phase III trials comparing crizotinib with standard chemotherapy solidified its position as the first-line treatment for ALK-positive NSCLC (Kwak et al., 2010).

Resistance posed a challenge to ALK inhibitors. Ceritinib and alectinib were developed to combat the problem of resistance. Both inhibitors effectively decreased the activity of ALK and could easily access the central nervous system. Prolonged improvements were observed in patients treated sequentially with crizotinib and a second-generation inhibitor. Comparisons between ceritinib and crizotinib showed that the second-generation inhibitor was more effective than crizotinib (Friboulet et al., 2014). In addition, ceritinib was effective in patients

who had developed crizotinib resistance (NCT01283516). Ceritinib was approved for the treatment of ALK-positive NSCLC because of its effectiveness in both patient groups, including those with brain metastases.

The other second-generation inhibitor, Alectinib, like ceritinib, showed promising results in treating NSCLC that had become resistant to crizotinib. Alectinib is a strong tyrosine kinase inhibitor that inhibits both ALK (IC50 = 1.9 nM) and RET (IC50 = 4.8 nM), and its main metabolite M4 has a similar profile (Kinoshita et al., 2012). Alectinib suppresses ALK autophosphorylation, phosphorylation of STAT3 and ALK, and growth inhibition of cell lines expressing activating mutations, fusions, or amplifications of ALK. In addition, alectinib suppresses tumor cell growth of NSCLC cell lines, including those with the ALK L1196M gatekeeper mutation (Sakamoto et al., 2011). Alectinib cannot bind the efflux transporters P-glycoprotein (P-gp) or breast cancer resistance protein (BCRP). Being unable to bind P-gp or BCRP allows for alectinib to cross the blood brain barrier to treat central nervous system ALK-positive tumors (Hu et al., 2016). Like ceritinib, Alectinib exhibits activity against crizotinib-resistant mutations and has unique CNS penetration due to its transport properties. Although initially effective, treatment with Alectinib can still lead to the onset of resistance mechanisms.

Despite the emergence of resistance, alectinib's CNS penetration, potency against ALK and RET, and safety profile allow for alectinib to be a valuable therapeutic for treating ALK-positive NSCLC. The pharmacokinetic profile of alectinib was established by using patients with ALK-positive NSCLC and healthy individuals. When taken orally, alectinib is rapidly absorbed and reaches peak plasma concentrations in individuals in 4-6 hours. Seven days of continuous dosage are required to reach steady-state concentrations. Alectinib should be given with meals

because a high-fat, high-calorie meal can quadruple exposure to the drug as compared to fasting settings. A significant volume of distribution indicates that alectinib and its primary metabolite, M4, have strong plasma protein binding and widespread tissue distribution. Alectinib enters the central nervous system but not M4. Plus, the pharmacokinetics of alectinib are unaffected by age, race, sex, body weight, or mild to moderate renal impairment (Agency, 2018).

Alectinib was found to be an effective first-line treatment for ALK-positive non-small cell lung cancer. The phase III J-ALEX research conducted in Japan demonstrated that patients who received alectinib 300 mg twice daily had a significantly greater PFS than those who received crizotinib 250 mg twice daily (Hida et al., 2017). The ALEX trial conducted in the EU and USA for patients with advanced ALK-positive NSCLC compared the efficacy of alectinib with crizotinib. Alectinib dramatically shortened the time to CNS progression, decreased the probability of disease progression or mortality, and increased PFS when compared to crizotinib. In addition, the 12-month cumulative incidence rate of CNS development was considerably reduced in the alectinib treated groups. While stable illness was more prevalent in the crizotinib group, there was no meaningful difference in ORR between the alectinib and crizotinib groups in the intent-to-treat population (Camidge et al., 2019).

Among the next-generation ALK inhibitors with significant preclinical efficacy in overcoming ALK resistance mutations are brigatinib and lorlatinib. Both have shown significant intracranial efficacy and clinically significant activity, which suggests they may be useful in treating patients who become resistant to conventional ALK inhibitors. Brigatinib targets ALK, ROS1, and EGFR and has shown promising crizotinib resistant mutations (Zhang et al., 2016). In

phase I/II clinical trial (NCT01449461) with participants with advanced cancer types, brigatinib demonstrated notable efficacy and a tolerable safety profile for both patients previously treated with crizotinib and those who had not received any ALK inhibitors (Gettinger et al., 2016). Of these, a significant majority (58%) were diagnosed with ALK-positive NSCLC. According to the study, patients who had previously had crizotinib treatment had a verified objective response rate of 62%, while individuals who had not received crizotinib treatment had an ORR of 100%. Furthermore, the group that had previously gotten crizotinib had a median PFS of 13.4 months, whereas the group that had not received crizotinib showed an undefinable PFS (Gettinger et al., 2016). Similar results were also seen for patients with NSCLC and positive for the oncogene ROS1 treated with lorlatinib. In phases I and II, patients were given twice-daily dosages of lorlatinib, and doses were increased for 21-day cycles. In phase II, lorlatinib treatment was continuous for 21-day cycles at a starting dose of 100 mg once daily. In both phases, researchers were able to see that lorlatinib was able to cross the blood brain barrier. In addition, lorlatinib was effective against crizotinib resistant cancers (Chen et al., 2021).

Entrectinib is effective in inhibiting several RTKs through its metabolite. Entrectinib inhibits ALK, ROS1, and nTRKs, but M5, the main active circulating metabolite of entrectinib, has potency and activity against several targets that are like entrectinib. Entrectinib was found to be substantially more effective than crizotinib against ROS1-dependent cells in preclinical assessments. It also effectively inhibited the proliferation of human tumor cell lines driven by nTRK1 or ALK fusions (Information, 2019). Additionally, it showed anticancer action and caused tumor regression in a variety of xenograft models containing fusions of nTRK, ROS1, or ALK, as well as in cell lines that had mutations in the nTRK1 kinase domain that made them resistant to

other TRK inhibitors (Drilon et al., 2017). Entrectinib's ability to bind to P-glycoprotein (P-gp) weakly makes it a valuable tool for prolonged central nervous system exposure. Entrectinib consistently showed a better ratio of unbound concentrations in the CSF to plasma, suggesting that it may penetrate the CNS efficiently (Fischer et al., 2020). This ability was subsequently shown in vivo when human tumor cell lines driven by nTRK or ALK fusions were intracranially injected into mouse models, and entrectinib suppressed tumor development and increased survival (Fischer et al., 2020). Entrectinib is mostly metabolized by CYP3A4, which forms M5. Uridine 5′-diphosphate-glucuronosyltransferase 1A4 then conjugates the drug to generate its N-glucuronide conjugate (M-11) (Drilon et al., 2017). The pharmacokinetic characteristics of entrectinib are mostly unchanged with respect to age, gender, body mass, ethnicity, mild to severe renal impairment, or mild hepatic impairment (Drilon et al., 2017).

Entrectinib has shown promising results in adult patients with inoperable or metastatic nTRK-positive solid tumors and ROS1-positive non-small cell lung cancers. Furthermore, entrectinib has been shown to work in tumors that have migrated to the central nervous system. These results were shown in several studies, including the one Phase II global basket trial (STARTRK-2) and the two Phase I trials (ALKA-372-001 and STARTRK-1) (Doebele et al., 2020). The phase I/II trials (ALKA-372-001, STARTRK-1, -2, and -NG) showed that entrectinib was generally well tolerated in patients with minimal side effects, and almost all patients showed a similar safety profile. In total, 504 individuals, including 475 adults, received entrectinib at least once and were exposed for a median of 5.5 months to test the safety profile of entrectinib. In summary, Entrectinib was effective at inhibiting tumor growth and crossing the blood brain

barrier, with minimal off-target side effects. Unfortunately, the onset of resistance mechanisms to entrectinib has been recently reported.

Chapter 2: Methods and materials used to determine the function of ALK receptor and its inhibitors in NEPC

Chapter 2.1 Current understanding of ALK in Neuroendocrine prostate cancer

Multiple variants of anaplastic lymphoma kinase receptors have been identified in various types of cancer, including breast, lung, and brain. However, knowledge about the role of ALK in NEPC is limited. Until now, only three studies have been conducted on this topic. The first study, published in 2018, suggested that ALK may have a role in NEPC treatment. The study found that a patient with small cell carcinoma of the prostate responded positively to ALK inhibitor treatment and expressed a specific mutant of ALK known as F1174C (Carneiro et al., 2018). The second study conducted by the same group of researchers followed up on the first study and demonstrated that the F1174C mutant of ALK functions with N-Myc to induce transdifferentiation of a mouse basal stem cell into an aggressive prostate cancer cell with neuroendocrine differentiation (Unno et al., 2021). The last study expanded on the understanding of ALK and NEPC by exploring current published RNA seq data of NEPC patient samples. The RNA seq data analyzed demonstrated that changes in ALK expression are rare in primary prostate cancer, but changes in ALK expression become more common in metastatic prostate cancer with neuroendocrine prostate differentiation (Patel et al., 2022).

For this thesis project, the current understanding of ALK and NEPC is expanded. To expand the understanding of ALK and NEPC, several NEPC cells were collected and treated with ALK inhibitors and assayed for cell viability and colony formation. De novo NEPC Tumor was implanted in mice and treated with ALK inhibitors, and then RNA samples were collected from cells and tumors for RNA sequencing. Cells treated with ALK inhibitors showed decreased cell growth and proliferation. Tumor treatment with ALK inhibitors also reduced tumor growth and mass. RNA sequencing of NEPC tumors and cells revealed that several pathways involved in cellular migration and proliferation are inhibited with ALK inhibitor treatment.

Chapter 2.2 Methods and materials

Cell culture

C4-2B, C4-2Benzer, and 42D prostate cancer cells were cultured in RPMI1640 with 10% FBS and 10mM enzalutamide and 20mM enzalutamide for 42D and C4-2Benzr respectively; NCI-H660 cells were cultured in HITES medium (RPMI1640 medium plus 0.005mg/ml Insulin, 0.01mg/ml Transferrin, 30nM Sodium selenite, 10nM Hydrocortisone, 10nM beta-estradiol and 2mM L-glutamine) with 5% FBS. Cells were grown at 37 °C in 5% CO2 incubators. C4-2B was from UroCor Inc. C4-2Benzr was generated in the lab. Cell lines were regularly tested to ensure negativity for mycoplasma.

Chemicals

Sources for chemicals are as follows: Alectinib (Cat: HY-13011) and entrectinib (Cat: HY-12678) were obtained from Med Chem Express (MCE); CM 272 (Cat: HY-101925) was obtained from Med Chem Express. Other chemicals are from Sigma-Aldrich, unless indicated otherwise.

qRT-PCR and immunoblotting analysis

Total RNA was isolated from cells six-well or 10-cm plates or from xenograft tumors, and cDNA was prepared, amplified, and measured in the presence of SYBR, as previously described. Briefly, the fluorescence values were collected, and a melting-curve analysis was performed. The fold difference was calculated as described previously. ± s.d. Cell lysates were analyzed by immunoblotting with antibodies specifically recognizing ALK (Cat: 3633), STAT3 (Cat: 12640), pSTAT3 (Cat: 9145), ERK1/2 (Cat: 9102), pERK1/2 (Cat: 4370), SYP (Cat: 36406), NSE (Cat: 24330), and BRN2 (Cat: 12137), and the indicated proteins. All antibodies used were obtained from Cell signaling technologies.

Cell viability, apoptosis and growth assays, and colony formation

For cell viability, cells were seeded in 96-well plates at 1,500–2,500 cells per well (optimum density for growth) in a total volume of 100 µl of media. Serially diluted compounds in 100 µl of media were added to the cells 24 h later. After 4-5 days of incubation, Cell-Titer GLO reagents (Promega) were added, and luminescence was measured on a GLOMAX microplate luminometer (Promega), according to the manufacturer's instructions. All experimental points were set up as sextuplicates as biological replication, and the entire experiment was repeated three times. The data are presented as a percentage of viable cells,

with vehicle-treated cells set at 100. The estimated in vitro half-maximal inhibitory concentration (IC50) values were calculated using GraphPad Prism 10 software (GraphPad).

For cell growth, cells were seeded in 6-well plates at 2×10^5 per well and treated as indicated. Total viable cell numbers were counted with a Coulter cell counter. For colony formation, 1000-2000 cells were seeded in a well of 6-well plates and cultured for 6d- 15d, with the medium changed every 3d. Cell colonies were collected after the time indicated, the medium was removed, and the cells were fixed with 10% formalin for 10 min. Then, the plates were washed with PBS two times, and the cell colonies were stained with 0.2% crystal violet (in 10% formalin) for 15 min. The numbers of cell colonies were counted using image j. The above assays were performed in triplicates, and the entire experiment was repeated three times.

RNA-seq data analysis

42D cells were treated with vehicle, alectinib, entrectinib, CM 272, or a combination of either CM 272 and alectinib or CM 272 and entrectinib. Treatment lasted for 24 and 48 hours before RNA extraction. RNA-seq libraries from 1 µg total RNA were prepared using Illumina Tru-Seq RNA Sample, according to the manufacturer's instructions. Libraries were validated with an Agilent Bioanalyzer (Agilent Technologies, Palo Alto, CA). Sequencing was performed on an Illumina HiSeq 2000 sequencer at BGI Tech (Hong Kong) and Novogene. The FASTQ-formatted sequence data were analyzed using a standard BWA-Bowtie-Cufflinks workflow59,60,61. In brief, sequence reads were mapped to the reference human-genome assembly (Feb. 2009, GRCh37/hg19) with BWA and Bowtie software. Subsequently, the Cufflinks package62 was applied for transcript assembly, quantification of normalized gene and isoform expression in

RPKM (reads per kilobase per million mapped reads) or FPKM (fragments per kilobase of exon model per million mapped reads), and testing for differential expression (Cuffdiff). To avoid spurious fold levels resulting from low expression values, only those genes with expression RPKM or FPKM values of >1 for either the vehicle control cell or the antagonist-treated cells (but need not be both) are included. The expression changes of at least 1.5-fold up or down were clustered with the k-means clustering algorithm in Cluster software63. The cluster was displayed with TreeView.

GSEA analysis

GSEA was performed using the Java desktop software (http://software.broadinstitute.org/gsea/index.jsp). Genes were ranked according to the shrunken limma $\log_2$ fold changes, and the GSEA tool was used in 'pre-ranked' mode with all default parameters. Previously reported genes in each analyzed pathway were analyzed using the RNA seq data.

Xenograft tumor models and chemical compound treatments

Four-week-old male mice (strain: C.B-17/scid) or athymic nude mice were purchased from Envigo, Inc. For establishing tumors, tumor fragments of NCI-H660 or LuCaP 173.1 were implanted. An animal group size of six or more was estimated to have a high statistical power, according to the power calculation (http://www.biomath.info/power/). When the tumor volume was approximately 50-150 mm3, the mice were randomized and then treated intraperitoneally (i.p.) or via oral gavage with vehicle (90% corn oil 10% DMSO), entrectinib

(oral gavage), alectinib (oral gavage), CM 272 (i.p.) 7 times a week for 30 days or until tumor reached 2cm in length. Tumor growth was monitored by calipers, and volume was calculated with the equation $V = \pi/6$ (length × width2). Body weight during the study was also monitored. At the end of the studies, mice were euthanized, and tumors were dissected and weighed. Mice were excluded from the study if they had no tumor or a tumor with a size twice as large or as small as the mean at the time of randomization.

Statistical analysis.

Cell culture–based experiments were performed three times or more, with assay points triplicated or sextuplicated, as indicated. The data are presented as mean values ± s.d. from three independent experiments. Statistics analysis was performed using two-tailed Student's t-tests to compare the means. $P < 0.05$ was considered to be significant.

Chapter 3: Characterization of ALK receptor and ALK inhibitors in NEPC

Chapter 3.1 ALK inhibitors inhibit NEPC cell growth and survival

Recent research indicates that ALK inhibitors can effectively inhibit the growth of NEPC tumors. Treatment with the ALK inhibitor alectinib has been shown to be successful in patients with ALK mutations in other cancer types. Previous research has also shown that crizotinib and ceritinib, both ALK inhibitors, can inhibit the growth of NEPC cells. Screening for compounds that could inhibit NEPC cell growth, it was observed that the nTRK/ALK/Ros1 inhibitor entrectinib blocked the growth of NCI-H660 cells. To validate that ALK inhibitors could inhibit NEPC cell growth, several prostate cancer cell lines were treated with the ALK inhibitors entrectinib and alectinib.

The results of the assays showed that treatment with ALK inhibitors effectively inhibited the proliferation and survival of NEPC cells. We tested several ALK inhibitors and found that alectinib and entrectinib were effective in blocking NEPC survival, with IC50 values ranging from 1.5-3.0 μM depending on the cell type (Figure 1a). However, lorlatinib did not show any response in the cells. Alectinib was found to block cell survival in both de novo and treatment

induced NEPC cells (Figure 1b). We also observed a decrease in colony formation when treated with alectinib using the colony formation assay (Figure 1c). These results confirm previous findings that ALK inhibitors can be used to block NEPC growth effectively. More importantly, alectinib and entrectinib could function as potential therapeutics for NEPC.

Chapter 3.2 Entrectinib and alectinib inhibit ALK signaling pathways in induced NEPC cells

It is known that the growth and survival of cancer cells can be influenced by ALK signaling. ALK is known to activate the RAS/MAPK and JAK/STAT pathways in different types of cancer, such as breast, lung, and prostate cancer. NEPC has also been reported to have these pathways activated. The next goal of the experiment was to verify whether entrectinib and alectinib can inhibit these pathways in NEPC and prostate cancer cells.

To answer this question, we conducted experiments using 42D, NCI-H660, and C4-2Benzr cells and treated them for 48 hours. We chose these specific cell types because they represent treated-induced (42D and C4-2Benzr) and de-novo NEPC (NCI-H660). ALK was found to be present in 42D and C4-2Benzr cells but absent in NCI-H660 (Figure 2). We also found that pSTAT3 is downregulated in all three cell types, and pERK1/2 is downregulated in C4-2Benzr and NCI-H660. Additionally, the expression of neuroendocrine markers such as CHGA and BRN2 is downregulated in 42D cells (Figure 2 a & b). However, in the case of NCI-H660, GAPDH is also downregulated, which presents a confounding issue (Figure 2. C).

Through observations, it was noted that ALK expression varies among different NEPC cell lines. ALK expression in NCI-H660 is low when compared to 42D and C42B-enzr. ALK

expression was not detected in the NCI-H660 cell line. Multiple attempts were made using different methods to detect ALK but were unsuccessful. In contrast, C4-2Benzr cells showed easily detectable ALK expression compared to 42D and NCI-H660. It is crucial to note that the proliferation rate of C4-2Benzr is double that of 42D and significantly faster than NCI-H660. Although ALK was not detected in NCI-H660, it was observed that these cells are more sensitive to alectinib and entrectinib treatment. These cells had a lower IC50 to alectinib and entrectinib when compared to 42D. More importantly, the MAPK and STAT3 pathways are active in NCI-H660 cells, which is why a decrease in growth is observed after treatment with ALK inhibitors.

Chapter 3.3 Entrectinib, alectinib, and CM 272 inhibit NEPC tumor growth

It was observed that ALK inhibitors, alectinib, and entrectinib, could inhibit NEPC cell growth in vitro. The next goal of the experiment was to determine if entrectinib and alectinib could inhibit NEPC tumor growth. Two de-novo NEPC tumor models were used: NCI-H660 and LuCaP 173.1. Mice were implanted with NEPC tumors, de-novo NCI-H660 tumors, or LuCaP 173.1 tumors and tumors were allowed to grow until they reached a size of 50-150mm3. Then, treatment with entrectinib, alectinib (oral gavage), or CM 272(IP) began. We treated the animals for 30 days and took measurements of mouse mass and tumor volume every three days. After treatment, tumors were harvested and weighed and then sent for RNA sequencing to Novogene.

ALK inhibitor treatment resulted in decreased tumor growth. Treatment with alectinib at 30mg/kg was effective at blocking NCI-H660 tumor growth. Similarly, CM 272 treatment was

also effective at blocking NCI-H660 growth (Figure 3a). The combination treatment of both drug types was significantly different from vehicle treatment alone but not significantly different from a single dose of CM 272(Figure 3a). Tumor mass was significantly different when compared to the vehicle for CM 272 and combination treatment (Figure 3a). However, we noted that body weight significantly decreased for the combination treatment.

Treatment of LuCaP 173.1 tumors with alectinib and entrectinib showed promising results. The low doses of entrectinib and alectinib were not very effective at blocking LuCaP 173.1 tumor growth (figure 3b). Treatment with CM 272 significantly inhibited tumor growth when compared to the vehicle. The combination treatment of alectinib with CM 272 or entrectinib with CM 272 was significantly different when compared to the vehicle. The tumor mass of both combination treatments was significantly different when compared to the vehicle (Figure 3B).

It is important to note that the tumor experiment involving NCI-H660 did not include entrectinib, and the doses for alectinib were higher. As mentioned earlier, both compounds target ALK and ROS1, but entrectinib also targets nTRKs. It was early that both alectinib and entrectinib had similar effects and similar IC50s in cells, which is why only alectinib was tested in NCI-H660 tumors. Later, it was revealed that entrectinib was better at inhibiting organoid growth than alectinib. Hence, it was decided to test in LuCaP 173.1 tumors.

Chapter 3.4 ALK inhibition downregulates cellular pathways associated with ALK and neuroendocrine signaling

As previously shown in Figures 1 and 3, alectinib and entrectinib can inhibit the growth of several NEPC and prostate cancer cell lines, as well as de-novo NEPC tumor growth, including LuCaP 173.1 and NCI-H660. To further investigate the cellular effects of ALK inhibition in NEPC cell and tumor growth, I conducted RNA sequencing.

To study the effects of alectinib and entrectinib on NEPC, the well-established and characterized 42D cell line was used. After treating the 42D cells with alectinib, entrectinib, or vehicle for 48 hours, RNA was isolated and sent for RNA sequencing. FPKM values were used to analyze RNA seq. Genes showing a 1.5-fold change in decreased expression were isolated. Afterward, the NIH tool, David, was used to determine which kegg cellular pathways were altered. Changes in the Neuroactive ligand-receptor interactions, cytokine to cytokine receptor interaction, JAK/STAT, aldosterone sodium reabsorption PI3K-AKT pathways were predicted to be altered in 42D cells treated with alectinib, entrectinib, and CM 272(Tables 1-3). These pathways are crucial for the proliferation and growth of cancer cells and have been implicated in several distinct cancers, including breast, lung, and prostate cancer, and will be discussed in greater detail.

For this study on the effects of ALK inhibition on NEPC cells, the focus was only on downregulated genes after the treatment. The reason for focusing on downregulated pathways is that it has been previously shown that RTK inhibition, specifically ALK inhibition, downregulates genes that support tumorigenesis. More importantly, ALK inhibition has been shown to inhibit these gene programs in other types of cancers, including breast and lung cancer.

42D cells treated with entrectinib, alectinib, and CM 272 showed changes in the Neuroactive ligand-receptor interaction pathway (NLRIP). The neuroactive ligand-receptor interaction signaling pathway is composed of receptors and ligands on the plasma membrane that are associated with extracellular and intracellular signaling. Bioinformatics analysis has revealed that the neuroactive pathway is involved in the progression of several cancers, including bladder, prostate, and renal cell carcinoma. To validate that the Neuroactive ligand-receptor interaction pathways were downregulated, a heatmap of genes associated with the pathway was generated using the RNA seq data. A total of 39 genes in the NLRIP pathway were altered after treatment (Figure 4A).

A closer look revealed that several genes in the neuroactive ligand-receptor interaction pathway were downregulated with all three treatments. The first gene that was downregulated was the nuclear receptor subfamily 3 group C member 1 (NR3C1) (Figure 4A). The gene encodes a glucocorticoid receptor that could also function as a transcription factor. The receptor is localized to the cytoplasm of cells, but once the ligand has bound, it is internalized and transported to the nucleus. NR3C1 is involved in several cellular pathways, including the inflammatory response, cellular proliferation, and differentiation. NR3C1 has been found to have low expression in prostate cancer (Morales et al., 2022). More interestingly, NR3C1 expression increases in patients who develop resistance. Furthermore, NR3C1 expression increases in patients treated with either arbiraterone or enzalutamide (Smith et al., 2020). In other cancers, NR3C1 has been found to activate anti-apoptotic pathways in breast cancer (West et al., 2016). More recently, it was revealed that inhibition of the NR3C1 decreased cellular proliferation and migration of renal cell carcinoma (Yan et al., 2023). Another gene that

was downregulated with all three treatments was glutamate ionotropic receptor AMPA type subunit 2 (GRIA2) (Figure 4A). Glutamate receptors are excitatory neurotransmitter receptors localized in the mammalian brain and are activated in several distinct physiological processes. Interestingly, the expression of GRIA2 and other glutamate receptors has been detected in several cancers, including prostate cancer. In prostate cancer serum, elevated levels of glutamate have been detected and have been correlated with Gleason score and prostate cancer aggressiveness. In addition, glutamate inhibition, or deprivation, decreased cellular growth, migration, invasion, and increased cell death (Kissick et al., 2015). Interestingly, in cancer, GRIA2 is a diagnostic cellular marker that detects solitary fibrous tumors. Gene knockdown of GRIA2 in lung cancer cells decreased proliferation and increased cell death (Rudin et al., 2012). Another gene that demonstrated decreased expression with all three treatments was 5-hydroxytryptamine (serotonin) receptor 5A (HTR5A) (Figure 4A). HTR5A serotonin receptor that binds to serotonin and helps regulate intracellular calcium levels. Inhibition of HTR5A had cytotoxic effects in prostate cancer cells. Interestingly, HTR5A expression increased in NEPC tumors after being grown in hypoxic conditions (Labrecque et al., 2019). HTR5A inhibition decreased breast cancer tumorsphere formation in breast cancer cell lines and patient-derived xenografts v(Gwynne et al., 2020). Several other genes in the NLRIP gene program showed decreased expression in alectinib and entrectinib treatment but not CM 272 and vice versa (Figure 4A).

Another pathway that was downregulated is the cytokine-to-cytokine receptor interaction pathway (Figure 4B). Cytokines are critical intracellular regulators and activators of cells involved in innate and adaptive immunity. Cytokine signaling is associated with host immunity, cell

growth, differentiation, apoptosis, angiogenesis, development, and restoration of homeostasis. Changes in the cytokine-to-cytokine receptor interaction pathway have been detected in prostate, breast, and colorectal cancers.

Several genes in the cytokine-to-cytokine receptor interaction pathway were downregulated with all three treatments of alectinib, entrectinib, and CM 272. Ciliary neurotrophic factor (CNTF) had decreased expression with all three treatment conditions (Figure 4B). CNTF is a part of the interleukin 6-type cytokine family. CNTF is a polypeptide hormone and neurotrophic factor that promotes neurotransmitter synthesis and neurite outgrowth within certain neuronal cell populations. In addition, CNTF is an important survival factor for neurons and oligodendrocytes. Using prostate cancer cell lines, researchers have found that CNTF has a role in CRPC environment remodeling and functions as a negative modulator of invasion processes (Fantone et al., 2020). More importantly, it seems that CTNF prevents cellular invasiveness by inhibiting several cellular pathways, including MAPK/ERK, PI3K/AKT, and JAK/STAT pathways (Tossetta et al., 2022). How CTNF functions in NEPC remains unclear; as mentioned earlier, data suggests IL-6 helps promote neuroendocrine differentiation in prostate cancer. CNTF has been shown to promote the transformation of astrocytes to neuroectodermal tumor cell lines in vitro (Taylor et al., 2023). CNTF and CNTFa receptor expression have been detected in human glioma cells. Another two genes that were downregulated by all three treatments were C-X-C motif chemokine 17 (CXCL17) and its receptor CXCR2(Figure 4B). CXCR2 and CXCL17 expression have been detected in primary prostate tumors and neuroendocrine prostate cancer. Evidence suggests that both CXCR2 and CXCL17 help promote prostate cancer growth and proliferation (Li et al., 2019a). The inhibition

of CXCL17 in breast cancer cell lines decreased proliferation and migration. More importantly, expression of CXC17 was associated with poor prognosis and lower survival in breast cancer (Hsu et al., 2019). In lung cancer, CXCL17 may be involved in the migration of lung cancer cells to the spine via Src/FAK signaling. Another gene that was downregulated by all three treatments was C-X-C motif Chemokine receptor 1 (CXCR1). CXCR1 is a g protein-coupled receptor that binds to interleukin 8 (IL8). Once CXCR1 binds to its ligand, it initiates a second messenger signaling cascade, which has been shown to inhibit embryonic oligodendrocyte precursor migration to the spinal cord. CXCR1, like CXCR2, helps promote prostate cancer cell growth and proliferation (Armstrong et al., 2020).

The next two pathways that showed decreased expression were the phosphatidylinositol 3-kinase (PI3K)/Akt and the JAK/STAT pathways (Figure 4 C&D). The PI3K/Akt pathway promotes cellular metabolism, proliferation, survival, growth, and angiogenesis. The JAK/STAT signaling pathway is critical for immunity, cell division, apoptosis, and tumor formation. PI3K/Akt signaling has been found to be perturbed in almost all human cancers, including lung, breast, colorectal, and prostate cancer. Constitutive activation of the JAK/STAT pathway is thought to contribute to the proliferation, metastasis, and survival of several distinct tumor cells. Overactivation of the JAK/STAT pathway has been shown to occur in breast, lung, pancreatic, and liver cancer.

A closer examination of both pathways revealed that several genes were downregulated with all three treatments. A critical gene that was downregulated with all three treatments in the PI3K/AKT pathway is T-cell Lymphoma/Leukemia 1B (TCL1B) (Figure 4C). TCL1B interacts with Akt and amplifies Akt kinase activity, functioning as a coactivator of Akt. The expression of

TCL1B is tightly regulated, and its expression is mostly during early development and maturing immune cells. Research of TCLB in prostate cancer is limited, but the activity of this protein has been observed in other cancers. Activity of TCL1B in the abnormal expression of TCL1B has been detected in T cell leukemias. It is thought to contribute to the pathogenicity of T cell leukemia by activating survival and proliferation cellular pathways (Haas et al., 1984). Another gene that showed decreased expression is Guanine nucleotide-binding protein subunit g8 (GNG8) (Figure 4C). GNG8 is a heterotrimeric G protein that is activated by G protein-coupled receptors. Normally, the heterotrimeric subunits a/b/g help mediate the cellular responses to extracellular signals. GNG8 expression has been detected in different regions of the rodent brain, including the olfactory, vomeronasal, and habenula. Altered expression of G protein subunits has been detected in prostate and lung cancer (El-Haibi et al., 2013). Research on GNG8 in cancer is limited, and it can present a new potential therapeutic target. PCa cells express several distinct G protein subunits, but GNG8 expression has not been reported. More interestingly, it seems GNG8 expression is detectable in 42D NEPC cells. Phosphoenolpyruvate carboxykinase 1 (PCK1) is another gene that was downregulated with all three treatments (Figure 4C). PCK1 is the central and main regulator of gluconeogenesis in the cell. PCK1 functions by catalyzing the formation of phosphoenolpyruvate from oxaloacetate. PCK1 has been found to help regulate neuroendocrine differentiation in CRPC. Increased expression of PCK1 leads to the increased expression of leukemia inhibitory factor LIF/ZBTB46, which induces the expression of neuroendocrine markers (Wen et al., 2022). In other cancers, PCK1 expression is increased in colon cancer and may help in the metabolic reprogramming of the cancer cell. However,

hepatocellular carcinoma has low expression of PCK1, and low expression of PCK1 hepatocellular carcinoma has been associated with poor prognosis.

The JAK/STAT pathway also showed several genes that were downregulated. Specifically, here, the focus will be on the genes that were downregulated with all three treatments. The first gene that was downregulated with all three treatments was the signal transducer and activator of transcription 5A (STAT5A). In the presence of cytokines and growth factors, STAT5A can become phosphorylated by receptor tyrosine kinases; once phosphorylated, STAT5A can become a homo or heterodimer and then be translocated to the nucleus, where it functions as a transcription factor. STAT5A expression is increased in human prostate cancers but not neighboring prostate tissue. More importantly, siRNA inhibition of STAT5A induces cell death in prostate cancer cells. Inhibition of STAT5A in xenograft prostate cancer tumors decreased incidence and growth (Maranto et al., 2018). STAT5A increased protein expression and STAT5A locus amplification have also been shown to be predictors of recurrence (Haddad et al., 2019). In other cancers, STAT5A has also been shown to help confer resistance.

LuCaP 173.1 tumors were treated with alectinib and entrectinib to study their effects on tumor models. Treatment lasted for 30 days, then RNA was isolated from tumors and sent for sequencing. Analysis of RNA seq data was like 42D data analysis. Like 42D cells alectinib and entrectinib was shown to downregulate the Neuroactive ligand receptor interactions, JAK/STAT, and PI3K-AKT pathways (Figure 5).

A closer look at the Neuroactive ligand-receptor interaction pathway in luCaP 173.1 revealed that most genes analyzed for the pathway were downregulated in all three treatments (Figure 5A). The Neuropeptide VF precursor (NPVF) RNA was downregulated in all three

treatments (Figure 5A). NPVF has been shown to be involved in several physiological processes, including food intake, blood pressure regulation, memory, insulin release, and neural regeneration. NPVF expression has been associated with an increased risk of prostate cancer, and it has also been detected in ovarian cancer. More importantly, altered expression of NPVF is an indicator of increased prostate cancer risk for men with African ancestry (Soh et al., 2023). Another gene that was downregulated in tumors was hypocretin neuropeptide precursor (HCRT). HCRT encodes for two neuropeptides, orexin A and orexin B. These neuropeptides have been associated with the following behaviors: sleep and arousal, metabolism, and cellular homeostasis. Elevated expression of orexin A has been detected in high-grade prostate cancers. Specifically, orexin A expression was elevated but not orexin B. More interestingly, is that DU-145 cells xenograft tumor size was decreased after treatment endogenous treatment with orexin A (Alain et al., 2021). Altered expression of orexin A and B have been detected in other cancers, including breast, colon, and pancreatic.

Most genes analyzed in the JAK/STAT pathway were downregulated with ALK and G9a/DMNT inhibition (Figure 5B). Interleukin 22 (IL22) was downregulated with all three treatments. IL22 is expressed by several distinct immune cells, and its expression is associated with cell survival, proliferation, and expression of antimicrobials. IL22 functions in wound healing and fighting infections against microbes. Unfortunately, cellular mechanisms involved in wound healing could be exploited by cancer cells. IL22 increases migration and invasion of androgen-independent prostate cancer cell lines. In other cancers, evidence suggests that increased expression of IL22 contributes to colorectal cancer stemness of cells. In addition, treatment with IL22 leads to the acquisition of chemoresistance in colorectal cancer. Increased

expression of IL22 has been seen in gastric and pancreatic cancer. Another gene that was downregulated is Growth hormone 1 (GH1) (Figure 5B). GH1 is necessary for the normal growth of the body's bones and tissues. GH1 increased expression has been detected in several cancers, including breast, endometrial, melanoma, and hepatocellular carcinoma. GH has been shown to increase cellular proliferation, survival, EMT transition, and cell migration in several cancers. Several other genes were downregulated in the JAK/STAT pathway, which requires more analysis.

The PI3K/Akt pathway showed several genes downregulated after treatment with alectinib and entrectinib in LuCaP 173.1 tumors. All tumors analyzed showed a decrease in the expression of FMS-like tyrosine kinase 4 (FLT4) RNA. FLT4 encodes for tyrosine kinase receptor that binds vascular endothelial growth factors C and D. This protein is involved in lymphangiogenesis and maintenance of the lymphatic endothelium. FLT4 has been shown to promote cancer angiogenesis and metastasis. Increased expression of FLT4 has been reported in primary prostate cancer. Furthermore, it has been reported that FLT4 expression is associated with prostate lymph node metastasis (Stearns et al., 2004). Inhibition of FLT4 suppressed colorectal cancer cell metastasis (Su et al., 2006). Analysis of gastric cancer cells revealed increased expression of FLT4 and vascular endothelial growth factor C (VEGF-C). More interestingly, VEGF-C was another factor that was downregulated in the PI3K-AKT pathway. VEGFC promotes angiogenesis and endothelial cell growth and increases blood vessel permeability. Increased expression of VEGFC has been detected in several cancers, including leukemia, lymphomas, solid malignant tumors, and prostate cancer (Su et al., 2006). Increased VEGF in tumors has been associated with increased angiogenesis, proliferation, and metastasis.

In prostate cancer, inhibition of VEGFC suppresses cellular growth and migration (Sun et al., 2014).

Figure 1

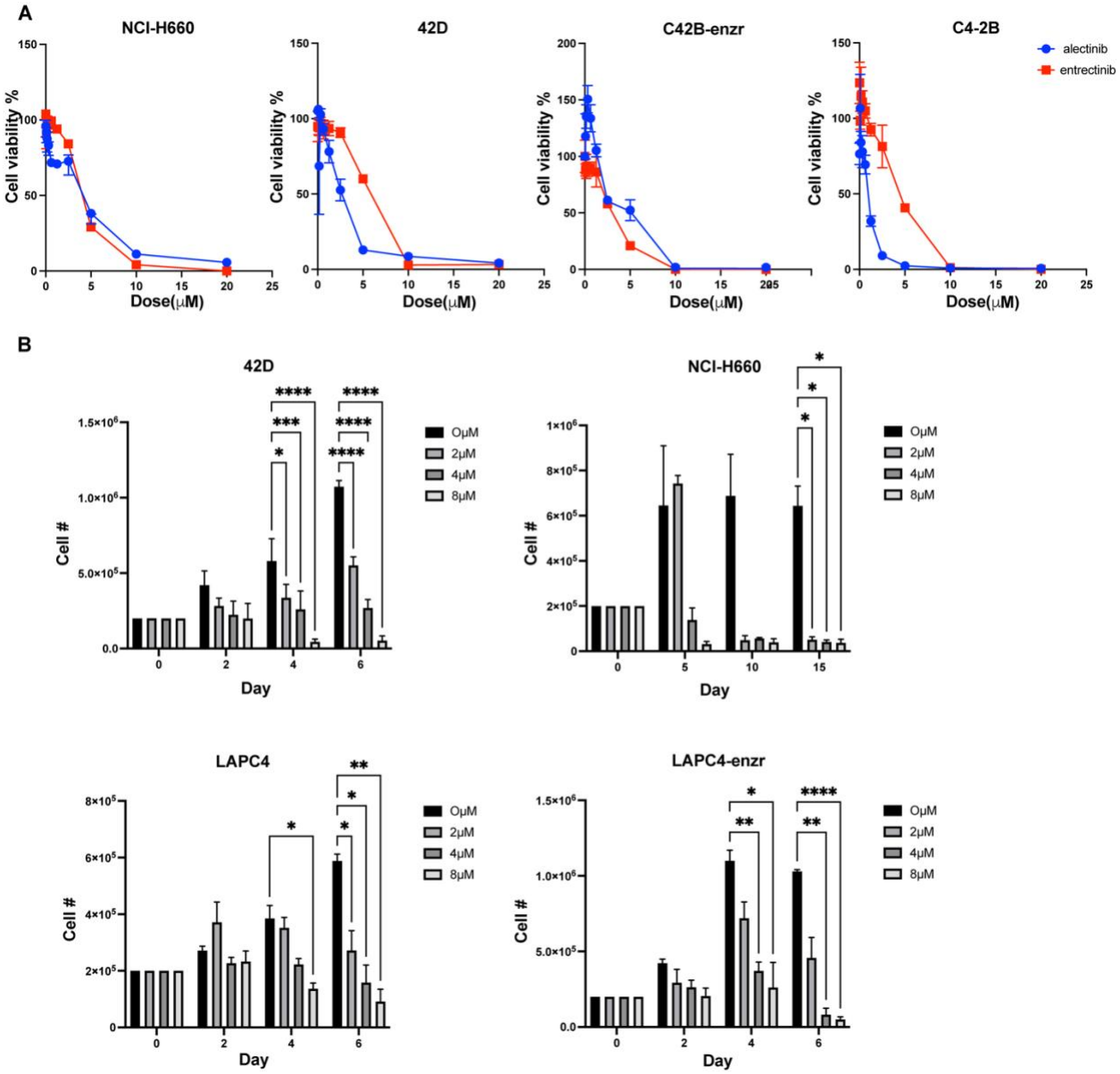
A
NCI-H660
42D
C42B-enzr
C4-2B
alectinib
entrectinib
Cell viability %
Dose(μM)
B
42D
NCI-H660
LAPC4
LAPC4-enzr
Cell #
Day
0μM
2μM
4μM
8μM

Figure 1 continued

C

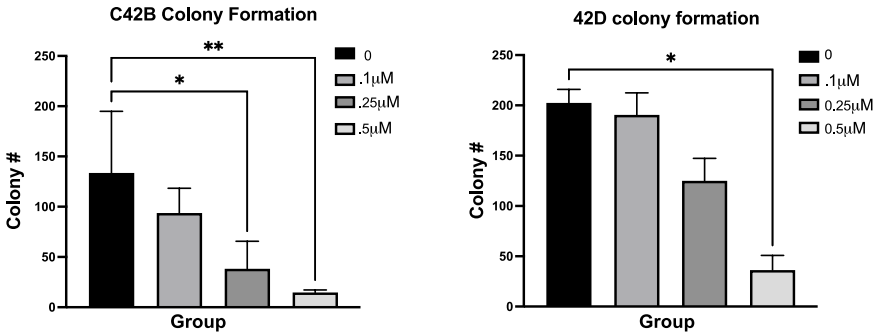

Figure 1. NEPC cell lines that represent treated and de novo NEPC were treated with ALK inhibitors entrectinib and alectinib. Treated and de novo NEPC cell growth and proliferation were inhibited with ALK inhibitor treatment. **A.** Cell viability assay of NCI-H660, 42D, C4-2Benzr, and C4-2B cells. Cells were plated in 96-well plates at a density of 2x103 cells per well. After four days, they were collected and measured. This assay was used to calculate IC50 for entrectinib and alectinib in different cell types. **B.** NCI-H660, 42D, LAPC4, and LAPC4enzr cells were seeded in 6 well plates at a density of 2x105 cells per well. Twenty-four hours after cells were seeded, they were treated with alectinib at the indicated doses. Cells were collected and counted on the days indicated using a cell counter. **C.** C42B and 42D cells were cultured in six-well plates at a density of 2x103 cells per well and treated with the indicated doses of alectinib. Colonies were stained and counted using Image J. The statistical analysis for cell # assay was a Two-way ANOVA where $p<0.05$. A One-way ANOVA multiple comparison was used for the colony formation assay where $p<0.05$.

Figure 2

A

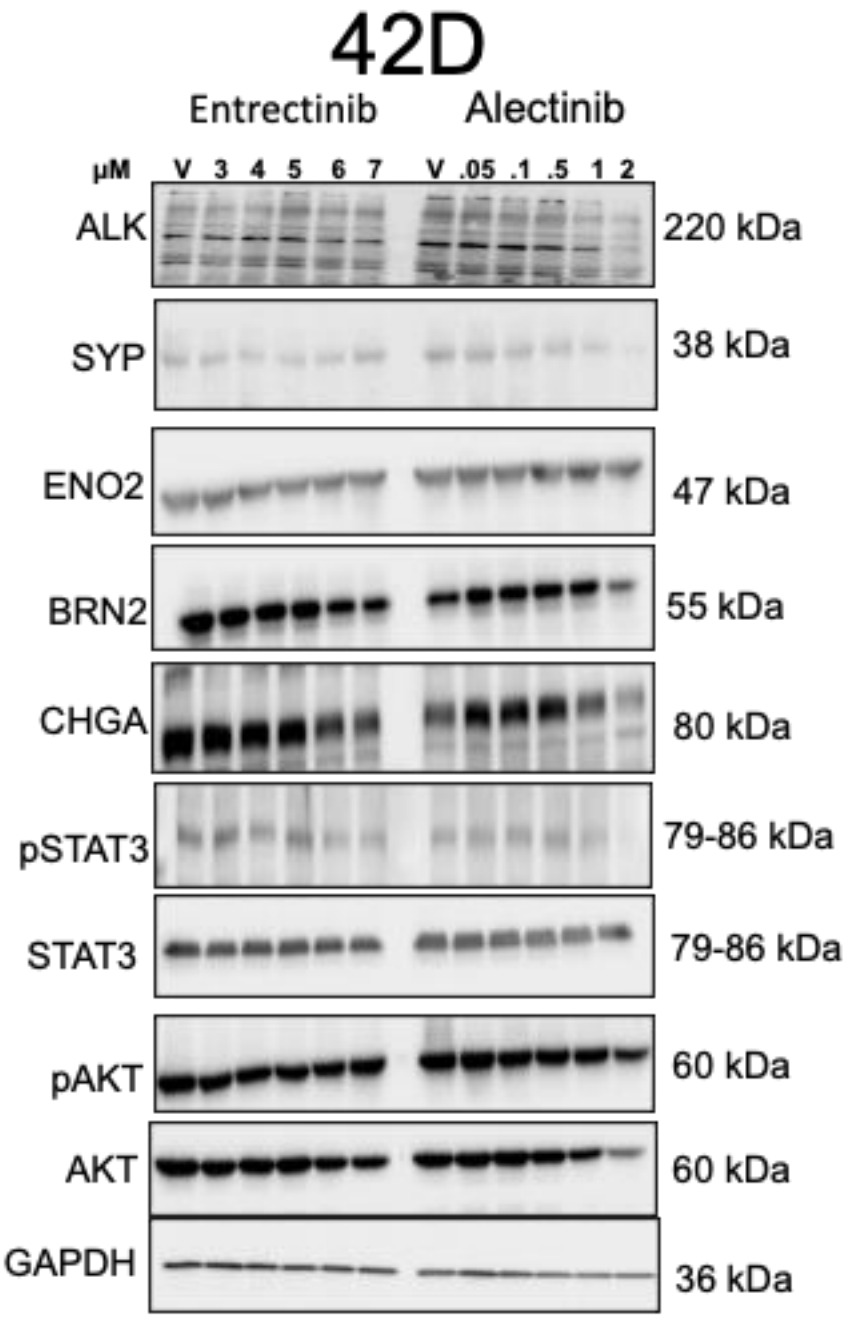
42D
Entrectinib
Alectinib
μM V 3 4 5 6 7 V .05 .1 .5 1 2
ALK
220 kDa
SYP
38 kDa
ENO2
47 kDa
BRN2
55 kDa
CHGA
80 kDa
pSTAT3
79-86 kDa
STAT3
79-86 kDa
pAKT
60 kDa
AKT
60 kDa
GAPDH
36 kDa

Figure 2 continued

B

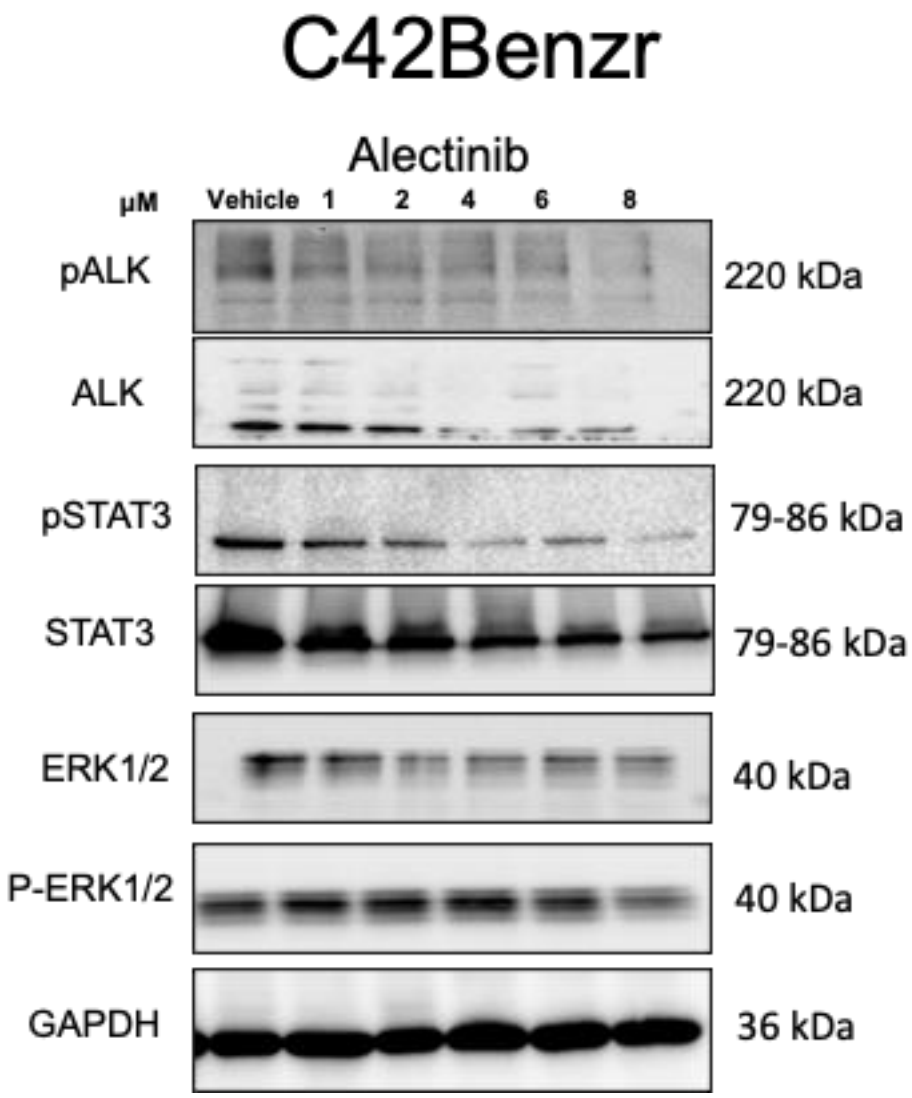

Figure 2 continued

C

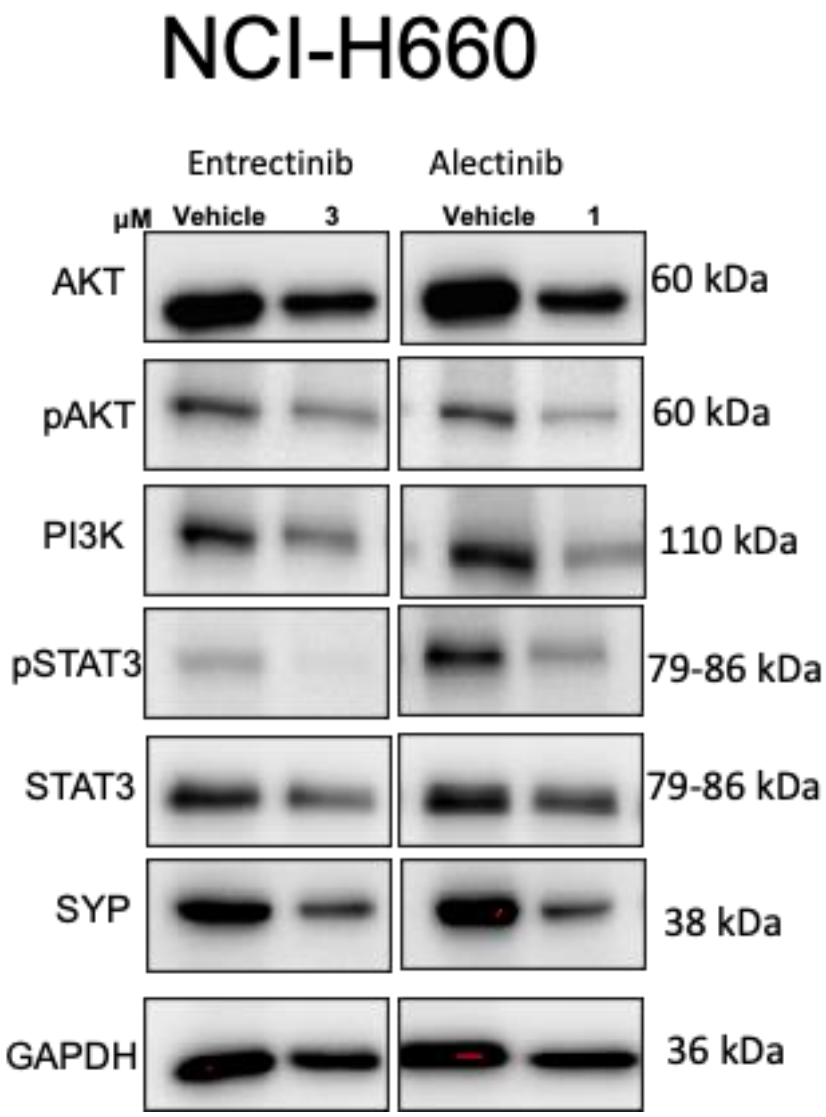

Figure 2. NEPC cell lines were treated with entrectinib and alectinib for 48 hours. Protein lysates were gathered from each treatment and quantified. Several cellular pathways involved in ALK signaling were downregulated. **A.** 42D cells were seeded at a density of 2.0x105 cells per well in six-well plates. Cells were treated with either entrectinib or alectinib alone for 48 hours. Cells were collected and lysed to collect protein. Protein concentrations were measured using a Bio-Rad protein assay kit. 10% SDS gels were prepared and loaded with the sample. Gels were then treated with the indicated primary antibody for 24hrs then treated with a secondary antibody for 1hr. Gels were imaged using a Bio-Rad imager. **B.** C4-2Benzr cells were seeded at a density of 2.0x105 cells per well in six-well plates. Cells were treated with alectinib for 48 hours. Cells were collected and lysed to collect protein. Protein concentrations were measured using a Bio-Rad protein assay kit. 10% SDS gels were prepared and loaded with the sample. Gels were then treated with the indicated primary antibody for 24hrs then treated with a secondary antibody for 1hr. Gels were imaged using a Bio-Rad imager **C.** NCI-H660 cells were seeded at the same concentration as above but in Matrigel-coated six-well plates. All other procedures and processes were the same as previously described.

Figure 3

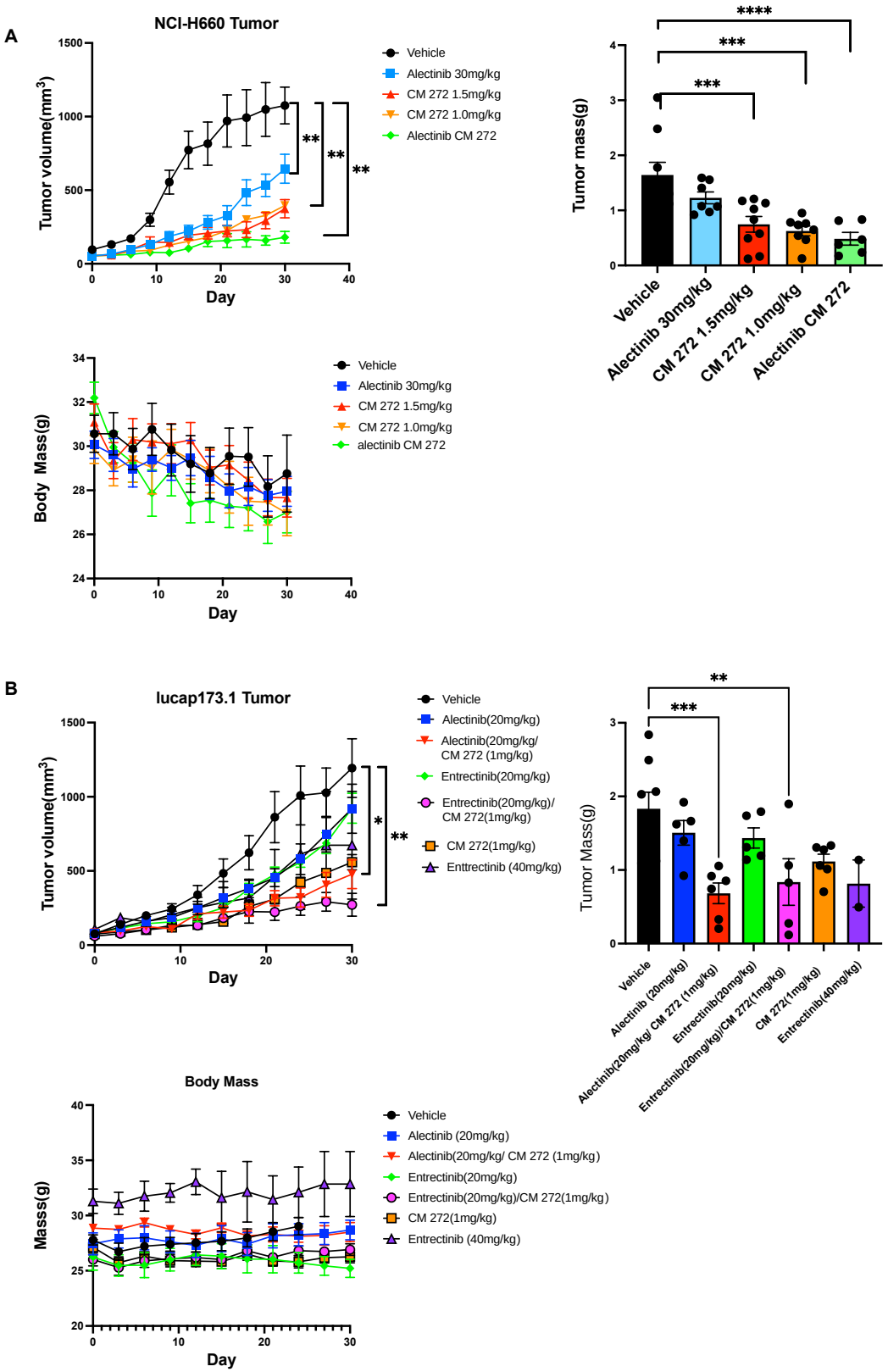
A
NCI-H660 Tumor
Tumor volume(mm3)
Day
Vehicle
Alectinib 30mg/kg
CM 272 1.5mg/kg
CM 272 1.0mg/kg
Alectinib CM 272
**
**
**
Body Mass(g)
alectinib CM 272
Tumor mass(g)
****
***
***
Vehicle
Alectinib 30mg/kg
CM 272 1.5mg/kg
CM 272 1.0mg/kg
Alectinib CM 272
B
lucap173.1 Tumor
Alectinib(20mg/kg)
Alectinib(20mg/kg/ CM 272 (1mg/kg)
Entrectinib(20mg/kg)
Entrectinib(20mg/kg)/ CM 272(1mg/kg)
CM 272(1mg/kg)
Enttrectinib (40mg/kg)
*
**
Tumor Mass(g)
**
***
Alectinib (20mg/kg)
Alectinib(20mg/kg/ CM 272 (1mg/kg)
Entrectinib(20mg/kg)
Entrectinib(20mg/kg)/CM 272(1mg/kg)
CM 272(1mg/kg)
Entrectinib(40mg/kg)
Body Mass
Masss(g)
Entrectinib (40mg/kg)

Figure 3. Mice were implanted with NEPC tumors and treated with ALK inhibitors and CM 272 for 30 days. Mice treated with alectinib and entrectinib showed decreased non-significant tumor growth. Combination treatment with ALK inhibitors and CM 272 showed a significant decrease in tumor growth. **A.** NCI-H660 tumors were implanted in 4–6-week-old mice. Once tumors reached a size between 50-100mM3, treatment begins. Alectinib was administered via oral gavage, while CM 272 was administered via intraperitoneal injections. Animal mass and tumor volume were measured every three days. Tumor volume was calculated using the formula Length x Width2/2. Animals were treated for 30 days, and tumors were harvested and weighed the next day. **B.** LuCaP 173.1 tumors were implanted following the same procedures as NCI-H660 tumors. Treatment began when tumor volume was in the range of 50-150mM3. As before, tumor volume and body mass were measured every three days. Before testing, all tumors were randomized and sorted to the best of our abilities. Statistical analysis involved using One-way ANOVA (tumor mass) or Two-way ANOVA (tumor volume over time) where $p<0.05$.

Table 1. Kegg pathways and genes downregulated 1.5 fold in 42D cells treated with 1.5µM alectinib for 48 hours.

Kegg Pathways	P-Value	Genes	Fold Enrichment
Neuroactive ligand-receptor interaction	5.27E-09	NPFFR2, VIPR2, CHRM1, NPFFR1, SCT, PMCH, HTR2B, RXFP4, GRIK4, GRIK1, TRH, PTH1R, NR3C1, GRM1, BRS3, CYSLTR1, GRM6, BDKRB2, LEPR, BDKRB1, SPX, GHSR, PAQR6, GRID1, PTH2R, PRLR, UTS2B, AGTR2, GRIA2, CALCA, GIPR, PTGER1, CHRNA4, LHB, PTH2, NTS, LYPD6, GHRHR, GLRA2, GRIN2A, PATE4, CNR2, CHRNG, TBXA2R, NPBWR1, NPVF, HRH4, KISS1R, DRD2, GABRP, P2RY10, P2RY14, HTR1D, GABRA3, SCTR, GPR50, NMBR, GRIN2B, TSHR, GRIN2D, GH2, P2RX7, KISS1, GRIN3B, MC1R, LPAR6, P2RX1, MC5R, GNRH1	2.072916087
Arachidonic acid metabolism	1.84E-05	PLA2G2F, GGT5, PLA2G2D, PLA2G12B, PLA2G4D, PLA2G2C, PLA2G1B, CYP4F2, PLA2G2A, PLAAT3, PLAAT2, PLA2G5, ALOX15B, PTGS1, ALOX5, PLA2G10, PTGDS, GGT1	3.253429241
Linoleic acid metabolism	3.43E-05	PLA2G2F, PLA2G2D, PLA2G12B, PLA2G4D, PLA2G2C, PLA2G1B, PLA2G2A, CYP1A2, PLA2G10, PLAAT3, PLAAT2, PLA2G5	4.410204082
alpha-Linolenic acid metabolism	4.85E-05	PLA2G2F, PLA2G2D, PLA2G12B, PLA2G4D, PLA2G2C, PLA2G1B, PLA2G2A, PLA2G10, PLAAT3, PLAAT2, PLA2G5	4.664638932
Ether lipid metabolism	9.46E-05	PLA2G2F, PLA2G2D, TMEM86B, PLA2G12B, PLA2G4D, PLA2G2C, PLA2G1B, PLA2G2A, PLAAT3, PLAAT2, PLA2G5, PLD2, PLA2G10, ENPP2, ENPP6	3.307653061
Protein digestion and absorption	1.07E-04	CELA3A, SLC15A1, SLC6A19, COL13A1, COL25A1, COL22A1, KCNJ13, CTRB1, COL23A1, ATP1A4, ATP1A3, ATP1B2, SLC8A2, SLC8A3, FXYD2, COL5A3, COL4A3, COL20A1, COL6A3, COL10A1, COL6A6, COL6A5, KCNN4	2.462007133
Taste transduction	5.75E-04	TAS2R8, TAS2R30, PDE1C, TAS2R10, HTR3E, HTR1D, GABRA3, HTR3C, TAS2R13, PKD2L1, HTR3A, HTR3B, ADCY8, GRM1, GNG13, SCNN1G, SCNN1B, SCNN1A, GNB3	2.435868533
Ras signaling pathway	6.30E-04	PLA2G1B, CALML6, FLT4, RASAL1, PLA2G5, RASGRP2, FGF3, PLD2, GRIN2A, FGF8, FGF9, FGF20, RAC2, GNG8, FGF23, PRKCG, PLA2G2F, PLA2G2D, ANGPT2, PLA2G12B, PLA2G4D, PRKCB, PLA2G2C, PLA2G2A, IGF2, FLT3LG, PLAAT3, PLAAT2, GRIN2B, GNG13, VEGFA, TIAM1, ZAP70, RASA4, FGF19, PLA2G10, GNB3, RIN1	1.775294016
Calcium signaling pathway	6.39E-04	RYR1, CHRM1, PDE1C, PTGER1, CALML6, FLT4, HTR2B, CXCR4, MST1R, ADCY8, SMIM6, FGF3, MYLK3, GRM1, SLC8A2, GRIN2A, CYSLTR1, FGF8, FGF9, TBXA2R, FGF20, BDKRB2, BDKRB1, FGF23, PRKCG, PRKCB, GRIN2B, TPCN2, GRIN2D, VEGFA, SLC8A3, P2RX7, GRIN3B, GNAL, P2RX1, FGF19, CAMK4, ITPKA, HRC, PLCD1	1.743163669
Cytokine-cytokine receptor interaction	0.00126345	ACVRL1, CNTFR, CSF3, CD40, CSF3R, EPO, IL23R, EBI3, CXCR4, TNFRSF13C, CXCL13, IL2RG, CX3CL1, EDA2R, IFNL2, THPO, CXCR1, CXCR2, LEPR, IL12B, CCR8, TNFRSF14, CCL19, IL12RB1, IFNL3, IL10, CCL24, TGFB1, IL37, IL34, TNFRSF18, TNFSF12, PRLR, IL2, GH2, IL22RA1, IL4, IL1A, CXCL11, IL7, ACKR4, RELL2, INHA, IL7R	1.633408919
Primary immunodeficiency	0.00158655	CD79A, ZAP70, CD40, CD19, BTK, TAP2, TNFRSF13C, IL7R, IL2RG, JAK3, ADA	3.191595059
Pancreatic secretion	0.00180061	PRKCG, PLA2G2F, CELA3A, PLA2G2D, PLA2G12B, PLA2G2C, PLA2G1B, SCT, PRKCB, CTRB1, PLA2G2A, ATP1A4, SCTR, ATP1A3, ATP1B2, PLA2G5, ADCY8, TPCN2, FXYD2, PLA2G10	2.161864746
Endocrine and other factor-regulated calcium reabsorption	0.00229999	PRKCG, KLK1, PRKCB, ATP1A4, ATP1A3, AP2A1, ATP1B2, PTH1R, SLC8A2, SLC8A3, FXYD2, TRPV5, BDKRB2	2.704370427
Bile secretion	0.0023278	UGT2B10, ABCC3, ABCB1, UGT1A1, SCT, AQP9, ATP1A4, SCTR, NR1H4, ATP1A3, ATP1B2, ADCY8, NR0B2, FXYD2, UGT1A8, SLC22A7, SLC27A5, UGT1A6	2.229878468
ECM-receptor interaction	0.0023278	ITGB4, LAMC3, ITGA3, MEPE, LAMC2, NPNT, THBS4, SV2B, IBSP, COL4A3, ITGA11, COL6A3, COL6A6, ITGB6, COL6A5, AGRN, FREM1, ITGA9	2.229878468
Proximal tubule bicarbonate reclamation	0.00327501	FXYD2, CA4, ATP1A4, ATP1A3, SLC25A10, ATP1B2, PCK1, SLC38A3	3.834960071
PI3K-Akt signaling pathway	0.00363744	CSF3, CSF3R, CHRM1, EPO, LAMC3, ITGB4, FLT4, LAMC2, FGF3, GYS2, FGF8, IBSP, FGF9, ITGB6, JAK3, ITGA3, FLT3LG, PRLR, EIF4E1B, COL4A3, COL6A3, COL6A6, COL6A5, SGK2, ITGA9, ATF6B, PKN3, IL2RG, THBS4, CD19, FGF20, GNG8, PCK1, FGF23, ANGPT2, IGF2, IL2, GNG13, VEGFA, GH2, IL4, CDK6, LPAR6, ARTN, IL7, FGF19, ITGA11, GNB3, IL7R	1.504874652
Cell adhesion molecules	0.00401712	CD40, CLDN2, VSIR, SPN, CDH4, HLA-DMB, SLITRK5, NTNG1, NTNG2, HLA-DRB5, CADM1, NEGR1, HLA-E, PTPRD, CLDN6, MAG, CLDN4, OCLN, CD6, CLDN34, CLDN7, CNTN1, CD226, CLDN16, CD22, ITGA9	1.814324464
Aldosterone-regulated sodium reabsorption	0.00478735	PRKCG, SCNN1G, PRKCB, SCNN1B, FXYD2, SCNN1A, ATP1A4, ATP1A3, SFN, ATP1B2	2.979867623
Glutamatergic synapse	0.00713337	PRKCG, GRIA2, PLA2G4D, PRKCB, GRIK4, GRIK1, ADCY8, SLC1A7, GRIN2B, GRM1, GNG13, PLD2, GRIN2D, GRIN2A, GRIN3B, GRM6, DLG4, GNB3, GNG8, SLC38A3	1.917480035
Retinol metabolism	0.00724375	UGT2B10, UGT1A1, RETSAT, CYP3A7, CYP26A1, CYP26C1, DHRS9, AWAT2, CYP1A2, CYP1A1, AOX1, BCO1, UGT1A8, UGT1A6	2.269957983
Complement and coagulation cascades	0.00973822	CFD, FGA, SERPINB2, SERPINC1, PLAUR, F3, C2, C4B, C4A, PROC, PLAU, BDKRB2, SERPING1, BDKRB1, VSIG4, CFB	2.051257712
Pathways in cancer	0.00978257	CSF3R, EPO, LAMC3, CALML6, HHIP, FLT4, IL23R, LAMC2, FZD10, FGF3, FGF8, FGF9, BDKRB2, RAC2, IL12B, BDKRB1, JAK3, PRKCG, WNT5B, PRKCB, ITGA3, DCC, FLT3LG, TRAF1, FOS, WNT16, MMP9, DDB2, PAX8, COL4A3, PPARD, PTGER1, EPAS1, GSTP1, CXCR4, IL2RG, ADCY8, RASGRP2, PLD2, WNT6, WNT11, TERT, FGF20, E2F1, GNG8, HES1, IL12RB1, WNT1, FGF23, STAT5A, TCF7L1, GSTM1, TGFB1, GADD45B, IGF2, IL2, GNG13, VEGFA, IL4, CDK6, LPAR6, IL7, FGF19, GNB3, IL7R	1.349638726
Fat digestion and absorption	0.01330982	PLA2G2F, PLA2G2D, PLA2G12B, PLA2G2C, PLA2G1B, MTTP, PLA2G2A, PLA2G10, PLA2G5, APOB	2.56407214
PPAR signaling pathway	0.01628083	UCP1, LPL, ILK, APOA5, FABP5, OLR1, ACSBG1, PLIN2, PLIN1, PCK1, PLTP, SLC27A5, PLIN5, PPARD	2.058095238
Viral protein interaction with cytokine and cytokine receptor	0.01725659	IL10, CCL24, IL37, IL34, CXCR4, CXCL13, IL2RG, IL2, CX3CL1, IL22RA1, CXCL11, CXCR1, CXCR2, ACKR4, CCR8, TNFRSF14, CCL19	1.874336735
Mineral absorption	0.01755868	SLC8A3, S100G, TF, SLC6A19, FXYD2, ATP1A4, CYBRD1, ATP1A3, MT1G, ATP1B2, TRPM6, SLC8A2	2.205102041
Nicotine addiction	0.02479356	GABRP, GRIA2, GRIN2A, GRIN3B, SLC32A1, CHRNA4, GABRA3, GRIN2B, GRIN2D	2.480739796
Staphylococcus aureus infection	0.0252096	IL10, CFD, HLA-DRB5, KRT13, KRT32, C2, KRT9, C4B, C4A, HLA-DMB, KRT39, KRT16, KRT15, KRT36, FCGR2B, CFB	1.837585034
JAK-STAT signaling pathway	0.02575913	IL10, STAT5A, CNTFR, CSF3, CSF3R, EPO, IL23R, IL2RG, PRLR, IL2, GH2, SOCS2, IL22RA1, IL4, IFNL2, THPO, IL7, LEPR, IL12B, AOX1, IL12RB1, IL7R, JAK3, IFNL3	1.594049668
Glycerophospholipid metabolism	0.03228108	DGKG, PLA2G2F, PLA2G2D, PLA2G12B, PLA2G4D, PLA2G2C, PLA2G1B, DGKA, PLA2G2A, PLAAT3, PLAAT2, PLA2G5, PLD2, LPCAT3, GPD1, PLA2G10	1.781900639
Pertussis	0.03955884	IL10, TICAM2, CALML6, FOS, C2, C4B, IL1A, C4A, IRF1, IRF8, SERPING1, IL12B, SFTPA1	1.885942535
Dilated cardiomyopathy	0.04383015	MYBPC3, TGFB1, CAV3, ITGB4, ITGA3, ADCY8, SLC8A2, SLC8A3, CACNG6, ITGA11, MYL3, SSPN, ITGB6, CACNG4, ITGA9, CACNG5	1.712700614
Amphetamine addiction	0.04472139	PRKCG, GRIA2, GRIN2A, GRIN3B, ATF6B, CALML6, PRKCB, CAMK4, PPP1R1B, FOS, GRIN2B, GRIN2D	1.917480035

Table 2. Kegg pathways and genes downregulated 1.5 fold in 42D cells treated with 1.5μM entrectinib for 48 hours.

Kegg pathways	P-Value	Genes	Fold Enrichment
Neuroactive ligand-receptor interaction	2.85E-12	NPFFR2, NPFFR1, SCT, CHRM4, MLNR, HTR2B, RXFP4, GRIK3, GRIK1, NR3C1, QRFP, GRM1, BRS3, MC4R, GRM3, GABRR2, GRM4, GRM6, GNRHR, BDKRB1, SPX, GHSR, GRID2, CHRNB3, PTH2R, AVPR1A, SSTR4, APLNR, AGTR2, GRIA2, CALCA, CALCB, PTGER1, NTS, CHRND, GRIN2A, P2RY4, CHRNG, CNR1, NPVF, HRH4, KISS1R, DRD2, GPR156, GRIA3, NTSR2, GRIA4, P2RY10, NMB, GABBR1, P2RY14, GPR50, NMBR, HTR5A, SLURP1, GH2, P2RX7, KISS1, P2RX3, LPAR6, P2RX1, MC5R, NMUR1	2.598681982
Cytokine-cytokine receptor interaction	1.29E-08	CSF3, CNTF, CTF1, CSF3R, IL20, EPO, IL23R, EBI3, CXCR5, CXCL17, CXCR4, IL2RG, CXCL14, CXCL5, CX3CL1, IFNL2, CXCR1, CXCR2, IL21R, IL12B, CCR8, CCL19, IL12RB1, CCL17, IL10, CCL25, IL33, XCR1, CCL22, CCL21, TNFSF14, IL34, TNFSF12, IL13, OSM, INHBB, NGF, GDF6, INHBC, IL2, GH2, IL4, CXCL10, CXCL11, IL7, TNFSF8, NODAL, IL17B	2.446602629
Taste transduction	5.20E-07	HCN4, TAS2R50, GABBR1, TAS2R8, TAS2R30, PDE1C, TAS2R31, HTR3C, TAS2R13, PKD2L1, HTR3B, ADCY8, TAS2R19, GRM1, SCNN1G, GRM4, P2RX3, P2RY4, SCN9A, SCN2A, TAS2R4	3.696574757
Viral protein interaction with cytokine and cytokine receptor	1.64E-06	CCL25, IL10, IL20, XCR1, CCL22, TNFSF14, CCL21, IL34, CXCR5, CXCR4, IL2RG, CXCL14, CXCL5, IL2, CX3CL1, CXCL10, CXCL11, CXCR1, CXCR2, CCR8, CCL19, CCL17	3.330437828
Staphylococcus aureus infection	4.58E-05	IL10, SELPLG, ITGAM, KRT13, DEFB1, KRT9, ICAM1, SELP, C4B, C4A, HLA-DMB, KRT16, KRT15, KRT36, KRT14, FCGR2B, HLA-DRB1, CAMP, CFB	2.996132516
Allograft rejection	1.26E-04	IL10, IL4, HLA-DMB, CD80, HLA-B, CD28, IL12B, HLA-A, HLA-DRB1, IL2, HLA-E	4.382155037
JAK-STAT signaling pathway	2.14E-04	CSF3, CNTF, CTF1, CSF3R, IL20, EPO, IL23R, IL2RG, SOCS3, IFNL2, STAT4, IL21R, IL12B, AOX1, STAT6, IL12RB1, IL10, STAT5A, IL13, OSM, IL2, GFAP, GH2, IL4, IL7	2.279872555
Complement and coagulation cascades	4.42E-04	CPB2, ITGAM, SERPINB2, F11, PLAT, C4BPA, F3, C4B, C4A, PROC, PLAU, ITGAX, SERPING1, BDKRB1, VSIG4, CFB	2.81643791
Cell adhesion molecules	6.56E-04	SELPLG, ITGAM, CD80, HLA-B, ICAM2, HLA-A, VSIR, ICAM1, HLA-E, SELP, SPN, CLDN6, IGSF11, HLA-DMB, PTPRC, CD28, CLDN19, CLDN18, ITGB8, CD226, SIGLEC1, CLDN16, HLA-DRB1	2.203684409
Inflammatory bowel disease	9.64E-04	IL10, IL23R, IL13, IL2RG, IL2, IL4, HLA-DMB, STAT4, IL21R, IL12B, STAT6, IL12RB1, HLA-DRB1	3.027670753
Protein digestion and absorption	0.00108106	COL28A1, CELA3A, SLC15A1, CPB2, SLC6A19, COL14A1, ATP1A4, ATP1B2, PGA5, SLC8A2, COL3A1, MEP1B, FXYD2, COL5A3, COL6A3, COL8A1, COL6A6	2.498563243
Chemokine signaling pathway	0.001783023	NCF1, CXCR5, CXCR4, ADCY8, CXCL14, CXCL5, CX3CL1, PAK1, GNGT2, CXCR1, GRK7, CXCR2, RAC2, CCR8, GNG8, CCL19, CCL17, CCL25, XCR1, CCL22, CCL21, PRKCB, CXCL10, HCK, CXCL11	1.971139813
Autoimmune thyroid disease	0.002120824	IL10, IL4, TPO, HLA-DMB, CD80, HLA-B, CD28, HLA-A, HLA-DRB1, IL2, HLA-E	3.14192248
Calcium signaling pathway	0.002403186	RYR2, PDE1C, CALML5, PTGER1, HTR2B, CXCR4, CALML3, ADCY8, FGF3, MYLK3, GRM1, SLC8A2, FGF5, GRIN2A, FGF9, BDKRB1, CD38, FGF23, PRKCB, ATP2B2, AVPR1A, NGF, HTR5A, P2RX7, P2RX3, P2RX1, FGF19, CAMK4, CASQ1, SLC25A31	1.795061711
Th1 and Th2 cell differentiation	0.002647162	RBPJL, STAT5A, IL13, IL2RG, IL2, DLL4, IL4, HLA-DMB, STAT4, IL12B, PRKCQ, STAT6, CD247, IL12RB1, HLA-DRB1	2.468209853
Pertussis	0.003832171	IL10, ITGAM, CALML5, CALML3, C4BPA, CXCL5, C4B, C4A, IRF1, IRF8, SERPING1, IL12B, CD14	2.589455249
Graft-versus-host disease	0.00545376	HLA-DMB, CD80, HLA-B, CD28, HLA-A, KIR3DL2, HLA-DRB1, IL2, HLA-E	3.24393295
Type I diabetes mellitus	0.006323422	HLA-DMB, CD80, HLA-B, CD28, IL12B, HLA-A, HLA-DRB1, IL2, HLA-E	3.168492649
Salivary secretion	0.007703323	CALML5, PRKCB, ATP1A4, CALML3, ATP2B2, LPO, ATP1B2, LYZ, ADCY8, DMBT1, FXYD2, PRB2, CD38, CAMP	2.278891965
Leukocyte transendothelial migration	0.00833063	ITGAM, NCF1, PRKCB, NCF2, MMP2, NCF4, CXCR4, THY1, MMP9, ICAM1, CLDN6, CLDN19, RAC2, CLDN18, CLDN16, MYL9	2.106205741
Glycosphingolipid biosynthesis - lacto and neolacto series	0.008656764	FUT5, B3GNT5, B3GALT2, B3GNT3, B3GALT5, ABO, FUT3	3.784588441
Hematopoietic cell lineage	0.012815523	CSF3, CSF3R, ITGAM, EPO, FLT3LG, CD1D, IL4, FCER2, HLA-DMB, IL7, CD38, CD14, CD36, HLA-DRB1	2.1407773
Intestinal immune network for IgA production	0.013912622	CCL25, IL10, IL4, HLA-DMB, CD80, CD28, CXCR4, HLA-DRB1, IL2	2.780513957
Amphetamine addiction	0.014388461	GRIA2, GRIN2A, MAOB, ATF6B, CALML5, TH, PRKCB, CAMK4, CALML3, GRIA3, GRIA4	2.413360745
C-type lectin receptor signaling pathway	0.018800582	IL10, EGR3, FCER1G, CCL22, SYK, KSR1, CLEC4M, CALML5, CALML3, IL2, PAK1, IRF1, IL12B, CCL17	2.037855315
cAMP signaling pathway	0.023528643	HCN4, GHSR, GRIA2, RYR2, GABBR1, CALML5, HHIP, ATP1A4, CALML3, ATP2B2, ATP1B2, ADCY8, PAK1, GRIN2A, FXYD2, CAMK4, RAC2, CNGA2, CNGB3, DRD2, MYL9, GRIA3, CNGB1, GRIA4	1.614757735
Th17 cell differentiation	0.024940054	STAT5A, IL23R, EBI3, IL2RG, IL2, IL4, HLA-DMB, IRF4, IL21R, PRKCQ, STAT6, CD247, IL12RB1, HLA-DRB1	1.962379192
Cardiac muscle contraction	0.027170321	CACNG6, MYL4, RYR2, FXYD2, MYL3, ATP1A4, CACNA2D3, ATP1B2, COX7A1, COX7B2, CACNG5, SLC8A2	2.088048795
Viral myocarditis	0.030847535	HLA-DMB, CD80, HLA-B, RAC2, CD28, HLA-A, HLA-DRB1, SGCG, ICAM1, HLA-E	2.259455786
Bile secretion	0.031508748	ABCB1, SCT, FXYD2, AQP9, ATP1A4, NR1H4, ATP1B2, SLC22A8, ADCY8, SLC22A7, CYP7A1, SLC4A5	2.04112635
ECM-receptor interaction	0.031508748	RELN, IBSP, SV2B, ITGA11, ITGB8, MEPE, COL6A3, COL6A6, DMP1, LAMC2, CD36, ITGB6	2.04112635
Pathways in cancer	0.032825531	CSF3R, CALML5, EPO, PTGER1, GSTP1, HHIP, IL23R, CXCR4, LAMC2, CALML3, IL2RG, ADCY8, FGF3, RASGRP4, FGF5, DLL4, WNT6, GNGT2, WNT11, FGF9, STAT4, RAC2, IL12B, GNG8, BDKRB1, STAT6, IL12RB1, FGF23, WNT2, HES5, STAT5A, CDKN2B, GSTM1, WNT5B, PRKCB, DCC, WNT3A, MMP2, IL13, FLT3LG, IGF1, MMP9, IL2, IL4, LPAR6, IL7, FGF19	1.339929618
Glutamatergic synapse	0.039059289	GRIA2, PRKCB, GRIK3, GRIK1, ADCY8, GRM1, GRM3, GRIN2A, GRM4, GNGT2, GRM6, GNG8, GRIA3, GRIA4	1.842930024
Phagosome	0.042252279	COLEC11, ITGAM, NCF1, CLEC4M, NCF2, NCF4, HLA-B, HLA-A, MPO, CTSS, HLA-E, HLA-DMB, OLR1, CD14, CD36, FCGR2B, HLA-DRB1	1.693105355
Adrenergic signaling in cardiomyocytes	0.046711332	RYR2, ATF6B, CALML5, ATP1A4, CACNA2D3, CALML3, ATP2B2, ATP1B2, ADCY8, SLC8A2, CACNG6, MYL4, PPP1R1A, FXYD2, MYL3, AGTR2, CACNG5	1.671116974
Cholesterol metabolism	0.048510875	LIPC, STAR, APOH, ANGPTL3, PCSK9, CD36, APOB, CYP7A1	2.374643728
PI3K-Akt signaling pathway	0.049303697	CSF3, CSF3R, ATF6B, EPO, LAMC2, IL2RG, FGF3, FGF5, GYS2, RELN, GNGT2, FGF9, IBSP, GNG8, ITGB8, ITGB6, PCK1, FGF23, ANGPT4, SYK, OSM, FLT3LG, IGF1, NGF, IL2, GH2, IL4, LPAR6, IL7, FGF19, ITGA11, COL6A3, COL6A6	1.391547839
Asthma	0.050119069	IL10, IL4, HLA-DMB, FCER1G, IL13, HLA-DRB1	2.930003955

Table 3. Kegg pathways and genes downregulated 1.5 fold in 42D cells treated with 300nM CM 272 for 48 hours.

Kegg pathways	P-Value	Genes	Fold Enrichment
Taste transduction	8.51E-08	GABBR1, TAS2R8, TAS2R30, PDE1C, TAS2R31, TAS2R10, HTR1D, HTR3C, TAS2R13, CACNA1A, HTR3B, TAS2R38, SCNN1G, P2RY4, SCNN1B, SCN9A, ASIC2, SCN2A, TAS2R5, TAS2R4	4.360591
Cytokine-cytokine receptor interaction	2.39E-04	CSF3, CSF3R, IL20, CXCR5, CXCL17, CXCR4, CXCL14, IFNL2, CXCR1, IL12B, CCL19, IL12RB1, IFNL3, CCR2, IL10, TNFSF18, CCL24, IL33, TNFSF14, TSLP, IL34, OSM, GDF6, IL2, GH2, IL4, CXCL10, CD4, CXCL11, CXCL12, IL7, IL7R	2.02026
Viral protein interaction with cytokine and cytokine receptor	7.84E-04	IL10, CCL24, IL20, TNFSF14, IL34, CXCR5, CXCR4, CXCL14, IL2, CXCL10, CXCL11, CXCL12, CXCR1, CCL19, CCR2	2.812581
Cell adhesion molecules	0.00431955	NTNG1, NLGN4Y, ITGAM, HLA-B, LRRC4, ICAM2, HLA-C, CLDN2, VSIR, SELP, SPN, IGSF11, CD4, PTPRC, SLITRK3, PDCD1, CLDN16, ITGA9	2.136138
Complement and coagulation cascades	0.00566533	C4B, C4A, FGA, ITGAM, PROC, SERPINC1, F11, ITGAX, C4BPA, VSIG4, F3, CFB	2.616355
Protein digestion and absorption	0.00833383	COL28A1, CELA3A, SLC15A1, SLC6A19, COL14A1, CTRB1, COL12A1, SLC3A1, PGA5, ACE2, XPNPEP2, FXYD2, COL6A3	2.366573
Calcium signaling pathway	0.00841324	NTRK2, PDE1C, PRKCB, HTR2B, CACNA1A, CXCR4, ADRA1D, HTR5A, FGF1, ADRA1B, CACNA1E, GRIN2B, FGF3, FGF5, FGF17, FGF7, GNA15, GRIN2A, FGF9, ERBB4, HRC, DRD1, SLC25A31, FGF23	1.778708
JAK-STAT signaling pathway	0.01525698	IL10, STAT5A, CSF3, CSF3R, IL20, TSLP, OSM, IL2, GH2, IL4, IFNL2, IL7, STAT4, IL12B, IL12RB1, IL7R, IFNL3	1.920236
PI3K-Akt signaling pathway	0.01621068	CSF3, CSF3R, ATF6B, FGF1, AREG, FGF3, FGF5, GYS2, TCL1B, FGF7, GNG2, FGF9, IBSP, ERBB4, TNN, GNG8, PCK1, FGF23, NTRK2, SYK, OSM, IL2, GH2, IL4, FGF17, IL7, EIF4E1B, COL6A3, IL7R, ITGA9	1.566898
Nicotine addiction	0.01809663	CHRNB2, GRIA2, GRIN2A, SLC32A1, CACNA1A, GRIN2B, GRIA3	3.281345
Th1 and Th2 cell differentiation	0.02389926	STAT5A, IL4, CD4, STAT4, IL12B, PRKCQ, GATA3, CD247, IL12RB1, RUNX3, IL2	2.241913
Virion - Human immunodeficiency virus	0.02538287	CD4, CLEC4M, CXCR4	11.25033
Staphylococcus aureus infection	0.03102982	C4B, IL10, SELP, C4A, ITGAM, KRT39, DEFB1, FCGR1A, CAMP, CFB, KRT9	2.1485
Serotonergic synapse	0.04199783	CYP2C8, GNG2, MAOB, PRKCB, HTR1D, HTR2B, HTR3C, CACNA1A, GNG8, HTR3B, HTR5A, ALOX15B	1.956578
Glutamatergic synapse	0.04199783	GRM3, GRIA2, GRIN2A, GNG2, GRM6, PRKCB, GRM8, CACNA1A, GNG8, GRIK2, GRIN2B, GRIA3	1.956578
Cocaine addiction	0.04429709	GRM3, GRIA2, GRIN2A, MAOB, ATF6B, DRD1, GRIN2B	2.678649
Pertussis	0.04811763	C4B, IL10, C4A, ITGAM, IL12B, LY96, C4BPA, CD14, SFTPA1	2.220459
Allograft rejection	0.0493018	IL10, IL4, HLA-B, HLA-C, IL12B, IL2	2.960612

Table 4. Kegg pathways and genes downregulated 1.5 fold in LuCaP 173.1 tumors treated with Entrectinib (40mg/kg).

Kegg pathways	P-Value	Genes	Fold Enrichment
Cytokine-cytokine receptor interaction	2.04E-10	ACVRL1, IL22, CSF3, CD40, IFNA7, IL20, CXCL8, IL25, MSTN, IFNA1, IL26, MPL, CXCL17, CXCL13, TNFSF13B, CXCL16, GHR, TNFSF10, CCR8, CCR2, IL15RA, IFNA14, IL15, IL1R2, NGF, EDAR, IL1A, IFNG, IL23A, IL1B, IFNK, CXCR6, IL2RG, ACVR1C, THPO, CXCR1, IL21R, TNFRSF17, CCL25, XCR1, IL31, IFNB1, TNFSF15, IL36G, BMP7, IFNW1, IL22RA1, GH1, IL6, IL5, IL2RB, ACKR3, IL17C, IL17B, IL18R1	2.536832
Neuroactive ligand-receptor interaction	2.75E-08	HTR2B, RXFP1, GHR, GRM3, CYSLTR1, EDNRA, GNRHR, BDKRB1, QRFPR, INSL5, PAQR9, EDN2, GLP2R, PTH2R, SSTR1, OPRM1, F2, GABRG2, SSTR4, UTS2B, AGTR2, PTGER4, NPB, GRIA2, CHRNA3, LHB, LPAR3, FPR3, LYPD6, GLRA1, MC2R, HRH1, CALCR, GALR3, NPVF, NPY, NPBWR2, P2RY1, HRH4, KISS1R, TAC4, HCRT, S1PR4, HTR1D, GCG, NMBR, HCRTR2, HCRTR1, GH1, P2RX3, P2RX2, LPAR6, SST, LYPD6B, F2RL1, RLN1, GALP, GPHB5	2.164947
Malaria	1.50E-06	CSF3, CD40, CXCL8, KLRB1, GYPC, HBA2, THBS2, SELE, SELP, COMP, IL6, KLRK1, IFNG, CR1L, IL1B, TLR4	4.383645
Taste transduction	3.68E-05	TAS2R7, TAS2R50, TAS2R30, TAS2R20, HTR1D, TAS2R13, TAS2R46, HTR3A, TAS2R16, ADCY8, TAS2R39, P2RX3, GNAT3, P2RX2, SCNN1A, P2RY1, TAS2R1, TAS2R3, TAS2R5	3.026499
JAK-STAT signaling pathway	6.06E-05	IL22, CSF3, IFNA7, IL20, IFNA1, IL26, MPL, IL2RG, GHR, SOCS1, THPO, IL21R, AOX1, IL15RA, IL31, IFNA14, IFNB1, IL15, STAT1, IFNW1, IL22RA1, GH1, IL6, IL5, IFNG, IL23A, IL2RB, IFNK	2.310656
NOD-like receptor signaling pathway	7.22E-05	IFNA7, CXCL8, IFNA1, MEFV, GPRC6A, PYCARD, CASP8, MAP1LC3A, NLRP6, CASP1, NLRP3, GBP2, GBP1, GBP4, GBP3, GBP5, CASR, GBP7, IFNA14, IFNB1, STAT1, CARD6, CYBA, IL6, OAS1, IL1B, CARD18, CARD16, RBCK1, TLR4	2.209498
PI3K-Akt signaling pathway	2.14E-04	CSF3, IFNA7, ATF6B, ITGB5, IFNA1, FLT4, LPAR3, THBS2, IL2RG, FGF2, EFNA4, IGF1R, INS, GHR, COMP, FGF7, FGF8, RELN, ERBB3, IBSP, PDGFC, SPP1, FGF20, ITGB8, ITGB7, ITGB6, PCK1, FGF22, NTRK2, IFNA14, LAMB3, IFNB1, VEGFC, FLT3LG, NGF, EREG, GH1, IL6, EFNA2, COL4A1, LPAR6, IL2RB, FGFR3, TP53, TLR4, SGK2	1.75529
Drug metabolism - cytochrome P450	5.90E-04	MAOB, UGT1A1, UGT2B15, MGST1, FMO1, FMO3, CYP3A4, FMO4, ADH6, ALDH3A1, ADH4, HPGDS, CYP2C8, AOX1, UGT1A6	2.853936
Inflammatory bowel disease	6.94E-04	IL22, STAT1, GATA3, IL2RG, IL1A, IL6, IL5, IFNG, IL23A, IL1B, IL21R, TLR4, IL18R1, HLA-DQB1	2.95053
Lipid and atherosclerosis	8.89E-04	IFNA7, CD40, CXCL8, IFNA1, NCF2, NCF4, LY96, PYCARD, CASP8, PPP3R2, CASP1, TNFSF10, NLRP3, LDLR, VAV3, IFNA14, HSPA5, IFNB1, HSPA6, NFATC2, APOA4, CYBA, SELE, POU2F3, SELP, CYP2C8, IL6, IL1B, TP53, TLR4	1.911473
Retinol metabolism	0.001083	UGT1A1, UGT2B15, CYP3A4, ADH6, CYP3A7, SDR16C5, ALDH1A3, ADH4, CYP2C8, CYP2S1, RDH16, AOX1, BCO1, UGT1A6	2.82036
Antigen processing and presentation	0.001347	CD74, CIITA, HSPA5, KLRC4, HSPA6, HLA-B, TAP2, HLA-C, TAP1, HLA-E, IFNG, PSME1, KLRD1, B2M, HLA-DQB1	2.634402
ECM-receptor interaction	0.001782	LAMB3, ITGB5, MEPE, DMP1, GP6, THBS2, DSPP, COMP, RELN, IBSP, COL4A1, SPP1, ITGB8, ITGB7, ITGB6, FREM2	2.462722
Cell adhesion molecules	0.002395	CD86, CD274, CD40, ITGAM, HLA-B, LRRC4, HLA-C, SELE, CLDN1, HLA-E, SELP, OCLN, CDH3, CDH1, CLDN14, CLDN7, ITGB8, ITGB7, SIGLEC1, CLDN16, TIGIT, CD99, HLA-DQB1	1.994142
Intestinal immune network for IgA production	0.002405	CCL25, CD86, IL15RA, IL6, CD40, IL5, IL15, TNFRSF17, ITGB7, TNFSF13B, HLA-DQB1	3.075261
Cytosolic DNA-sensing pathway	0.002731	ZBP1, IFNA7, IFNA14, IFNA1, IFNB1, DNASE2B, MEFV, PYCARD, IL6, CASP8, IL1B, CASP1, NLRP3, POLR3G	2.557126
Graft-versus-host disease	0.002764	CD86, IL1A, IL6, IFNG, IL1B, HLA-B, HLA-C, KLRD1, HLA-E, HLA-DQB1	3.261641
IL-17 signaling pathway	0.003094	CSF3, CEBPB, CXCL8, IL25, MUC5AC, FOSL1, IL6, CASP8, IL5, IFNG, IL1B, S100A9, IL17C, S100A8, IL17B, S100A7	2.331726
Tuberculosis	0.005763	CD74, CIITA, IFNA7, CEBPB, ITGAM, IFNA14, IFNA1, IFNB1, STAT1, MALT1, TLR1, IL1A, IL6, FCGR2A, CASP8, PPP3R2, IFNG, CR1L, CLEC7A, IL23A, IL1B, ATP6V0A4, TLR4, HLA-DQB1	1.826519
Influenza A	0.006312	CIITA, IFNA7, IFNA14, CXCL8, IFNA1, RSAD2, IFNB1, STAT1, MX2, IFIH1, PYCARD, IL1A, IL6, CASP8, IFNG, OAS1, IL1B, CASP1, TNFSF10, NLRP3, SLC25A31, TLR4, HLA-DQB1	1.842541
Phagosome	0.00702	MSR1, ITGAM, ITGB5, TUBAL3, NCF2, NCF4, HLA-B, TAP2, HLA-C, TAP1, CYBA, THBS2, HLA-E, COMP, MARCO, FCGR2A, CLEC7A, ATP6V0A4, NOS1, TLR4, HLA-DQB1	1.89261
Calcium signaling pathway	0.009763	MYLK2, FLT4, HTR2B, ADCY8, FGF2, HRH1, FGF7, CYSLTR1, EDNRA, FGF8, PPP3R2, PLN, PLCZ1, ERBB3, PDGFC, FGF20, BDKRB1, NOS1, FGF22, NTRK2, TNNC2, VEGFC, NFATC2, NGF, P2RX3, P2RX2, GNAS, SLC25A31, FGFR3, CAMK1G	1.624374
Ovarian steroidogenesis	0.010507	PLA2G4D, ALOX5, LHB, HSD17B2, GNAS, ADCY8, LDLR, CYP17A1, IGF1R, INS	2.686057
Type I diabetes mellitus	0.011326	CD86, IL1A, IFNG, IL1B, HLA-B, HLA-C, HLA-E, INS, HLA-DQB1	2.86721
Toll-like receptor signaling pathway	0.01136	CD86, IFNA7, CD40, IFNA14, CXCL8, IFNA1, IFNB1, STAT1, LY96, TLR1, IL6, CASP8, IL1B, SPP1, TLR8, TLR4	2.029465
Viral protein interaction with cytokine and cytokine receptor	0.013271	CCL25, IL20, XCR1, CXCL8, CXCL13, IL2RG, IL22RA1, IL6, CXCR1, IL2RB, TNFSF10, ACKR3, CCR8, IL18R1, CCR2	2.054834
Steroid hormone biosynthesis	0.013427	HSD11B2, UGT1A1, CYP11B1, UGT2B15, HSD17B2, CYP3A4, HSD17B8, CYP7A1, UGT1A6, CYP17A1, CYP3A7	2.430448
Autoimmune thyroid disease	0.013449	CD86, IFNA7, CD40, IFNA14, IL5, IFNA1, HLA-B, HLA-C, HLA-E, HLA-DQB1	2.584696
Rap1 signaling pathway	0.018285	ITGAM, FLT4, LPAR3, ADCY8, FGF2, EFNA4, IGF1R, INS, PARD6B, FGF7, FGF8, CDH1, PDGFC, P2RY1, FGF20, FGF22, VAV3, VEGFC, NGF, EFNA2, GNAS, LCP2, FGFR3, PFN3, SKAP1	1.63082
Allograft rejection	0.018333	CD86, CD40, IL5, IFNG, HLA-B, HLA-C, HLA-E, HLA-DQB1	2.883977
Osteoclast differentiation	0.018526	IFNB1, NCF2, STAT1, NCF4, NFATC2, CYBA, LILRB4, SIRPB1, FOSL2, FOSL1, IL1A, FCGR2A, SOCS1, CALCR, PPP3R2, IFNG, IL1B, LCP2	1.826519
Legionellosis	0.018949	PYCARD, IL6, ITGAM, CXCL8, CASP8, CR1L, IL1B, HSPA6, CASP1, TLR4	2.44623
Thyroid hormone synthesis	0.01927	GPX2, TTR, ATF6B, HSPA5, ATP1A4, GNAS, LRP2, ADCY8, SLC26A4, SERPINA7, ASGR2, PDIA4	2.191823
Leishmaniasis	0.023065	IL1A, FCGR2A, ITGAM, IFNG, NCF2, CR1L, STAT1, IL1B, NCF4, CYBA, TLR4, HLA-DQB1	2.134892
Metabolism of xenobiotics by cytochrome P450	0.025155	ALDH3A1, ADH4, HPGDS, CYP2A13, UGT1A1, CYP2S1, UGT2B15, MGST1, DHDH, CYP3A4, ADH6, UGT1A6	2.107522
Chemical carcinogenesis - DNA adducts	0.02948	CYP2C8, HPGDS, CYP2A13, UGT1A1, CYP3A43, UGT2B15, MGST1, CYP3A4, SULT1A4, UGT1A6, CYP3A7	2.152683
RIG-I-like receptor signaling pathway	0.032167	IFIH1, IFNA7, IFNA14, CXCL8, CASP8, RNF125, IFNA1, IFNB1, DHX58, IFNK, IFNW1	2.122363
cAMP signaling pathway	0.03782	GRIA2, GPR119, HHIP, LHB, ATP1A4, ADCY8, GLI3, HCAR2, HCAR3, EDNRA, MC2R, PLN, NPY, CNGA4, VAV3, EDN2, HTR1D, GCG, SSTR1, SST, PDE3A, GNAS, CNGB3, CNGB1, GPHB5	1.522099
Human papillomavirus infection	0.039534	PTGER4, IFNA7, ITGB5, IFNA1, WNT8A, FZD10, THBS2, COMP, PARD6B, CASP8, RELN, WNT11, IBSP, SPP1, ITGB8, ITGB7, ATP6V0A4, ITGB6, HES6, JAG1, IFNA14, LAMB3, IFNB1, STAT1, WNT3A, MX2, HLA-B, HLA-C, HLA-E, COL4A1, TBPL2, GNAS, TP53, CRB3	1.407137
Necroptosis	0.04064	ZBP1, IFNA7, IFNA14, PLA2G4D, IFNA1, IFNB1, STAT1, PYCARD, IL1A, GLUD2, CASP8, IFNG, IL1B, CASP1, TNFSF10, NLRP3, SLC25A31, RBCK1, TLR4	1.636974
Measles	0.042914	IFNA7, IFNA14, IFNA1, IFNB1, STAT1, MX2, HSPA6, IL2RG, IFIH1, IL1A, IL6, CASP8, OAS1, IL1B, IL2RB, TP53, TLR4	1.687545
Starch and sucrose metabolism	0.043747	MGAM2, AGL, AMY1B, SI, TREH, ENPP3, HK2	2.663673
Tyrosine metabolism	0.043747	ALDH3A1, ADH4, MAOB, TH, AOX1, HPD, ADH6	2.663673
Complement and coagulation cascades	0.047035	PROCR, ITGAM, C6, SERPINE2, C7, CR1L, CFHR4, C9, F11, BDKRB1, PLAT, F2	1.911473
Pertussis	0.048194	PYCARD, IL1A, IL6, ITGAM, CXCL8, IL23A, IL1B, CASP1, NLRP3, LY96, TLR4	1.982734
African trypanosomiasis	0.049131	IL6, IFNG, IL1B, F2RL1, HBA2, APOL1, SELE	2.591682

Table 5. Kegg pathways and genes downregulated 1.5 fold in LuCaP 173.1 tumors treated with Entrectinib (20mg/kg).

Kegg pathways	P-Value	Genes	Fold Enrichment
Neuroactive ligand-receptor interaction	1.51E-12	GLP1R, OXTR, VIPR2, HTR2B, PRL, ADRA1B, QRFP, RXFP1, BRS3, CYSLTR1, QRFPR, INSL5, PTGDR, PAQR9, CHRNB4, CHRNB3, OPRM1, F2, GABRG3, GABRG2, VGF, CCKBR, AGTR2, GRIA1, CHRNA3, PTGER1, PTGER2, CHRNA7, LHB, CHRNA6, PTGER3, FPR3, MCHR1, CRHR1, KNG1, GHRHR, GLRA1, MC2R, HRH1, CALCR, GALR3, CNR2, P2RY2, PATE2, NPVF, DRD1, HCRT, S1PR4, GABRA1, GABRA5, GCGR, GCG, GRIN2D, GH1, P2RX3, LPAR6, RLN1, GALP, GPHB5	2.751752232
Cytokine-cytokine receptor interaction	8.60E-06	ACVRL1, IL22, IFNA7, CXCL9, CTF1, IL20, IFNA1, IL26, CXCR5, CXCL17, CSF2RB, IL27, PRL, CXCL13, EDA2R, CXCR1, CCR8, IFNA21, CCL25, NGFR, IFNA14, IFNB1, IL37, TNFSF15, IL36G, GDF5, BMP7, IFNW1, BMP5, IL22RA1, GH1, BMP3, CXCL10, CXCL11, IL6, IFNG, ACKR4, IL17C	2.190032337
Toll-like receptor signaling pathway	4.62E-05	CD86, IFNA7, CXCL9, TICAM2, IFNA14, IFNA1, IFNB1, STAT1, TLR1, CXCL10, CXCL11, IL6, SPP1, TLR8, IRF5, TLR7, TLR3, TLR2, IFNA21	3.011294463
Nicotine addiction	3.90E-04	GRIA1, GABRA1, GABRA5, CHRNA7, CHRNA6, SLC17A6, SLC17A7, GABRG3, GABRG2, GRIN2D	4.279207921
JAK-STAT signaling pathway	6.28E-04	PDGFRA, IL22, IFNA7, IL20, CTF1, IFNA14, IFNA1, IFNB1, STAT1, IL26, FHL1, IL27, CSF2RB, PRL, IFNW1, IL22RA1, GH1, IL6, CCND2, IFNG, JAK3, IFNA21	2.268495765
Cell adhesion molecules	8.33E-04	CD86, CD274, SELPLG, ITGAM, HLA-B, HLA-C, ITGAL, SELE, HLA-E, SELP, CDH3, ALCAM, SLITRK2, CDH1, CLDN14, CLDN34, ITGA8, CNTN2, CLDN16, ITGA9, LRRC4B	2.275021933
Human papillomavirus infection	8.54E-04	IFNA7, IFNA1, WNT8A, FZD10, COMP, CCND2, SPP1, ATP6V0A4, ITGB6, HES3, WNT1, HES5, HES4, IFNA21, FZD1, APC2, IFNA14, LAMB3, IFNB1, STAT1, WNT3A, MX2, HLA-B, HLA-C, ISG15, HLA-E, COL2A1, COL1A2, TBPL2, COL6A1, ITGA11, ITGA8, TP53, TLR3, ITGA9	1.809936885
PI3K-Akt signaling pathway	9.46E-04	IFNA7, FLT1, ATF6B, IFNA1, FLT4, PRL, INS, COMP, GNG3, CCND2, SPP1, GNG8, ITGB6, PCK1, JAK3, IFNA21, NGFR, PDGFRA, IFNA14, LAMB3, IFNB1, IGF2, VEGFC, EREG, GH1, IL6, COL2A1, EFNA2, COL1A2, LPAR6, COL6A1, ITGA11, ITGA8, TEK, TP53, ITGA9, TLR2	1.764130285
Morphine addiction	0.002249	GABRA1, KCNJ6, PDE1C, KCNJ9, GABRA5, OPRM1, ADCY8, GABRG3, GABRG2, GNG3, PDE3A, GNG8, PDE7B, DRD1	2.63335872
Dilated cardiomyopathy	0.002498	CAV3, ADCY8, CACNG7, ACTC1, PLN, SGCD, TNNT2, ITGA11, ITGA8, SSPN, ITGB6, CACNG1, MYH6, ITGA9, MYH7	2.492742478
Phagosome	0.003147	COLEC11, ITGAM, TUBAL3, NCF1, SFTPA2, NCF4, HLA-B, TAP2, HLA-C, TAP1, CYBA, HLA-E, COMP, TUBA3E, FCGR2A, TUBB2A, OLR1, ATP6V0A4, TLR2	2.13960396
Hypertrophic cardiomyopathy	0.003978	CAV3, CACNG7, IL6, ACTC1, SGCD, TNNT2, ITGA11, ITGA8, SSPN, ITGB6, CACNG1, MYH6, ITGA9, MYH7	2.470470552
Mucin type O-glycan biosynthesis	0.004182	GALNT14, GALNT4, B3GNT6, GCNT4, GALNTL6, ST6GALNAC3, C1GALT1C1L, GALNT10	3.803740374
ECM-receptor interaction	0.00529	LAMB3, MEPE, DMP1, COMP, COL2A1, COL1A2, SV2B, COL6A1, ITGA11, ITGA8, SPP1, ITGB6, ITGA9	2.500211369
Protein digestion and absorption	0.006652	CPA2, COL26A1, CPA1, CPB2, KCNJ13, CTRB1, ATP1A4, ATP1B4, DPP4, COL2A1, COL1A2, XPNPEP2, COL6A1, COL8A1	2.326559646
Malaria	0.007766	SELP, COMP, IL6, IFNG, GYPC, HBA2, ITGAL, SELE, TLR2	3.081029703
Taste transduction	0.010951	TAS2R7, GABRA1, TAS2R30, P2RX3, PDE1C, GNAT3, GABRA5, TAS2R46, TAS2R1, TAS2R16, ADCY8, TAS2R39	2.388395119
Cytosolic DNA-sensing pathway	0.011296	CXCL10, IL6, IFNA7, IFNA14, IFNA1, IFNB1, DNASE2B, NLRP3, CGAS, SAMHD1, IFNA21	2.510468647
Viral protein interaction with cytokine and cytokine receptor	0.013146	CCL25, CXCL9, IL20, IL37, CXCR5, CXCL13, IL22RA1, CXCL10, CXCL11, IL6, CXCR1, ACKR4, CCR8	2.225188119
Viral myocarditis	0.015138	CD86, SGCD, CAV3, HLA-B, SSPN, HLA-C, ITGAL, MYH6, MYH7, HLA-E	2.554750997
Coronavirus disease - COVID-19	0.016324	IFNA7, IFNA14, IFNA1, IFNB1, STAT1, MX2, MMP3, CGAS, ISG15, F2, SELP, CXCL10, RPS17, IL6, FCGR2A, C6, C9, TLR8, NLRP3, TLR7, TLR3, TLR2, IFNA21	1.696927279
Arrhythmogenic right ventricular cardiomyopathy	0.023671	CACNG7, SGCD, CAV3, ITGA11, LEF1, SSPN, ITGA8, CTNNA3, CACNG1, ITGB6, ITGA9	2.241489863
Epstein-Barr virus infection	0.026391	IFNA7, IFNA14, IFNA1, IFNB1, STAT1, HLA-B, TAP2, HLA-C, TAP1, ISG15, ITGAL, HLA-E, CXCL10, IL6, CCND2, BLNK, JAK3, TP53, TLR2, IFNA21	1.69473581
Complement and coagulation cascades	0.027399	PROCR, F7, CPB2, ITGAM, C6, PLAU, C9, PLAT, A2M, F2, KNG1	2.189362192
Linoleic acid metabolism	0.028076	PLA2G4F, CYP2C8, PLA2G12B, PLA2G2A, PLAAT3, PLA2G5	3.423366337
Basal cell carcinoma	0.029054	FZD1, APC2, SHH, WNT3A, LEF1, WNT8A, FZD10, WNT1, TP53	2.445261669
Autoimmune thyroid disease	0.033072	CD86, IFNA7, IFNA14, IFNA1, HLA-B, HLA-C, IFNA21, HLA-E	2.583672707
Pathways in cancer	0.037112	ALK, IFNA7, IFNA1, PTGER1, FLT4, PTGER2, PTGER3, LEF1, WNT8A, CSF2RB, KLK3, FZD10, ADCY8, KNG1, RASGRP3, DLL3, DLL4, SHH, GNG3, CCND2, CDH1, GNG8, CTNNA3, WNT1, JAK3, HES5, IFNA21, FZD1, APC2, PDGFRA, IFNA14, LAMB3, STAT1, WNT3A, MMP2, IGF2, VEGFC, F2, IL6, IFNG, LPAR6, TP53	1.353873692
Calcium signaling pathway	0.038652	PDGFRA, OXTR, FLT1, PDE1C, PTGER1, CHRNA7, FLT4, PTGER3, HTR2B, VEGFC, ADCY8, ADRA1B, GRIN2D, HRH1, CYSLTR1, PLN, P2RX3, PLCZ1, CCKBR, SLN, CASQ1, DRD1, SLC25A6	1.556075608
Human cytomegalovirus infection	0.038948	PDGFRA, IFNA7, IFNA14, ATF6B, IFNA1, IFNB1, PTGER1, PTGER2, PTGER3, HLA-B, TAP2, HLA-C, TAP1, CGAS, ADCY8, HLA-E, GNG3, IL6, GNG8, TP53, IFNA21	1.597570957
NOD-like receptor signaling pathway	0.043437	GBP5, IFNA7, GBP7, IFNA14, IFNA1, IFNB1, STAT1, CYBA, IL6, CASP12, CARD18, PYDC1, NLRP3, GBP2, GBP1, GBP4, GBP3, IFNA21	1.656467582

Table 6. Kegg pathways and genes downregulated 1.5 fold in LuCaP 173.1 tumors treated with alectinib (20mg/kg).

Kegg pathways	P-Value	Genes	Fold Enrichment
Neuroactive ligand-receptor interaction	2.22E-09	SCT, PTH1R, ADRA1A, RXFP1, RXFP3, GABRR1, CYSLTR1, EDNRA, HTR7, INSL5, TSHB, PTGDR, CHRNB3, TACR2, SSTR1, OPRM1, F2, PRLR, GABRG2, SSTR4, UTS2B, AGTR2, GRIA1, NPB, GRIA2, CHRNA6, LPAR3, LYPD6, MC2R, CALCR, GALR3, P2RY2, PATE2, NPVF, NPBWR2, HRH4, KISS1R, DRD1, HCRT, S1PR4, GABRA1, GABBR1, GCG, NMBR, APLN, KISS1, GH1, P2RX3, LPAR6, GPHB5	2.527160248
Estrogen signaling pathway	3.74E-04	GABBR1, SHC3, ATF6B, CALML5, KCNJ9, MMP2, KRT24, TGFA, KRT32, OPRM1, KRT31, ADCY8, EGFR, KRT33A, KRT16, GPER1, GNAQ, KRT15, KRT14	2.572538454
Cytokine-cytokine receptor interaction	6.26E-04	ACVRL1, IL22, IFNA7, CXCL9, CSF3R, IL25, IL26, CXCR5, CXCL13, CXCL16, IL1RL2, CXCR1, TNFSF10, CCR8, CCR7, XCR1, IFNA14, GDF5, PRLR, IFNW1, IL22RA1, GH1, BMP3, CXCL10, CXCL11, IL6, IL5, IFNG, XCL2, IL18R1, IL17B	1.936128091
Steroid hormone biosynthesis	0.00158816	UGT1A1, CYP11A1, CYP11B1, UGT2B15, AKR1D1, HSD17B2, AKR1C2, HSD17B8, UGT1A6, CYP17A1, CYP3A7	3.291014814
PI3K-Akt signaling pathway	0.00173901	IFNA7, PHLPP1, CSF3R, ATF6B, LAMA1, FLT4, LAMA3, TGFA, LPAR3, EFNA4, EGFR, IGF1R, INS, COMP, RELN, CCND2, MYC, CHAD, SPP1, ITGB7, FGF22, IFNA14, FN1, VEGFC, FLT3LG, PRLR, EREG, GH1, IL6, LPAR6, ITGA8, TEK, EPHA2, TLR2	1.756763542
Toll-like receptor signaling pathway	0.00186108	IFNA7, CXCL9, TICAM2, IFNA14, STAT1, LY96, TLR1, CXCL10, CXCL11, IL6, SPP1, TLR8, TLR6, TLR3, TLR2	2.576299475
Influenza A	0.00205215	CIITA, IFNA7, IFNA14, RSAD2, STAT1, MX2, PABPN1L, IFIH1, CXCL10, IL6, NXF3, IFNG, OAS1, OAS2, OAS3, CASP1, TNFSF10, NLRP3, TLR3, SLC25A6	2.169515348
NOD-like receptor signaling pathway	0.00234519	GBP5, IFNA7, GBP7, IFNA14, STAT1, IL6, CASP12, CASP5, OAS1, NLRP6, OAS2, OAS3, CASP1, CARD18, NLRP3, CARD16, GBP2, GBP1, GBP4, BIRC3, GBP3	2.094282154
Viral protein interaction with cytokine and cytokine receptor	0.00260552	CXCL9, XCR1, CXCR5, CXCL13, IL22RA1, CXCL10, CXCL11, IL6, CXCR1, TNFSF10, XCL2, CCR8, CCR7, IL18R1	2.596909871
Hepatitis C	0.00481273	IFNA7, IFNA14, RSAD2, STAT1, MX2, EGFR, CXCL10, IFNG, OAS1, CLDN14, OAS2, MYC, OAS3, CLDN23, CLDN34, CLDN7, CLDN16, TLR3	2.113217798
Malaria	0.00481862	COMP, IL6, KLRK1, VCAM1, IFNG, GYPC, HBA2, SELE, TLR2	3.33888412
Taste transduction	0.00613551	TAS2R7, GABRA1, GABBR1, TAS2R30, P2RX3, GNAT3, TAS2R46, TAS2R1, PKD2L1, TAS2R16, ADCY8, SCN2A	2.588282264
Focal adhesion	0.0063524	SHC3, LAMA1, FLT4, CAV1, LAMA3, FN1, VEGFC, EMP1, EGFR, IGF1R, MYLK4, COMP, RELN, CCND2, CHAD, ITGA8, SPP1, MYL10, ITGB7, TLN2, BIRC3	1.91889892
Cortisol synthesis and secretion	0.00760458	MC2R, ATF6B, CYP11A1, CYP11B1, GNAQ, KCNA4, ADCY8, KCNK2, CACNA1G, CYP17A1	2.853747111
Retinol metabolism	0.01017587	SDR16C5, CYP26A1, ADH4, UGT1A1, DHRS9, UGT2B15, BCO1, CYP2C18, UGT1A6, CYP3A7	2.727846503
Cell adhesion molecules	0.01080259	CD274, VCAM1, HLA-B, HLA-C, SELE, SPN, VCAN, CLDN14, CLDN23, CLDN34, CLDN7, ITGA8, MADCAM1, ITGB7, PDCD1, CLDN16, CD99	1.995816809
Mucin type O-glycan biosynthesis	0.01153936	GALNT4, GALNT3, GALNTL5, GCNT4, ST6GALNAC3, C1GALT1C1L, GALNT10	3.606819266
African trypanosomiasis	0.01316503	IL6, VCAM1, IFNG, GNAQ, HBA2, APOL1, SELE	3.509337664
Coronavirus disease - COVID-19	0.01344748	IFNA7, IFNA14, STAT1, MX2, F2, RPL17-C18ORF32, EGFR, IFIH1, CXCL10, RPS17, IL6, FCGR2A, C8G, OAS1, OAS2, OAS3, C9, CASP1, TLR8, NLRP3, TLR3, TLR2	1.758990676
JAK-STAT signaling pathway	0.01674245	IL22, IFNA7, CSF3R, IFNA14, STAT1, IL26, PRLR, EGFR, IFNW1, IL22RA1, GH1, IL6, IL5, CCND2, IFNG, MYC, STAT4	1.899632866
Ovarian steroidogenesis	0.01852416	PLA2G4F, CYP11A1, HSD17B2, ACOT1, ADCY8, CYP17A1, IGF1R, INS	2.909702937
GnRH secretion	0.02068539	KISS1, GABBR1, KCNJ9, TRPC4, GPER1, GNAQ, SPP1, KISS1R, CACNA1G	2.608503219
ECM-receptor interaction	0.02073928	COMP, RELN, LAMA1, LAMA3, CHAD, ITGA8, SPP1, FN1, MEPE, ITGB7, FREM2	2.292617061
Inflammatory bowel disease	0.02252129	IL22, IL6, MAF, IL5, IFNG, STAT1, STAT4, IL18R1, TLR2	2.5683724
Chemical carcinogenesis - DNA adducts	0.0334393	HPGDS, CYP2A13, UGT1A1, CYP3A43, UGT2B15, AKR1C2, CYP2C18, UGT1A6, CYP3A7	2.384917229
Lipid and atherosclerosis	0.04109125	IFNA7, TICAM2, VCAM1, IFNA14, CALML5, NCF4, LY96, APOA4, SELE, CASP7, IL6, CASP1, TNFSF10, OLR1, NLRP3, TLR6, APOB, MAP3K5, TLR2	1.639245434
TNF signaling pathway	0.04249713	CXCL10, IL6, CASP7, VCAM1, JAG1, ATF6B, IRF1, VEGFC, SELE, IL18R1, MAP3K5, BIRC3	1.952563813
Cytosolic DNA-sensing pathway	0.04749486	CXCL10, IL6, IFNA7, CASP7, IFNA14, CASP1, NLRP3, POLR3G, SAMHD1	2.225922747

Tables 1-3. 42D cells were treated with ALK inhibitors, alectinib and entrectinib, and CM 272 for 48hrs. RNA was isolated and sent for sequencing by BGI. The tables were generated by identifying genes that were downregulated 1.5 and using the online tool NIH DAVID tool https://david.ncifcrf.gov/. Tables display the predicted changes in pathways and genes in 42D cells after treatment. **Tables 4-6** LuCaP 173.1 tumors were treated with ALK inhibitors entrectinib and alectinib for 30 days. The tables display Kegg pathways and genes downregulated by ALK inhibitor treatment. The tables 4-6 were created using the same protocol as 42D cells. All tables list pathways that are predicted to be altered with a p-value < .05.

Figure 4

A

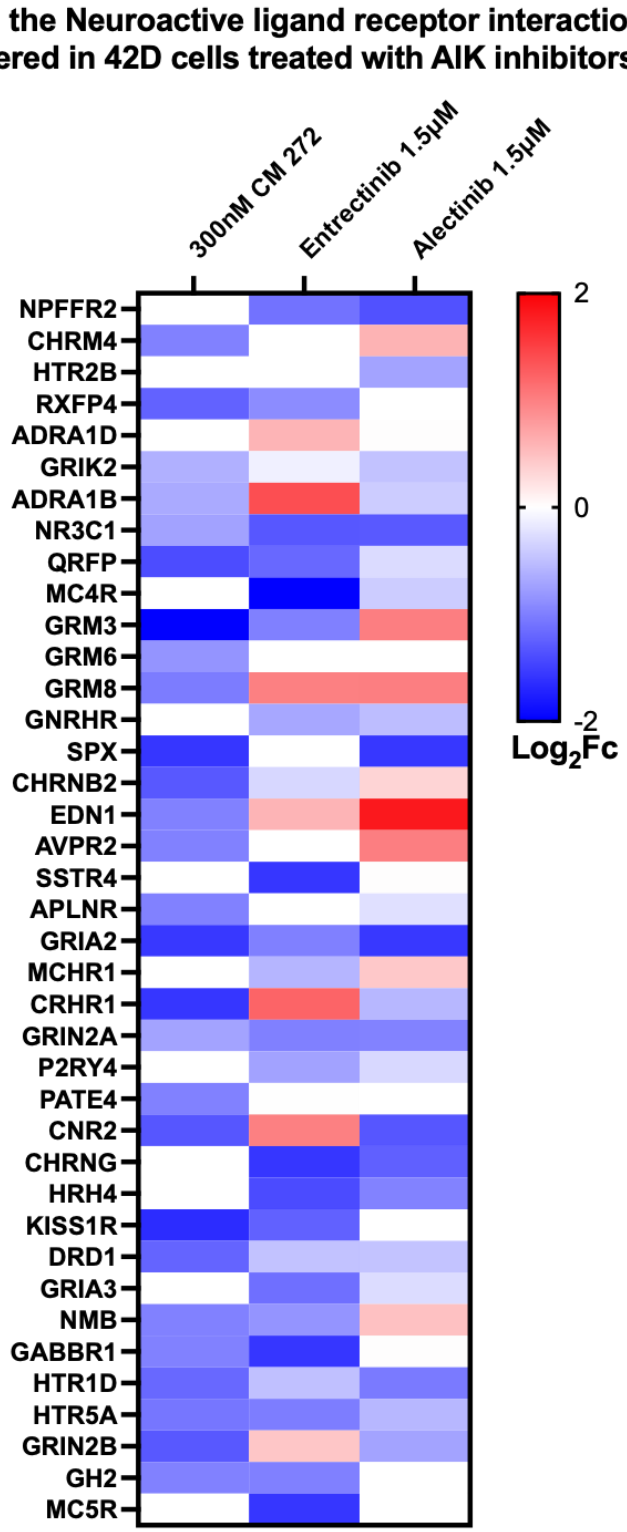
Changes in the Neuroactive ligand receptor interaction gene program were altered in 42D cells treated with AIK inhibitors and CM 272
300nM CM 272
Entrectinib 1.5μM
Alectinib 1.5μM
NPFFR2
CHRM4
HTR2B
RXFP4
ADRA1D
GRIK2
ADRA1B
NR3C1
QRFP
MC4R
GRM3
GRM6
GRM8
GNRHR
SPX
CHRNB2
EDN1
AVPR2
SSTR4
APLNR
GRIA2
MCHR1
CRHR1
GRIN2A
P2RY4
PATE4
CNR2
CHRNG
HRH4
KISS1R
DRD1
GRIA3
NMB
GABBR1
HTR1D
HTR5A
GRIN2B
GH2
MC5R
2
0
-2
Log2Fc

Figure 4 continued

B

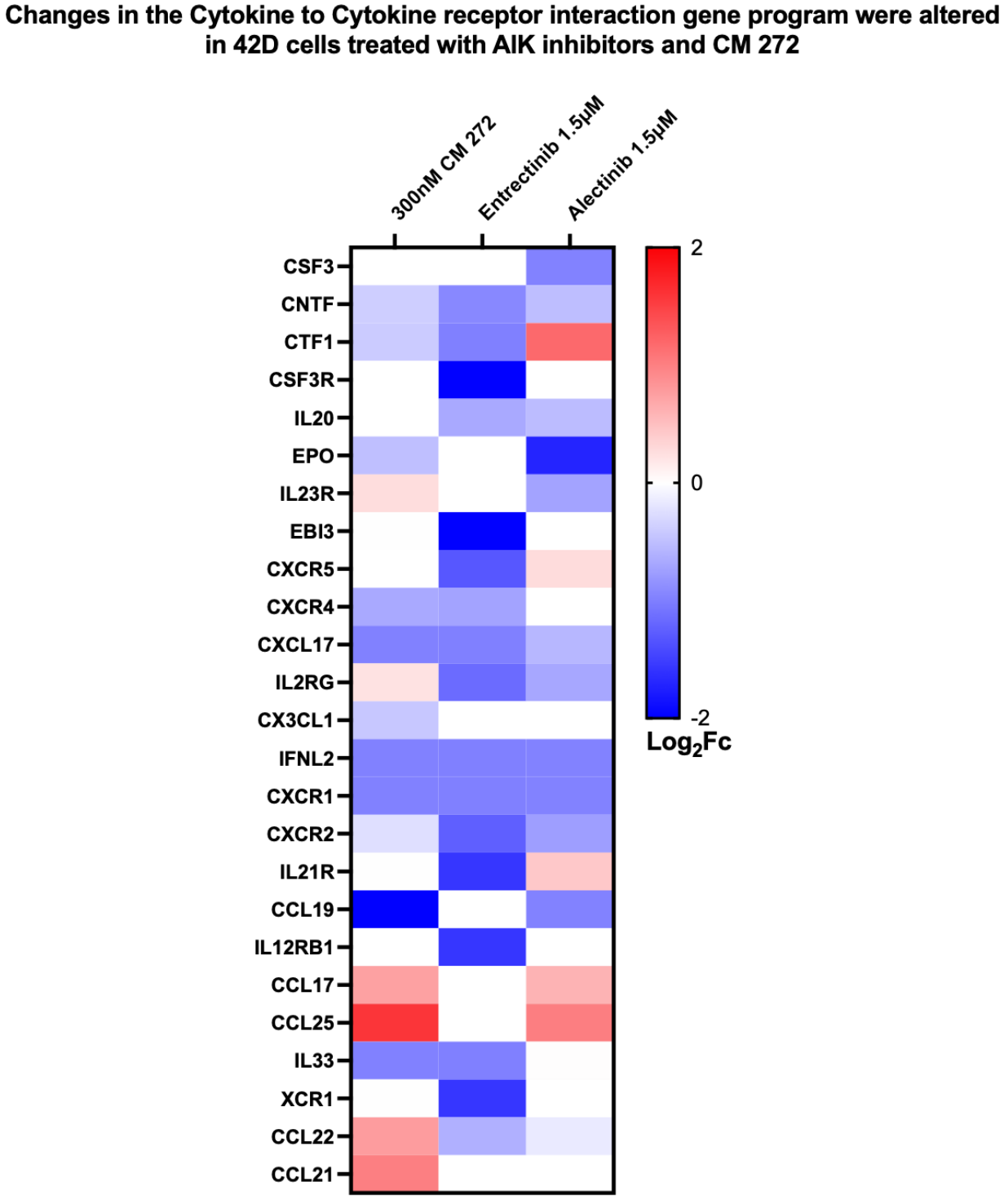

Figure 4 continued

C

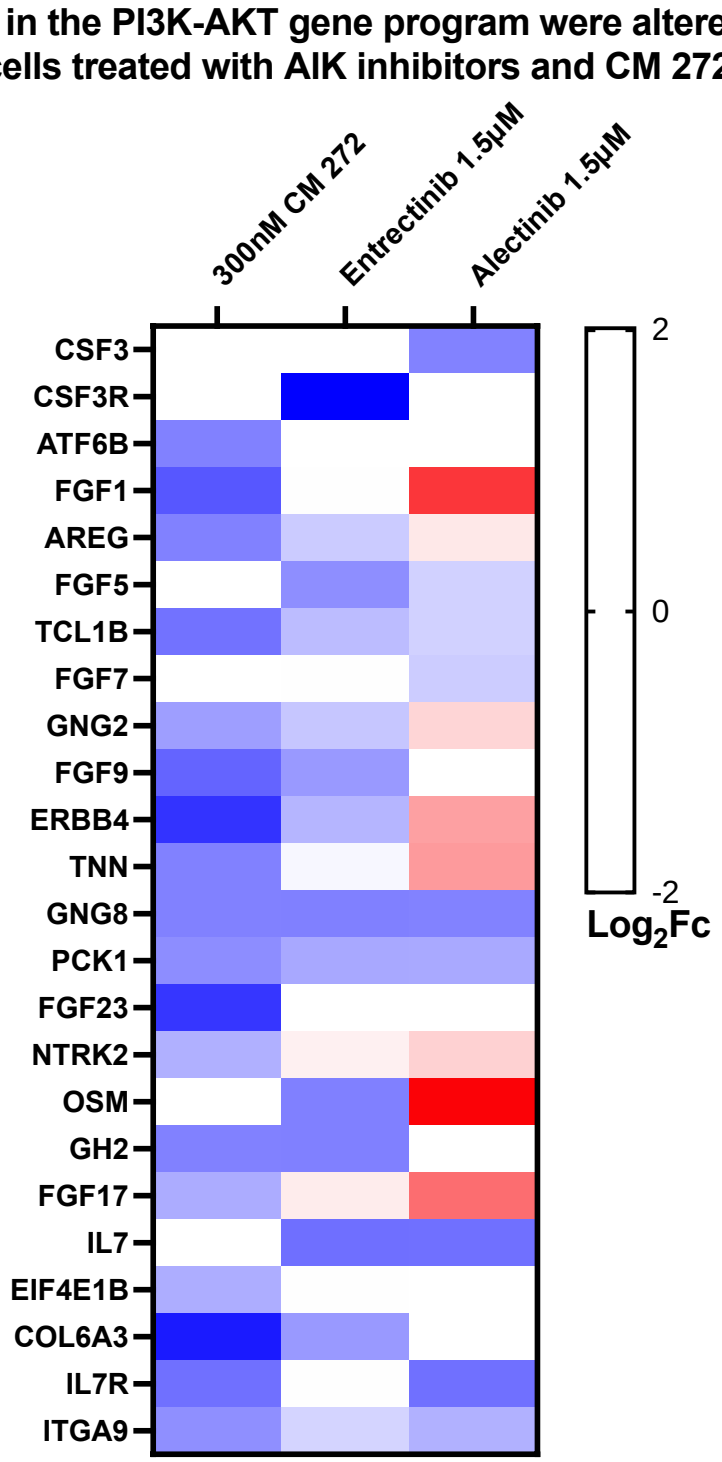

Figure 4 continued

D

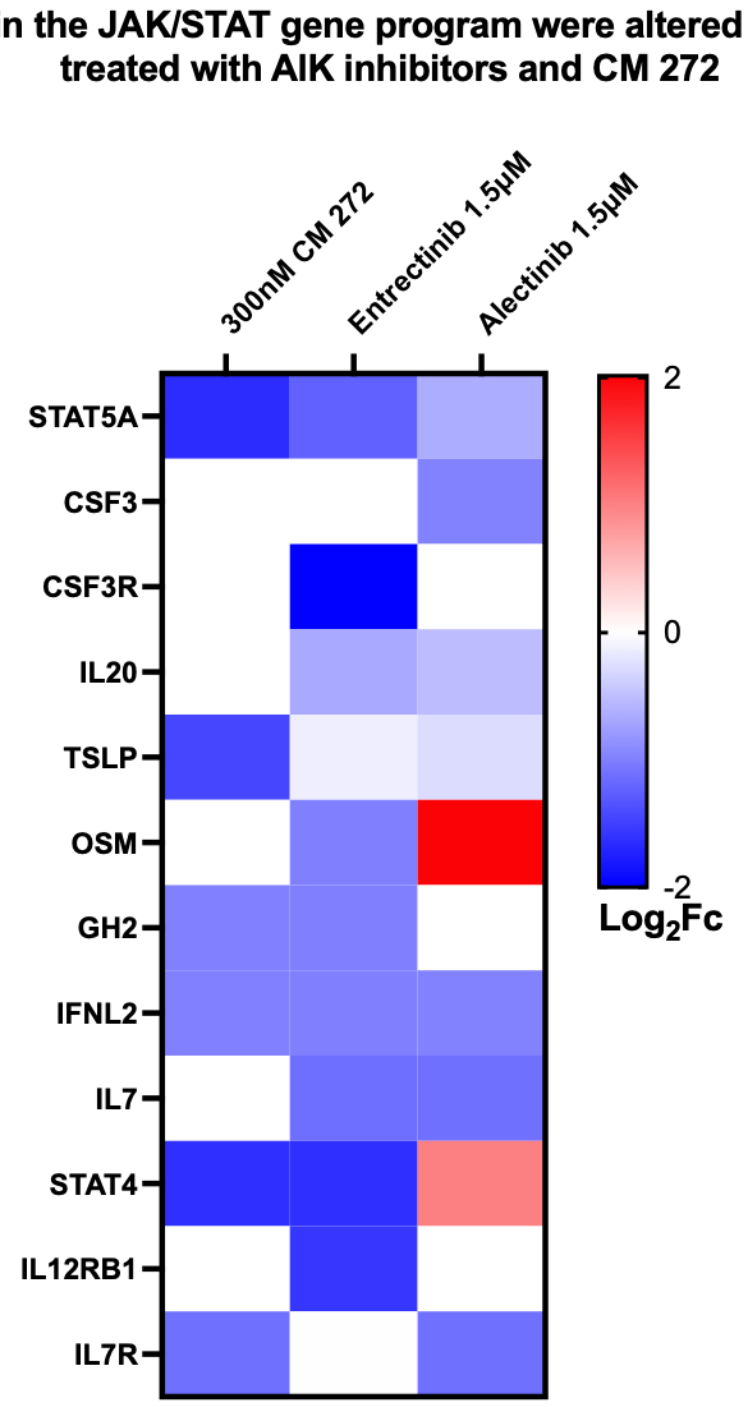

Figure 4. 42D cells were treated with the ALK inhibitors entrectinib and alectinib for 48hrs and RNA was isolated and sent for sequencing by BGI. RNA sequencing was analyzed using DAVID then verified by looking at gene programs listed by DAVID. **A.** The genes in the Neuroactive ligand receptor gene program were analyzed. RNA seq data showed that several genes in the Neuroactive ligand receptor pathway were downregulated after treatment. **B.** The genes in the cytokine-to-cytokine receptor interaction gene pathway were analyzed. Several genes in the cytokine-to-cytokine receptor interaction gene pathway were downregulated. **C.** The genes in the PI3K-AKT gene program were analyzed. RNA seq data showed that several genes in the PI3K-AKT pathway were downregulated after treatment. **D.** The genes in the JAK/STAT gene program were analyzed. RNA seq data showed that several genes in the JAK/STAT pathway were downregulated after treatment.

Figure 5

A

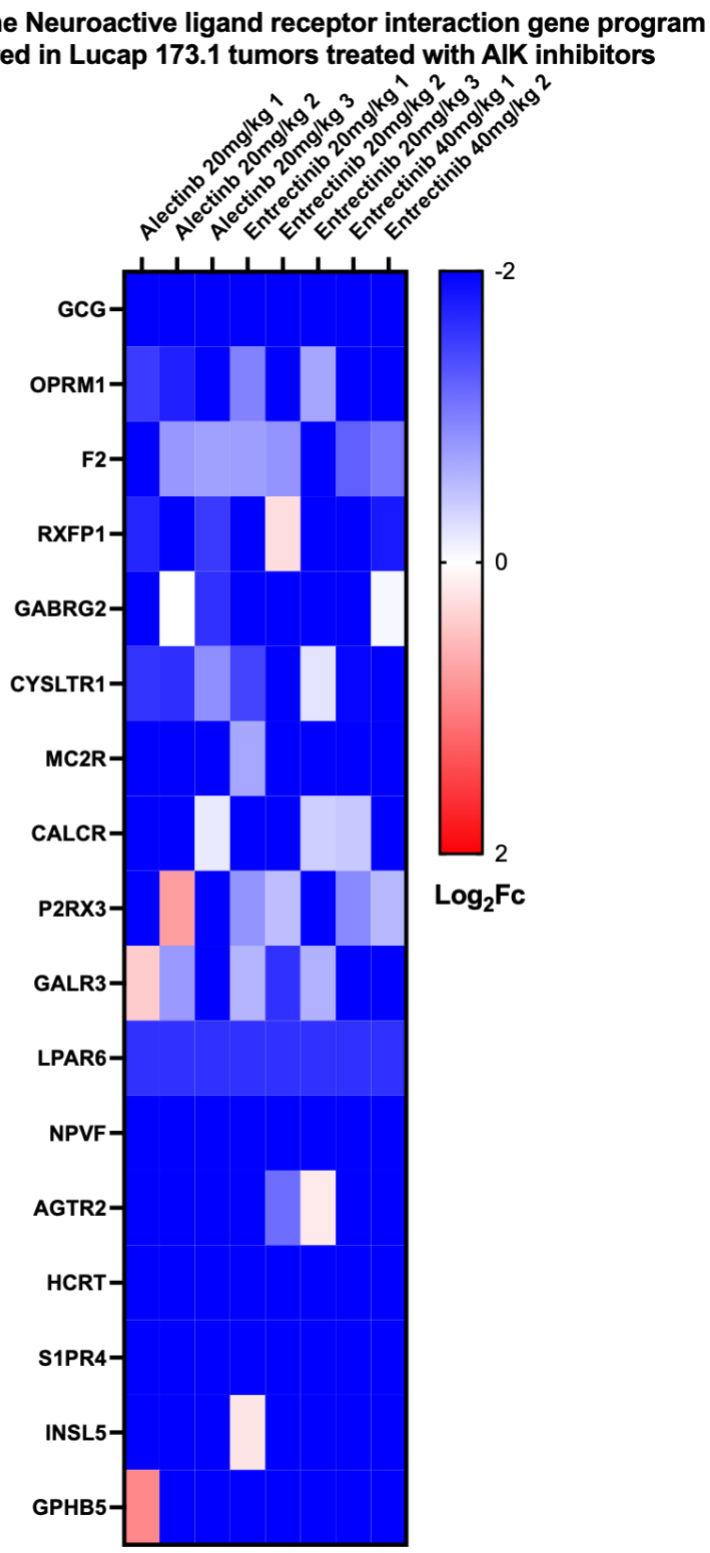
Changes in the Neuroactive ligand receptor interaction gene program were altered in Lucap 173.1 tumors treated with AlK inhibitors
Alectinb 20mg/kg 1
Alectinb 20mg/kg 2
Alectinb 20mg/kg 3
Entrectinib 20mg/kg 1
Entrectinib 20mg/kg 2
Entrectinib 20mg/kg 3
Entrectinib 40mg/kg 1
Entrectinib 40mg/kg 2
GCG
OPRM1
F2
RXFP1
GABRG2
CYSLTR1
MC2R
CALCR
P2RX3
GALR3
LPAR6
NPVF
AGTR2
HCRT
S1PR4
INSL5
GPHB5
-2
0
2
Log2Fc

Figure 5 continued

B

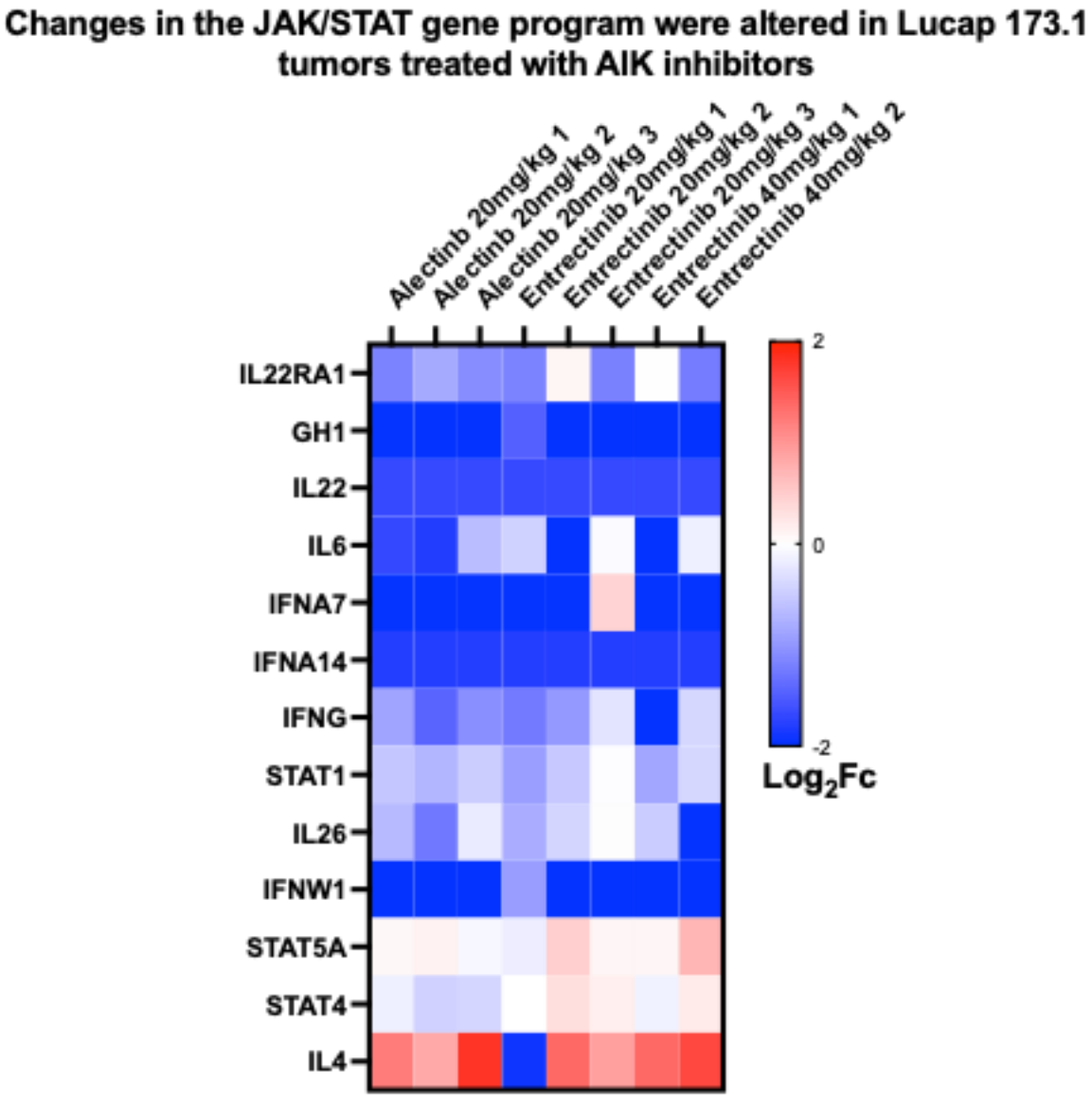

Figure 5 continued

C

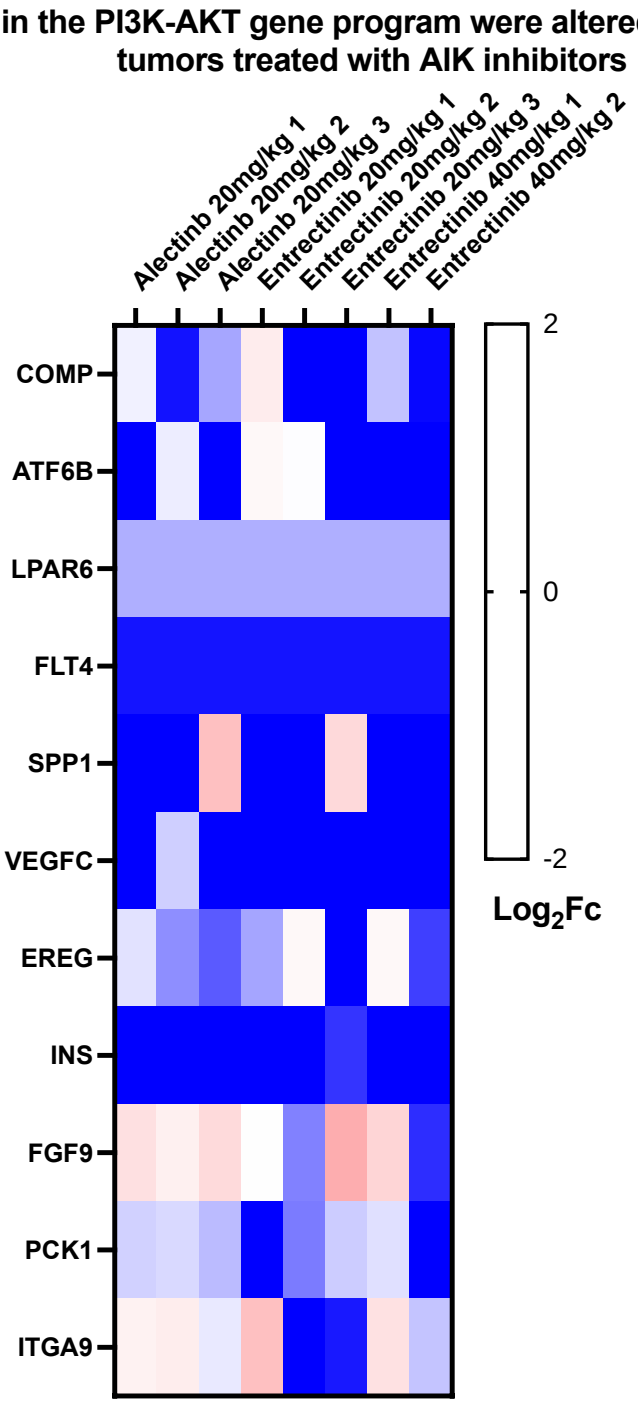

Figure 5. RNA seq analysis of LuCaP 173.1 tumors treated with alectinib and entrectinib for 30 days. After treatment tumors showed a decrease in volume and mass after treatment. LuCaP 173.1 tumors were dissected and digested for RNA isolation. RNA was sequenced by Novogene. **A.** The genes in the Neuroactive ligand receptor gene program were analyzed. RNA seq data showed that several genes in the Neuroactive ligand receptor pathway were downregulated after treatment in LuCaP 173.1 tumors. **B.** The genes in the JAK/STAT gene program were individually analyzed. RNA seq data showed that several genes in the JAK/STAT pathway were downregulated after treatment in LuCaP 173.1 tumors. **C.** The genes in the PI3K-AKT gene program were individually analyzed. RNA seq data showed that several genes in the PI3K-AKT pathway were downregulated after treatment in LuCaP 173.1 tumors.

Chapter 4: ALK receptors and NEPC discussion

Chapter 4.1 Discussion of ALK receptors in NEPC

This project aimed to expand the understanding of the functional role of ALK in NEPC. This project demonstrated that ALK inhibitors block cellular growth and proliferation of NEPC cells. This project showed that ALK inhibitors successfully inhibit de novo NEPC tumor growth. Unfortunately, these findings have previously been described using distinct ALK inhibitors and different cell lines (Patel et al., 2022). More importantly, the ALK inhibitor Alectinib has been shown to be a viable potential therapeutic for NEPC treatment (Carneiro et al., 2018). What is unique and informative about this project is that it expands upon the cellular pathways that are altered with ALK inhibitors. More importantly, it suggests potential synergistic partners that could work with ALK inhibitors in combination treatments.

Several distinct NEPC and CRPC cell lines were prepared and treated with ALK inhibitors. NCI-H660 and 42D cells have been extensively studied and have been shown to be suitable representatives for de novo and treatment-induced NEPC. C4-2Benzr is a treatment-induced NEPC cell line generated in the lab. Like NCI-H660 and 42D, C4-2Benzr expresses several NEPC markers, such as SYP, NSE, and CHGA. These three cell lines responded favorably to alectinib and entrectinib treatment. Interestingly, the C4-2B cell line, a CRPC representative, also responded to ALK inhibition. This project also tested the ALK/ROS1 inhibitor lorlatinib, but none of the cell lines responded to treatment. These experiments were also tested with the 42f cell

line, and a similar response was observed with all three ALK inhibitors. Lastly, Alectinib and entrectinib successfully inhibited cell growth and colony formation.

The next phase of this project was to establish that ALK was present in our NEPC cell lines and that ALK signaling was altered in the presence of ALK inhibitors. The cell lines 42D and C4-2Benzr showed robust expression of ALK, while NCI-H660 had little to no expression. More importantly, when looking at the JAK/STAT and PI3K-MAPK pathways, a decrease in phosphorylation of STAT3, AKT, and ERK is observed. In addition, the expression of NEPC markers such as SYP and CHGA decreased.

The next aim of the study was to show that these compounds could be used to inhibit tumor growth in animal models. The use of alectinib and entrectinib slowed tumor growth in NCI-H660 and LuCaP 173.1 tumors. More importantly, when examining tumor mass, ALK inhibitor treatment decreased tumor mass. The compound CM 272 could also be used in combination with alectinib or entrectinib to inhibit tumor growth further. This demonstrates that these two compounds are viable therapeutics for NEPC.

Alectinib and entrectinib inhibited tumor growth, so the next step was to characterize altered cellular pathways in 42D cells and de novo NEPC tumors treated with alectinib and entrectinib. Using the online tool NIH DAVID Bioinformatics, several pathways were predicted to be downregulated in cells treated with alectinib and entrectinib. These results align with our western blot results and our understanding of NEPC. Pathways such as Neuroactive ligand, JAK/STAT, and PI3K-AKT pathways were predicted to be altered in 42D cells treated with alectinib and entrectinib. These findings are further supported by the RNA seq data and

evaluation of each gene in the listed pathways. Several genes associated with the JAK/STAT and PI3K-AKT pathways were downregulated.

LuCaP 173.1 tumors demonstrated a similar result in downregulated pathways when treated with ALK inhibitors. The NIH David predicted altered pathways included Neuroactive ligand-receptor interaction, JAK/STAT, and PI3K-AKT. More interestingly, cytokine-to-cytokine receptor interaction pathway genes were altered in 42D and LuCaP 173.1 tumors. I next looked at the gene expression profile of each of these pathways, but upon closer examination of these pathways, the results became more ambiguous. Several genes were downregulated in all the listed pathways, but other genes were completely missing, even in the vehicle group. This suggests heterogeneity among the tumors and that more analysis is required.

Although several of these experiments are successful, there are several limitations within each of the experiments. These limitations include the fact that cell lines do not adequately represent tumors. Another limitation is that the tumors used in the experiment do not represent all variations of NEPC tumors, and results varied with each tumor. Lastly, RNA seq data does not capture changes within the DNA. Later, these limitations and the strategies to circumvent these problems are discussed in greater detail.

To find viable therapeutic drugs for treating NEPC, the lab conducted a large screening of several compounds and discovered that entrectinib successfully inhibited NEPC cell growth. This was initially done with one cell line and only one ALK inhibitor. Currently, several ALK inhibitors are used for cancer treatment. Different ALK inhibitors were acquired and tested to determine if they could inhibit NEPC cell growth. The complete list of cell lines used in the first experiment includes 42D, 42f, C4-2B, C4-2Benzr, Lapc4, Lapc4-enzr, and NCI-H660. The ALK inhibitors

alectinib and entrectinib inhibited cell growth in all these cell lines, including the lung cancer cell lines A549 and H1299. Although cells do not represent tumors, a large sample size of cells responding similarly to treatment does warrant further investigation. This experiment aimed to discover and verify compounds that could inhibit NEPC cell growth, which was successfully achieved.

The next goal of our experiment was to demonstrate that ALK inhibition disrupts ALK signaling in NEPC cells. Unfortunately, this experiment has several limitations that could not be overcome with Western blot. This technique only allows for the screening of proteins known to be present and does not reveal interactions between cellular pathways. Fortunately, this technique was used to verify our results for each experiment, such as a decrease in the phosphorylation of pAKT and pSTAT3, and more importantly, to confirm the presence of ALK in NEPC cells and the decrease in the expression of NEPC markers. This technique also enables us to visualize RNA sequencing data acquired through GSEA and David analysis.

To further verify our results, NEPC tumor models were prepared. NCI-H660 and LuCaP 173.1 tumors represent de novo NEPC. A limitation of using these tumor models is that they do not represent treated NEPC. Moreover, this project only used two different tumor models, although several NEPC tumor models are available. Despite this limitation, the advantage is that de novo NEPC represents the lethal form of NEPC. Thus, any successful experiment using these tumor models warrants further investigation. In various experiments, different tumors, although of the same type, can potentially respond differently to treatment. This limitation was mitigated by using a high tumor count for each treatment and randomizing the tumors.

The last experiment was RNA sequencing of 42D cells and LuCaP 173.1 tumors treated with alectinib and entrectinib. RNA sequencing is an excellent technique for capturing snapshots of proteins that are potentially in the process of being expressed. It captures all RNA available to be potentially translated or degraded, but this technique does not account for the latter.

This research project has made significant contributions to the field of NEPC and ALK inhibitors. For example, this project suggests that cytokine-to-cytokine receptor interactions contribute to NEPC cell and tumor growth. Alectinib and entrectinib treatment downregulated the cytokine-to-cytokine receptor interaction pathway in 42D cells and tumors. The field of NEPC research has established that cytokines and chemokines contribute to NEPC growth and survival and to CSC and EMT transitions (Adekoya and Richardson, 2020). Several potential therapeutic pathways have been identified using the RNA sequencing data, but further analysis is required.

The aldosterone sodium reabsorption pathway has recently been implicated in cancers. This pathway appeared in our results for cells and tumors treated with alectinib and entrectinib. The renin-angiotensin-aldosterone system (RAAS) is a biological system that has garnered much attention due to its role in cancer (Sun et al., 2017). The RAAS pathway could increase tumor growth and metastasis through angiotensin signaling, specifically via the AT1 receptor (Hassani et al., 2023). Although the RAAS pathway could have dual roles by releasing anti-inflammatory cytokines, it might also suppress tumor growth.

Our current RNA-seq data aligns with published results of ALK signaling. Treatment with either alectinib or entrectinib suppresses the JAK/STAT and PI3K-AKT pathways. More

importantly, cellular proliferation and tumor growth decrease is observed after treatment. This dataset corresponds with published results for lung cancer tumors and tumors with ALK mutations (Camidge et al., 2019). Significantly, our dataset is consistent with results from tumors with similar physiology, such as neuroblastomas. Neuroblastoma patients treated with ALK inhibitors show promising results, but in 14% of cases, they also develop resistance (Pastorino et al., 2023). Another type of cancer that our data correlates with is glioblastoma. Interestingly, ALK inhibition in glioblastomas induced cell death and stopped cell growth (Kalamatianos et al., 2018).

Our current dataset fits our understanding of ALK inhibition, but further exploration is necessary. A significant amount of data currently requires analysis. Only five pathways have been investigated, which represents a small subset of cancer cellular pathways. More importantly, results need to be reviewed and validated with wet lab experiments. qPCR of 42D cells and tumor RNA could further support current findings. Lastly, synergistic partners that could work with ALK inhibitors must be explored.

Chapter 4.2 The future of ALK and NEPC

As mentioned, the research relating ALK to NEPC is limited to only three studies. The first explains that mutant ALK F1174C was expressed in a patient, and this patient responded to ALK inhibition with Alectinib (Carneiro et al., 2018). A follow-up study by the same group explains that ALK functions with N-Myc to drive neuroendocrine differentiation (Unno et al., 2021). The last study explains that ALK expression is decreased in primary prostate cancer but

increased in a subset of mCRPC (Patel et al., 2022). This study expands on this knowledge by showing that de novo NEPC tumors respond to ALK inhibitors alectinib and entrectinib. In addition, this study highlights several potential therapeutic targets for the treatment of NEPC. Lastly, this study highlights a potential therapeutic combination treatment, alectinib or entrectinib, with CM 272.

ALK has a critical role in the survival and growth of a subset of Neuroendocrine prostate cancer. ALK inhibition with entrectinib and alectinib decreased cell growth and proliferation. NCI-H660 and LuCaP 173.1, de novo NEPC tumors, demonstrated decreased growth when treated with alectinib or entrectinib. More importantly, the G9a inhibitor further suppressed tumor growth when combined with ALK inhibition. RNA seq analysis revealed that several pathways related to ALK signaling, such as JAK/STAT and PI3K-pAKt pathways, were inhibited. In addition, the Neuroactive ligand-receptor pathway was suppressed. More data analysis of the RNA seq data is needed to expand on the results.

This project seeks to explore several areas of research. ALK inhibitors decrease cellular growth and survival, but how they change gene expression and alter DNA accessibility in NEPC remains unclear. Also, ALKi resistance frequently arises through the G1269A and G1202R mutations in ALK (Pan et al., 2021). It remains to be explored if ALKi treatment will lead to the onset of these mutations in NEPC tumors. Another area of exploration is what triggers the alteration of ALK in prostate cancer. A subset of mCRPC has been reported to have increased expression of ALK, but what triggers this increased expression (Patel et al., 2022)? More importantly, another question is why ALK mutations are rare in prostate cancer but more common in other types of cancer. As mentioned earlier, there are several distinct mutations in

ALK, which include chromosomal translocations, point mutations, and gain of function mutations, but these mutations are rare in prostate cancer. This begs the question: What is different in the DNA structure of the prostate cell that prevents or slows ALK mutation?

Another area of research that needs to be explored is the role of nTRKs and Ros1 in mCRPC and NEPC. The ALK inhibitor entrectinib targets nTRKs, ALK, and Ros1. In some cases, it was observed that entrectinib performed better than alectinib. This suggests that either nTRK or Ros1 have a critical role in NEPC. nTRK mutations, splice variants, and TRK overexpression have been detected in several cancers, including colorectal, lung, melanoma, and NSClC (Manea et al., 2022). A gene fusion of IRF2BP2-nTRK1 has been reported in prostatic adenocarcinoma (Yeh et al., 2019). More importantly, gene fusions of nTRK have been reported in neuroendocrine tumors (Bongarzone et al., 1989). A patient with the first report of nTRK fusion Neuroendocrine cancer reported a favorable response to combination treatment with entrectinib (Doebele et al., 2020). This result highlights the need to explore nTRKs in NEPC.

References

1. Abida, W., Cyrta, J., Heller, G., Prandi, D., Armenia, J., Coleman, I., Cieslik, M., Benelli, M., Robinson, D., Van Allen, E. M.*, et al.* (2019). Genomic correlates of clinical outcome in advanced prostate cancer. Proc Natl Acad Sci U S A *116*, 11428-11436.
2. Adams, J. (1853). The case of scirrhous of the prostate gland with corresponding affliction of the lymphatic glands in the lumbar region and in the pelvis. Lancet.
3. Adekoya, T. O., and Richardson, R. M. (2020). Cytokines and Chemokines as Mediators of Prostate Cancer Metastasis. Int J Mol Sci *21*.
4. Agency, E. M. (2018). Alecensa (alectinib): summary of product characteristics.
5. Akamatsu, S., Wyatt, A. W., Lin, D., Lysakowski, S., Zhang, F., Kim, S., Tse, C., Wang, K., Mo, F., Haegert, A.*, et al.* (2015). The Placental Gene PEG10 Promotes Progression of Neuroendocrine Prostate Cancer. Cell Rep *12*, 922-936.
6. Akaza, H., Hinotsu, S., Usami, M., Arai, Y., Kanetake, H., Naito, S., and Hirao, Y. (2009). Combined androgen blockade with bicalutamide for advanced prostate cancer: long-term follow-up of a phase 3, double-blind, randomized study for survival. Cancer *115*, 3437-3445.
7. Alain, C., Pascal, N., Valérie, G., and Thierry, V. (2021). Orexins/Hypocretins and Cancer: A Neuropeptide as Emerging Target. Molecules *26*.
8. Alexander, S. P., Mathie, A., and Peters, J. A. (2011). Guide to Receptors and Channels (GRAC), 5th edition. Br J Pharmacol *164 Suppl 1*, S1-324.

9. Alva, A., and Hussain, M. (2013). The changing natural history of metastatic prostate cancer. Cancer J *19*, 19-24.

10. Anderson, K. M., and Liao, S. (1968). Selective retention of dihydrotestosterone by prostatic nuclei. Nature *219*, 277-279.

11. Antonarakis, E. S., Lu, C., Luber, B., Wang, H., Chen, Y., Zhu, Y., Silberstein, J. L., Taylor, M. N., Maughan, B. L., Denmeade, S. R.*, et al.* (2017). Clinical Significance of Androgen Receptor Splice Variant-7 mRNA Detection in Circulating Tumor Cells of Men With Metastatic Castration-Resistant Prostate Cancer Treated With First- and Second-Line Abiraterone and Enzalutamide. J Clin Oncol *35*, 2149-2156.

12. Antonarakis, E. S., Lu, C., Wang, H., Luber, B., Nakazawa, M., Roeser, J. C., Chen, Y., Mohammad, T. A., Chen, Y., Fedor, H. L.*, et al.* (2014). AR-V7 and resistance to enzalutamide and abiraterone in prostate cancer. N Engl J Med *371*, 1028-1038.

13. Armstrong, A. J., Halabi, S., Luo, J., Nanus, D. M., Giannakakou, P., Szmulewitz, R. Z., Danila, D. C., Healy, P., Anand, M., Rothwell, C. J.*, et al.* (2019a). Prospective Multicenter Validation of Androgen Receptor Splice Variant 7 and Hormone Therapy Resistance in High-Risk Castration-Resistant Prostate Cancer: The PROPHECY Study. J Clin Oncol *37*, 1120-1129.

14. Armstrong, A. J., Szmulewitz, R. Z., Petrylak, D. P., Holzbeierlein, J., Villers, A., Azad, A., Alcaraz, A., Alekseev, B., Iguchi, T., Shore, N. D.*, et al.* (2019b). ARCHES: A Randomized, Phase III Study of Androgen Deprivation Therapy With Enzalutamide or Placebo in Men With Metastatic Hormone-Sensitive Prostate Cancer. J Clin Oncol *37*, 2974-2986.

15. Armstrong, C. W. D., Coulter, J. A., Ong, C. W., Maxwell, P. J., Walker, S., Butterworth, K. T., Lyubomska, O., Berlingeri, S., Gallagher, R., O'Sullivan, J. M.*, et al.* (2020). Clinical and functional characterization of CXCR1/CXCR2 biology in the relapse and radiotherapy resistance of primary PTEN-deficient prostate carcinoma. NAR Cancer *2*, zcaa012.

16. Arora, V. K., Schenkein, E., Murali, R., Subudhi, S. K., Wongvipat, J., Balbas, M. D., Shah, N., Cai, L., Efstathiou, E., Logothetis, C.*, et al.* (2013). Glucocorticoid receptor confers resistance to antiandrogens by bypassing androgen receptor blockade. Cell *155*, 1309-1322.

17. Asangani, I. A., Dommeti, V. L., Wang, X., Malik, R., Cieslik, M., Yang, R., Escara-Wilke, J., Wilder-Romans, K., Dhanireddy, S., Engelke, C.*, et al.* (2014). Therapeutic targeting of BET bromodomain proteins in castration-resistant prostate cancer. Nature *510*, 278-282.

18. Aubry, A., Galiacy, S., Ceccato, L., Marchand, C., Tricoire, C., Lopez, F., Bremner, R., Racaud-Sultan, C., Monsarrat, B., Malecaze, F., and Allouche, M. (2015). Peptides derived from the dependence receptor ALK are proapoptotic for ALK-positive tumors. Cell Death Dis *6*, e1736.

19. Aytes, A., Mitrofanova, A., Kinkade, C. W., Lefebvre, C., Lei, M., Phelan, V., LeKaye, H. C., Koutcher, J. A., Cardiff, R. D., Califano, A.*, et al.* (2013). ETV4 promotes metastasis in response to activation of PI3-kinase and Ras signaling in a mouse model of advanced prostate cancer. Proc Natl Acad Sci U S A *110*, E3506-3515.

20. Baade, P. D., Youlden, D. R., and Krnjacki, L. J. (2009). International epidemiology of prostate cancer: geographical distribution and secular trends. Mol Nutr Food Res *53*, 171-184.

21. Beer, T. M., Armstrong, A. J., Rathkopf, D. E., Loriot, Y., Sternberg, C. N., Higano, C. S., Iversen, P., Bhattacharya, S., Carles, J., Chowdhury, S*., et al.* (2014). Enzalutamide in metastatic prostate cancer before chemotherapy. N Engl J Med *371*, 424-433.

22. Beltran, H., Oromendia, C., Danila, D. C., Montgomery, B., Hoimes, C., Szmulewitz, R. Z., Vaishampayan, U., Armstrong, A. J., Stein, M., Pinski, J*., et al.* (2019). A Phase II Trial of the Aurora Kinase A Inhibitor Alisertib for Patients with Castration-resistant and Neuroendocrine Prostate Cancer: Efficacy and Biomarkers. Clin Cancer Res *25*, 43-51.

23. Beltran, H., Rickman, D. S., Park, K., Chae, S. S., Sboner, A., MacDonald, T. Y., Wang, Y., Sheikh, K. L., Terry, S., Tagawa, S. T*., et al.* (2011). Molecular characterization of neuroendocrine prostate cancer and identification of new drug targets. Cancer Discov *1*, 487-495.

24. Beltran, H., Tomlins, S., Aparicio, A., Arora, V., Rickman, D., Ayala, G., Huang, J., True, L., Gleave, M. E., Soule, H*., et al.* (2014). Aggressive variants of castration-resistant prostate cancer. Clin Cancer Res *20*, 2846-2850.

25. Berry, T., Luther, W., Bhatnagar, N., Jamin, Y., Poon, E., Sanda, T., Pei, D., Sharma, B., Vetharoy, W. R., Hallsworth, A*., et al.* (2012). The ALK(F1174L) mutation potentiates the oncogenic activity of MYCN in neuroblastoma. Cancer Cell *22*, 117-130.

26. Bilir, B., Osunkoya, A. O., Wiles, W. G. t., Sannigrahi, S., Lefebvre, V., Metzger, D., Spyropoulos, D. D., Martin, W. D., and Moreno, C. S. (2016). SOX4 Is Essential for Prostate Tumorigenesis Initiated by PTEN Ablation. Cancer Res *76*, 1112-1121.

27. Bishop, J. L., Thaper, D., Vahid, S., Davies, A., Ketola, K., Kuruma, H., Jama, R., Nip, K. M., Angeles, A., Johnson, F*., et al.* (2017). The Master Neural Transcription Factor BRN2 Is an

Androgen Receptor-Suppressed Driver of Neuroendocrine Differentiation in Prostate Cancer. Cancer Discov *7*, 54-71.

28. Blee, A. M., Liu, S., Wang, L., and Huang, H. (2016). BET bromodomain-mediated interaction between ERG and BRD4 promotes prostate cancer cell invasion. Oncotarget *7*, 38319-38332.

29. Bongarzone, I., Pierotti, M. A., Monzini, N., Mondellini, P., Manenti, G., Donghi, R., Pilotti, S., Grieco, M., Santoro, M., Fusco, A., and et al. (1989). High frequency of activation of tyrosine kinase oncogenes in human papillary thyroid carcinoma. Oncogene *4*, 1457-1462.

30. Bossi, R. T., Saccardo, M. B., Ardini, E., Menichincheri, M., Rusconi, L., Magnaghi, P., Orsini, P., Avanzi, N., Borgia, A. L., Nesi, M.*, et al.* (2010). Crystal structures of anaplastic lymphoma kinase in complex with ATP competitive inhibitors. Biochemistry *49*, 6813-6825.

31. Bruchovsky, N., and Wilson, J. D. (1968). The intranuclear binding of testosterone and 5-alpha-androstan-17-beta-ol-3-one by rat prostate. J Biol Chem *243*, 5953-5960.

32. Brummer, T., Schmitz-Peiffer, C., and Daly, R. J. (2010). Docking proteins. Febs j *277*, 4356-4369.

33. Cai, C., He, H. H., Chen, S., Coleman, I., Wang, H., Fang, Z., Chen, S., Nelson, P. S., Liu, X. S., Brown, M., and Balk, S. P. (2011). Androgen receptor gene expression in prostate cancer is directly suppressed by the androgen receptor through recruitment of lysine-specific demethylase 1. Cancer Cell *20*, 457-471.

34. Camidge, D. R., Dziadziuszko, R., Peters, S., Mok, T., Noe, J., Nowicka, M., Gadgeel, S. M., Cheema, P., Pavlakis, N., de Marinis, F.*, et al.* (2019). Updated Efficacy and Safety Data and Impact of the EML4-ALK Fusion Variant on the Efficacy of Alectinib in Untreated ALK-

Positive Advanced Non-Small Cell Lung Cancer in the Global Phase III ALEX Study. J Thorac Oncol *14*, 1233-1243.

35. Carén, H., Abel, F., Kogner, P., and Martinsson, T. (2008). High incidence of DNA mutations and gene amplifications of the ALK gene in advanced sporadic neuroblastoma tumours. Biochem J *416*, 153-159.

36. Carneiro, B. A., Pamarthy, S., Shah, A. N., Sagar, V., Unno, K., Han, H., Yang, X. J., Costa, R. B., Nagy, R. J., Lanman, R. B.*, et al.* (2018). Anaplastic Lymphoma Kinase Mutation (ALK F1174C) in Small Cell Carcinoma of the Prostate and Molecular Response to Alectinib. Clin Cancer Res *24*, 2732-2739.

37. Chang, K. H., Li, R., Kuri, B., Lotan, Y., Roehrborn, C. G., Liu, J., Vessella, R., Nelson, P. S., Kapur, P., Guo, X.*, et al.* (2013). A gain-of-function mutation in DHT synthesis in castration-resistant prostate cancer. Cell *154*, 1074-1084.

38. Chen, C. D., Welsbie, D. S., Tran, C., Baek, S. H., Chen, R., Vessella, R., Rosenfeld, M. G., and Sawyers, C. L. (2004). Molecular determinants of resistance to antiandrogen therapy. Nat Med *10*, 33-39.

39. Chen, H., Tu, S. W., and Hsieh, J. T. (2005). Down-regulation of human DAB2IP gene expression mediated by polycomb Ezh2 complex and histone deacetylase in prostate cancer. J Biol Chem *280*, 22437-22444.

40. Chen, J., O'Gorman, M. T., James, L. P., Klamerus, K. J., Mugundu, G., and Pithavala, Y. K. (2021). Pharmacokinetics of Lorlatinib After Single and Multiple Dosing in Patients with Anaplastic Lymphoma Kinase (ALK)-Positive Non-Small Cell Lung Cancer: Results from a Global Phase I/II Study. Clin Pharmacokinet *60*, 1313-1324.

41. Chen, W. S., Aggarwal, R., Zhang, L., Zhao, S. G., Thomas, G. V., Beer, T. M., Quigley, D. A., Foye, A., Playdle, D., Huang, J.*, et al.* (2019). Genomic Drivers of Poor Prognosis and Enzalutamide Resistance in Metastatic Castration-resistant Prostate Cancer. Eur Urol *76*, 562-571.

42. Chen, Y., Takita, J., Choi, Y. L., Kato, M., Ohira, M., Sanada, M., Wang, L., Soda, M., Kikuchi, A., Igarashi, T.*, et al.* (2008). Oncogenic mutations of ALK kinase in neuroblastoma. Nature *455*, 971-974.

43. Chi, K. N., Chowdhury, S., Bjartell, A., Chung, B. H., Pereira de Santana Gomes, A. J., Given, R., Juárez, A., Merseburger, A. S., Özgüroğlu, M., Uemura, H.*, et al.* (2021). Apalutamide in Patients With Metastatic Castration-Sensitive Prostate Cancer: Final Survival Analysis of the Randomized, Double-Blind, Phase III TITAN Study. J Clin Oncol *39*, 2294-2303.

44. Choi, Y. L., Takeuchi, K., Soda, M., Inamura, K., Togashi, Y., Hatano, S., Enomoto, M., Hamada, T., Haruta, H., Watanabe, H.*, et al.* (2008). Identification of novel isoforms of the EML4-ALK transforming gene in non-small cell lung cancer. Cancer Res *68*, 4971-4976.

45. Chong, J. T., Oh, W. K., and Liaw, B. C. (2018). Profile of apalutamide in the treatment of metastatic castration-resistant prostate cancer: evidence to date. Onco Targets Ther *11*, 2141-2147.

46. Conteduca, V., Wetterskog, D., Sharabiani, M. T. A., Grande, E., Fernandez-Perez, M. P., Jayaram, A., Salvi, S., Castellano, D., Romanel, A., Lolli, C.*, et al.* (2017). Androgen receptor gene status in plasma DNA associates with worse outcome on enzalutamide or abiraterone for castration-resistant prostate cancer: a multi-institution correlative biomarker study. Ann Oncol *28*, 1508-1516.

47. Corao, D. A., Biegel, J. A., Coffin, C. M., Barr, F. G., Wainwright, L. M., Ernst, L. M., Choi, J. K., Zhang, P. J., and Pawel, B. R. (2009). ALK expression in rhabdomyosarcomas: correlation with histologic subtype and fusion status. Pediatr Dev Pathol *12*, 275-283.

48. Crawford, E. D., Stanton, W., and Mandair, D. (2020). Darolutamide: An Evidenced-Based Review of Its Efficacy and Safety in the Treatment of Prostate Cancer. Cancer Manag Res *12*, 5667-5676.

49. Culig, Z. (2014). Proinflammatory cytokine interleukin-6 in prostate carcinogenesis. Am J Clin Exp Urol *2*, 231-238.

50. Culig, Z., and Santer, F. R. (2014). Androgen receptor signaling in prostate cancer. Cancer Metastasis Rev *33*, 413-427.

51. Dardenne, E., Beltran, H., Benelli, M., Gayvert, K., Berger, A., Puca, L., Cyrta, J., Sboner, A., Noorzad, Z., MacDonald, T*., et al.* (2016). N-Myc Induces an EZH2-Mediated Transcriptional Program Driving Neuroendocrine Prostate Cancer. Cancer Cell *30*, 563-577.

52. Davis, I. D., Martin, A. J., Stockler, M. R., Begbie, S., Chi, K. N., Chowdhury, S., Coskinas, X., Frydenberg, M., Hague, W. E., Horvath, L. G*., et al.* (2019). Enzalutamide with Standard First-Line Therapy in Metastatic Prostate Cancer. N Engl J Med *381*, 121-131.

53. Del Grosso, F., De Mariano, M., Passoni, L., Luksch, R., Tonini, G. P., and Longo, L. (2011). Inhibition of N-linked glycosylation impairs ALK phosphorylation and disrupts pro-survival signaling in neuroblastoma cell lines. BMC Cancer *11*, 525.

54. Di Croce, L., and Helin, K. (2013). Transcriptional regulation by Polycomb group proteins. Nat Struct Mol Biol *20*, 1147-1155.

55. Dirix, L. (2019). Predictive Significance of Androgen Receptor Splice Variant 7 in Patients With Metastatic Castration-Resistant Prostate Cancer: The PROPHECY Study. J Clin Oncol *37*, 2180-2181.

56. Doebele, R. C., Drilon, A., Paz-Ares, L., Siena, S., Shaw, A. T., Farago, A. F., Blakely, C. M., Seto, T., Cho, B. C., Tosi, D.*, et al.* (2020). Entrectinib in patients with advanced or metastatic NTRK fusion-positive solid tumours: integrated analysis of three phase 1-2 trials. Lancet Oncol *21*, 271-282.

57. Drilon, A., Siena, S., Ou, S. I., Patel, M., Ahn, M. J., Lee, J., Bauer, T. M., Farago, A. F., Wheler, J. J., Liu, S. V.*, et al.* (2017). Safety and Antitumor Activity of the Multitargeted Pan-TRK, ROS1, and ALK Inhibitor Entrectinib: Combined Results from Two Phase I Trials (ALKA-372-001 and STARTRK-1). Cancer Discov *7*, 400-409.

58. Duan, L., Chen, Z., Lu, J., Liang, Y., Wang, M., Roggero, C. M., Zhang, Q. J., Gao, J., Fang, Y., Cao, J.*, et al.* (2019). Histone lysine demethylase KDM4B regulates the alternative splicing of the androgen receptor in response to androgen deprivation. Nucleic Acids Res *47*, 11623-11636.

59. Duff, J., and McEwan, I. J. (2005). Mutation of histidine 874 in the androgen receptor ligand-binding domain leads to promiscuous ligand activation and altered p160 coactivator interactions. Mol Endocrinol *19*, 2943-2954.

60. Efstathiou, E., Titus, M., Wen, S., Hoang, A., Karlou, M., Ashe, R., Tu, S. M., Aparicio, A., Troncoso, P., Mohler, J., and Logothetis, C. J. (2015). Molecular characterization of enzalutamide-treated bone metastatic castration-resistant prostate cancer. Eur Urol *67*, 53-60.

61. El-Haibi, C. P., Sharma, P., Singh, R., Gupta, P., Taub, D. D., Singh, S., and Lillard, J. J. W. (2013). Differential G protein subunit expression by prostate cancer cells and their interaction with CXCR5. Molecular Cancer *12*, 64.

62. Esposito, S., Russo, M. V., Airoldi, I., Tupone, M. G., Sorrentino, C., Barbarito, G., Di Meo, S., and Di Carlo, E. (2015). SNAI2/Slug gene is silenced in prostate cancer and regulates neuroendocrine differentiation, metastasis-suppressor and pluripotency gene expression. Oncotarget *6*, 17121-17134.

63. Faivre, E. J., Wilcox, D., Lin, X., Hessler, P., Torrent, M., He, W., Uziel, T., Albert, D. H., McDaniel, K., Kati, W., and Shen, Y. (2017). Exploitation of Castration-Resistant Prostate Cancer Transcription Factor Dependencies by the Novel BET Inhibitor ABBV-075. Mol Cancer Res *15*, 35-44.

64. Fan, L., Zhang, F., Xu, S., Cui, X., Hussain, A., Fazli, L., Gleave, M., Dong, X., and Qi, J. (2018). Histone demethylase JMJD1A promotes alternative splicing of AR variant 7 (AR-V7) in prostate cancer cells. Proc Natl Acad Sci U S A *115*, E4584-e4593.

65. Fantone, S., Tossetta, G., Montironi, R., Senzacqua, M., Marzioni, D., and Mazzucchelli, R. (2020). Ciliary neurotrophic factor (CNTF) and its receptor (CNTFRα) signal through MAPK/ERK pathway in human prostate tissues: a morphological and biomolecular study. Eur J Histochem *64*.

66. Farooqi, A. A., and Siddik, Z. H. (2015). Platelet-derived growth factor (PDGF) signalling in cancer: rapidly emerging signalling landscape. Cell Biochem Funct *33*, 257-265.

67. Fischer, H., Ullah, M., de la Cruz, C. C., Hunsaker, T., Senn, C., Wirz, T., Wagner, B., Draganov, D., Vazvaei, F., Donzelli, M.*, et al.* (2020). Entrectinib, a TRK/ROS1 inhibitor with anti-CNS

tumor activity: differentiation from other inhibitors in its class due to weak interaction with P-glycoprotein. Neuro Oncol *22*, 819-829.

68. Fizazi, K., Scher, H. I., Molina, A., Logothetis, C. J., Chi, K. N., Jones, R. J., Staffurth, J. N., North, S., Vogelzang, N. J., Saad, F*., et al.* (2012). Abiraterone acetate for treatment of metastatic castration-resistant prostate cancer: final overall survival analysis of the COU-AA-301 randomised, double-blind, placebo-controlled phase 3 study. Lancet Oncol *13*, 983-992.

69. Fizazi, K., Shore, N., Tammela, T. L., Ulys, A., Vjaters, E., Polyakov, S., Jievaltas, M., Luz, M., Alekseev, B., Kuss, I*., et al.* (2020). Nonmetastatic, Castration-Resistant Prostate Cancer and Survival with Darolutamide. N Engl J Med *383*, 1040-1049.

70. Fizazi, K., Smith, M. R., and Tombal, B. (2018). Clinical Development of Darolutamide: A Novel Androgen Receptor Antagonist for the Treatment of Prostate Cancer. Clin Genitourin Cancer *16*, 332-340.

71. Fizazi, K., Tran, N., Fein, L., Matsubara, N., Rodriguez-Antolin, A., Alekseev, B. Y., Özgüroğlu, M., Ye, D., Feyerabend, S., Protheroe, A*., et al.* (2019). Abiraterone acetate plus prednisone in patients with newly diagnosed high-risk metastatic castration-sensitive prostate cancer (LATITUDE): final overall survival analysis of a randomised, double-blind, phase 3 trial. Lancet Oncol *20*, 686-700.

72. Fragoso, M. A., Patel, A. K., Nakamura, R. E., Yi, H., Surapaneni, K., and Hackam, A. S. (2012). The Wnt/β-catenin pathway cross-talks with STAT3 signaling to regulate survival of retinal pigment epithelium cells. PLoS One *7*, e46892.

73. Friboulet, L., Li, N., Katayama, R., Lee, C. C., Gainor, J. F., Crystal, A. S., Michellys, P. Y., Awad, M. M., Yanagitani, N., Kim, S.*, et al.* (2014). The ALK inhibitor ceritinib overcomes crizotinib resistance in non-small cell lung cancer. Cancer Discov *4*, 662-673.

74. Gazdar, A. F. (2009). Activating and resistance mutations of EGFR in non-small-cell lung cancer: role in clinical response to EGFR tyrosine kinase inhibitors. Oncogene *28 Suppl 1*, S24-31.

75. Gettinger, S. N., Bazhenova, L. A., Langer, C. J., Salgia, R., Gold, K. A., Rosell, R., Shaw, A. T., Weiss, G. J., Tugnait, M., Narasimhan, N. I.*, et al.* (2016). Activity and safety of brigatinib in ALK-rearranged non-small-cell lung cancer and other malignancies: a single-arm, open-label, phase 1/2 trial. Lancet Oncol *17*, 1683-1696.

76. Grasso, C. S., Wu, Y. M., Robinson, D. R., Cao, X., Dhanasekaran, S. M., Khan, A. P., Quist, M. J., Jing, X., Lonigro, R. J., Brenner, J. C.*, et al.* (2012). The mutational landscape of lethal castration-resistant prostate cancer. Nature *487*, 239-243.

77. Greer, J. M., and McCombe, P. A. (2012). The role of epigenetic mechanisms and processes in autoimmune disorders. Biologics *6*, 307-327.

78. Grindstad, T., Andersen, S., Al-Saad, S., Donnem, T., Kiselev, Y., Nordahl Melbø-Jørgensen, C., Skjefstad, K., Busund, L. T., Bremnes, R. M., and Richardsen, E. (2015). High progesterone receptor expression in prostate cancer is associated with clinical failure. PLoS One *10*, e0116691.

79. Grossmann, M., and Zajac, J. D. (2011). Management of side effects of androgen deprivation therapy. Endocrinol Metab Clin North Am *40*, 655-671, x.

80. Guan, J., Umapathy, G., Yamazaki, Y., Wolfstetter, G., Mendoza, P., Pfeifer, K., Mohammed, A., Hugosson, F., Zhang, H., Hsu, A. W*., et al.* (2015). FAM150A and FAM150B are activating ligands for anaplastic lymphoma kinase. Elife *4*, e09811.

81. Gwynne, W. D., Shakeel, M. S., Girgis-Gabardo, A., Kim, K. H., Ford, E., Dvorkin-Gheva, A., Aarts, C., Isaac, M., Al-Awar, R., and Hassell, J. A. (2020). Antagonists of the serotonin receptor 5A target human breast tumor initiating cells. BMC Cancer *20*, 724.

82. Haas, M., Altman, A., Rothenberg, E., Bogart, M. H., and Jones, O. W. (1984). Mechanism of T-cell lymphomagenesis: transformation of growth-factor-dependent T-lymphoblastoma cells to growth-factor-independent T-lymphoma cells. Proc Natl Acad Sci U S A *81*, 1742-1746.

83. Haddad, B. R., Erickson, A., Udhane, V., LaViolette, P. S., Rone, J. D., Kallajoki, M. A., See, W. A., Rannikko, A., Mirtti, T., and Nevalainen, M. T. (2019). Positive STAT5 Protein and Locus Amplification Status Predicts Recurrence after Radical Prostatectomy to Assist Clinical Precision Management of Prostate Cancer. Cancer Epidemiol Biomarkers Prev *28*, 1642-1651.

84. Harris, W. P., Mostaghel, E. A., Nelson, P. S., and Montgomery, B. (2009). Androgen deprivation therapy: progress in understanding mechanisms of resistance and optimizing androgen depletion. Nat Clin Pract Urol *6*, 76-85.

85. Hassani, B., Attar, Z., and Firouzabadi, N. (2023). The renin-angiotensin-aldosterone system (RAAS) signaling pathways and cancer: foes versus allies. Cancer Cell International *23*, 254.

86. He, Y. W., Beers, C., Deftos, M. L., Ojala, E. W., Forbush, K. A., and Bevan, M. J. (2000). Down-regulation of the orphan nuclear receptor ROR gamma t is essential for T lymphocyte maturation. J Immunol *164*, 5668-5674.

87. Herbst, R. S. (2004). Review of epidermal growth factor receptor biology. Int J Radiat Oncol Biol Phys *59*, 21-26.

88. Hida, T., Nokihara, H., Kondo, M., Kim, Y. H., Azuma, K., Seto, T., Takiguchi, Y., Nishio, M., Yoshioka, H., Imamura, F*., et al.* (2017). Alectinib versus crizotinib in patients with ALK-positive non-small-cell lung cancer (J-ALEX): an open-label, randomised phase 3 trial. Lancet *390*, 29-39.

89. Hirayama, Y., Tam, T., Jian, K., Andersen, R. J., and Sadar, M. D. (2020). Combination therapy with androgen receptor N-terminal domain antagonist EPI-7170 and enzalutamide yields synergistic activity in AR-V7-positive prostate cancer. Mol Oncol *14*, 2455-2470.

90. Hoyle, A. P., Ali, A., James, N. D., Cook, A., Parker, C. C., de Bono, J. S., Attard, G., Chowdhury, S., Cross, W. R., Dearnaley, D. P*., et al.* (2019). Abiraterone in "High-" and "Low-risk" Metastatic Hormone-sensitive Prostate Cancer. Eur Urol *76*, 719-728.

91. Hsu, Y. L., Yen, M. C., Chang, W. A., Tsai, P. H., Pan, Y. C., Liao, S. H., and Kuo, P. L. (2019). CXCL17-derived CD11b(+)Gr-1(+) myeloid-derived suppressor cells contribute to lung metastasis of breast cancer through platelet-derived growth factor-BB. Breast Cancer Res *21*, 23.

92. Hu, H., Qing Lin, W., Zhu, Q., Wen Yang, X., Wang, H. D., and Kuang, Y. K. (2016). Is there a benefit of first- or second-line crizotinib in locally advanced or metastatic anaplastic

lymphoma kinase-positive non-small cell lung cancer? a meta-analysis. Oncotarget *7*, 81090-81098.

93. Huang, H. (2018). Anaplastic Lymphoma Kinase (ALK) Receptor Tyrosine Kinase: A Catalytic Receptor with Many Faces. Int J Mol Sci *19*.

94. Huang, L., and Xu, A. M. (2017). SET and MYND domain containing protein 3 in cancer. Am J Transl Res *9*, 1-14.

95. Hubbard, G. K., Mutton, L. N., Khalili, M., McMullin, R. P., Hicks, J. L., Bianchi-Frias, D., Horn, L. A., Kulac, I., Moubarek, M. S., Nelson, P. S.*, et al.* (2016). Combined MYC Activation and Pten Loss Are Sufficient to Create Genomic Instability and Lethal Metastatic Prostate Cancer. Cancer Res *76*, 283-292.

96. Huggins, C., and Hodges, C. V. (1972). Studies on prostatic cancer. I. The effect of castration, of estrogen and androgen injection on serum phosphatases in metastatic carcinoma of the prostate. CA Cancer J Clin *22*, 232-240.

97. Huggins, C., and Scott, W. W. (1945). Bilateral Adrenalectomy in Prostatic Cancer: Clinical Features and Urinary Excretion of 17-Ketosteroids and Estrogen. Ann Surg *122*, 1031-1041.

98. Hussong, M., Börno, S. T., Kerick, M., Wunderlich, A., Franz, A., Sültmann, H., Timmermann, B., Lehrach, H., Hirsch-Kauffmann, M., and Schweiger, M. R. (2014). The bromodomain protein BRD4 regulates the KEAP1/NRF2-dependent oxidative stress response. Cell Death Dis *5*, e1195.

99. Information, U. F. a. D. A. C. f. D. E. a. R. R. P. (2019).

100. Itakura, J., Ishiwata, T., Shen, B., Kornmann, M., and Korc, M. (2000). Concomitant over-expression of vascular endothelial growth factor and its receptors in pancreatic cancer. Int J Cancer *85*, 27-34.

101. Iwahara, T., Fujimoto, J., Wen, D., Cupples, R., Bucay, N., Arakawa, T., Mori, S., Ratzkin, B., and Yamamoto, T. (1997). Molecular characterization of ALK, a receptor tyrosine kinase expressed specifically in the nervous system. Oncogene *14*, 439-449.

102. James, N. D., de Bono, J. S., Spears, M. R., Clarke, N. W., Mason, M. D., Dearnaley, D. P., Ritchie, A. W. S., Amos, C. L., Gilson, C., Jones, R. J.*, et al.* (2017). Abiraterone for Prostate Cancer Not Previously Treated with Hormone Therapy. N Engl J Med *377*, 338-351.

103. Jang, M. K., Mochizuki, K., Zhou, M., Jeong, H. S., Brady, J. N., and Ozato, K. (2005). The bromodomain protein Brd4 is a positive regulatory component of P-TEFb and stimulates RNA polymerase II-dependent transcription. Mol Cell *19*, 523-534.

104. Janoueix-Lerosey, I., Lequin, D., Brugières, L., Ribeiro, A., de Pontual, L., Combaret, V., Raynal, V., Puisieux, A., Schleiermacher, G., Pierron, G.*, et al.* (2008). Somatic and germline activating mutations of the ALK kinase receptor in neuroblastoma. Nature *455*, 967-970.

105. Jarrard, D. F., Bova, G. S., Ewing, C. M., Pin, S. S., Nguyen, S. H., Baylin, S. B., Cairns, P., Sidransky, D., Herman, J. G., and Isaacs, W. B. (1997). Deletional, mutational, and methylation analyses of CDKN2 (p16/MTS1) in primary and metastatic prostate cancer. Genes Chromosomes Cancer *19*, 90-96.

106. JF, P. (1837). The works of John Hunter, F.R.S.;with notes. Br Foreign Med Rev *4*, 75-87.

107. Ji, S., Shi, Y., Yang, L., Zhang, F., Li, Y., and Xu, F. (2022). miR-145-5p Inhibits Neuroendocrine Differentiation and Tumor Growth by Regulating the SOX11/MYCN Axis in Prostate cancer. Front Genet *13*, 790621.

108. Jia, H., Morris, C. D., Williams, R. M., Loring, J. F., and Thomas, E. A. (2015). HDAC inhibition imparts beneficial transgenerational effects in Huntington's disease mice via altered DNA and histone methylation. Proc Natl Acad Sci U S A *112*, E56-64.

109. Kalamatianos, T., Denekou, D., Stranjalis, G., and Papadimitriou, E. (2018). Anaplastic Lymphoma Kinase in Glioblastoma: Detection/Diagnostic Methods and Therapeutic Options. Recent Pat Anticancer Drug Discov *13*, 209-223.

110. Kim, J., Roh, M., Doubinskaia, I., Algarroba, G. N., Eltoum, I. E., and Abdulkadir, S. A. (2012). A mouse model of heterogeneous, c-MYC-initiated prostate cancer with loss of Pten and p53. Oncogene *31*, 322-332.

111. Kinoshita, K., Asoh, K., Furuichi, N., Ito, T., Kawada, H., Hara, S., Ohwada, J., Miyagi, T., Kobayashi, T., Takanashi, K.*, et al.* (2012). Design and synthesis of a highly selective, orally active and potent anaplastic lymphoma kinase inhibitor (CH5424802). Bioorg Med Chem *20*, 1271-1280.

112. Kissick, H. T., On, S. T., Dunn, L. K., Sanda, M. G., Asara, J. M., Pellegrini, K. L., Noel, J. K., and Arredouani, M. S. (2015). The transcription factor ERG increases expression of neurotransmitter receptors on prostate cancer cells. BMC Cancer *15*, 604.

113. Knighton, D. R., Zheng, J. H., Ten Eyck, L. F., Ashford, V. A., Xuong, N. H., Taylor, S. S., and Sowadski, J. M. (1991). Crystal structure of the catalytic subunit of cyclic adenosine monophosphate-dependent protein kinase. Science *253*, 407-414.

114. Komura, K., Jeong, S. H., Hinohara, K., Qu, F., Wang, X., Hiraki, M., Azuma, H., Lee, G. S., Kantoff, P. W., and Sweeney, C. J. (2016). Resistance to docetaxel in prostate cancer is associated with androgen receptor activation and loss of KDM5D expression. Proc Natl Acad Sci U S A *113*, 6259-6264.

115. Konduri, K., Gallant, J. N., Chae, Y. K., Giles, F. J., Gitlitz, B. J., Gowen, K., Ichihara, E., Owonikoko, T. K., Peddareddigari, V., Ramalingam, S. S.*, et al.* (2016). EGFR Fusions as Novel Therapeutic Targets in Lung Cancer. Cancer Discov *6*, 601-611.

116. Ku, S. Y., Rosario, S., Wang, Y., Mu, P., Seshadri, M., Goodrich, Z. W., Goodrich, M. M., Labbé, D. P., Gomez, E. C., Wang, J.*, et al.* (2017). Rb1 and Trp53 cooperate to suppress prostate cancer lineage plasticity, metastasis, and antiandrogen resistance. Science *355*, 78-83.

117. Kunath, F., Borgmann, H., Blümle, A., Keck, B., Wullich, B., Schmucker, C., Sikic, D., Roelle, C., Schmidt, S., Wahba, A., and Meerpohl, J. J. (2015). Gonadotropin-releasing hormone antagonists versus standard androgen suppression therapy for advanced prostate cancer A systematic review with meta-analysis. BMJ Open *5*, e008217.

118. Kwak, E. L., Bang, Y. J., Camidge, D. R., Shaw, A. T., Solomon, B., Maki, R. G., Ou, S. H., Dezube, B. J., Jänne, P. A., Costa, D. B.*, et al.* (2010). Anaplastic lymphoma kinase inhibition in non-small-cell lung cancer. N Engl J Med *363*, 1693-1703.

119. Labrecque, M. P., Coleman, I. M., Brown, L. G., True, L. D., Kollath, L., Lakely, B., Nguyen, H. M., Yang, Y. C., da Costa, R. M. G., Kaipainen, A.*, et al.* (2019). Molecular profiling stratifies diverse phenotypes of treatment-refractory metastatic castration-resistant prostate cancer. The Journal of Clinical Investigation *129*, 4492-4505.

120. Lasek, A. W., Lim, J., Kliethermes, C. L., Berger, K. H., Joslyn, G., Brush, G., Xue, L., Robertson, M., Moore, M. S., Vranizan, K.*, et al.* (2011). An evolutionary conserved role for anaplastic lymphoma kinase in behavioral responses to ethanol. PLoS One *6*, e22636.

121. Lee, E., Madar, A., David, G., Garabedian, M. J., Dasgupta, R., and Logan, S. K. (2013). Inhibition of androgen receptor and β-catenin activity in prostate cancer. Proc Natl Acad Sci U S A *110*, 15710-15715.

122. Lee, T. I., Jenner, R. G., Boyer, L. A., Guenther, M. G., Levine, S. S., Kumar, R. M., Chevalier, B., Johnstone, S. E., Cole, M. F., Isono, K.*, et al.* (2006). Control of developmental regulators by Polycomb in human embryonic stem cells. Cell *125*, 301-313.

123. Lemmon, M. A., and Schlessinger, J. (2010). Cell signaling by receptor tyrosine kinases. Cell *141*, 1117-1134.

124. Li, D., Sun, H., Sun, W. J., Bao, H. B., Si, S. H., Fan, J. L., Lin, P., Cui, R. J., Pan, Y. J., Wen, S. M.*, et al.* (2016a). Role of RbBP5 and H3K4me3 in the vicinity of Snail transcription start site during epithelial-mesenchymal transition in prostate cancer cell. Oncotarget *7*, 65553-65567.

125. Li, H., Wang, L., Li, Z., Geng, X., Li, M., Tang, Q., Wu, C., and Lu, Z. (2020). SOX2 has dual functions as a regulator in the progression of neuroendocrine prostate cancer. Lab Invest *100*, 570-582.

126. Li, J., Alyamani, M., Zhang, A., Chang, K. H., Berk, M., Li, Z., Zhu, Z., Petro, M., Magi-Galluzzi, C., Taplin, M. E.*, et al.* (2017a). Aberrant corticosteroid metabolism in tumor cells enables GR takeover in enzalutamide resistant prostate cancer. Elife *6*.

127. Li, N., Dhar, S. S., Chen, T. Y., Kan, P. Y., Wei, Y., Kim, J. H., Chan, C. H., Lin, H. K., Hung, M. C., and Lee, M. G. (2016b). JARID1D Is a Suppressor and Prognostic Marker of Prostate Cancer Invasion and Metastasis. Cancer Res *76*, 831-843.

128. Li, N., Xue, W., Yuan, H., Dong, B., Ding, Y., Liu, Y., Jiang, M., Kan, S., Sun, T., Ren, J.*, et al.* (2017b). AKT-mediated stabilization of histone methyltransferase WHSC1 promotes prostate cancer metastasis. J Clin Invest *127*, 1284-1302.

129. Li, W., Cohen, A., Sun, Y., Squires, J., Braas, D., Graeber, T. G., Du, L., Li, G., Li, Z., Xu, X.*, et al.* (2016c). The Role of CD44 in Glucose Metabolism in Prostatic Small Cell Neuroendocrine Carcinoma. Mol Cancer Res *14*, 344-353.

130. Li, X., Xu, Y., Chen, Y., Chen, S., Jia, X., Sun, T., Liu, Y., Li, X., Xiang, R., and Li, N. (2013). SOX2 promotes tumor metastasis by stimulating epithelial-to-mesenchymal transition via regulation of WNT/β-catenin signal network. Cancer Lett *336*, 379-389.

131. Li, Y., He, Y., Butler, W., Xu, L., Chang, Y., Lei, K., Zhang, H., Zhou, Y., Gao, A. C., Zhang, Q.*, et al.* (2019a). Targeting cellular heterogeneity with CXCR2 blockade for the treatment of therapy-resistant prostate cancer. Sci Transl Med *11*.

132. Li, Y., Zhang, Q., Lovnicki, J., Chen, R., Fazli, L., Wang, Y., Gleave, M., Huang, J., and Dong, X. (2019b). SRRM4 gene expression correlates with neuroendocrine prostate cancer. Prostate *79*, 96-104.

133. Liu, C., Lou, W., Zhu, Y., Nadiminty, N., Schwartz, C. T., Evans, C. P., and Gao, A. C. (2014). Niclosamide inhibits androgen receptor variants expression and overcomes enzalutamide resistance in castration-resistant prostate cancer. Clin Cancer Res *20*, 3198-3210.

134. Liu, G., Chen, T., Ding, Z., Wang, Y., Wei, Y., and Wei, X. (2021). Inhibition of FGF-FGFR and VEGF-VEGFR signalling in cancer treatment. Cell Prolif *54*, e13009.

135. Longatto Filho, A., Martins, A., Costa, S. M., and Schmitt, F. C. (2005). VEGFR-3 expression in breast cancer tissue is not restricted to lymphatic vessels. Pathol Res Pract *201*, 93-99.

136. Lorén, C. E., Englund, C., Grabbe, C., Hallberg, B., Hunter, T., and Palmer, R. H. (2003). A crucial role for the Anaplastic lymphoma kinase receptor tyrosine kinase in gut development in Drosophila melanogaster. EMBO Rep *4*, 781-786.

137. Lu, C., Terbuch, A., Dolling, D., Yu, J., Wang, H., Chen, Y., Fountain, J., Bertan, C., Sharp, A., Carreira, S.*, et al.* (2020). Treatment with abiraterone and enzalutamide does not overcome poor outcome from metastatic castration-resistant prostate cancer in men with the germline homozygous HSD3B1 c.1245C genotype. Ann Oncol *31*, 1178-1185.

138. Lu, N. Z., Wardell, S. E., Burnstein, K. L., Defranco, D., Fuller, P. J., Giguere, V., Hochberg, R. B., McKay, L., Renoir, J. M., Weigel, N. L.*, et al.* (2006). International Union of Pharmacology. LXV. The pharmacology and classification of the nuclear receptor superfamily: glucocorticoid, mineralocorticoid, progesterone, and androgen receptors. Pharmacol Rev *58*, 782-797.

139. Mahajan, N. P., Liu, Y., Majumder, S., Warren, M. R., Parker, C. E., Mohler, J. L., Earp, H. S., and Whang, Y. E. (2007). Activated Cdc42-associated kinase Ack1 promotes prostate cancer progression via androgen receptor tyrosine phosphorylation. Proc Natl Acad Sci U S A *104*, 8438-8443.

140. Mahon, K. L., Qu, W., Devaney, J., Paul, C., Castillo, L., Wykes, R. J., Chatfield, M. D., Boyer, M. J., Stockler, M. R., Marx, G.*, et al.* (2014). Methylated Glutathione S-transferase 1

(mGSTP1) is a potential plasma free DNA epigenetic marker of prognosis and response to chemotherapy in castrate-resistant prostate cancer. Br J Cancer *111*, 1802-1809.

141. Maina, P. K., Shao, P., Liu, Q., Fazli, L., Tyler, S., Nasir, M., Dong, X., and Qi, H. H. (2016). c-MYC drives histone demethylase PHF8 during neuroendocrine differentiation and in castration-resistant prostate cancer. Oncotarget *7*, 75585-75602.

142. Mainwaring, W. I. (1969). A soluble androgen receptor in the cytoplasm of rat prostate. J Endocrinol *45*, 531-541.

143. Malinowska, K., Neuwirt, H., Cavarretta, I. T., Bektic, J., Steiner, H., Dietrich, H., Moser, P. L., Fuchs, D., Hobisch, A., and Culig, Z. (2009). Interleukin-6 stimulation of growth of prostate cancer in vitro and in vivo through activation of the androgen receptor. Endocr Relat Cancer *16*, 155-169.

144. Manea, C. A., Badiu, D. C., Ploscaru, I. C., Zgura, A., Bacinschi, X., Smarandache, C. G., Serban, D., Popescu, C. G., Grigorean, V. T., and Botnarciuc, V. (2022). A review of NTRK fusions in cancer. Ann Med Surg (Lond) *79*, 103893.

145. Manning, G., Whyte, D. B., Martinez, R., Hunter, T., and Sudarsanam, S. (2002). The protein kinase complement of the human genome. Science *298*, 1912-1934.

146. Maranto, C., Udhane, V., Hoang, D. T., Gu, L., Alexeev, V., Malas, K., Cardenas, K., Brody, J. R., Rodeck, U., Bergom, C.*, et al.* (2018). STAT5A/B Blockade Sensitizes Prostate Cancer to Radiation through Inhibition of RAD51 and DNA Repair. Clin Cancer Res *24*, 1917-1931.

147. Marcelli, M., Ittmann, M., Mariani, S., Sutherland, R., Nigam, R., Murthy, L., Zhao, Y., DiConcini, D., Puxeddu, E., Esen, A.*, et al.* (2000). Androgen receptor mutations in prostate cancer. Cancer Res *60*, 944-949.

148. Marín-Aguilera, M., Codony-Servat, J., Reig, Ò., Lozano, J. J., Fernández, P. L., Pereira, M. V., Jiménez, N., Donovan, M., Puig, P., Mengual, L.*, et al.* (2014). Epithelial-to-mesenchymal transition mediates docetaxel resistance and high risk of relapse in prostate cancer. Mol Cancer Ther *13*, 1270-1284.

149. Matsuo, H., Baba, Y., Nair, R. M., Arimura, A., and Schally, A. V. (1971). Structure of the porcine LH- and FSH-releasing hormone. I. The proposed amino acid sequence. Biochem Biophys Res Commun *43*, 1334-1339.

150. McKeithen, D., Graham, T., Chung, L. W., and Odero-Marah, V. (2010). Snail transcription factor regulates neuroendocrine differentiation in LNCaP prostate cancer cells. Prostate *70*, 982-992.

151. Metz, E. P., Wilder, P. J., Dong, J., Datta, K., and Rizzino, A. (2020). Elevating SOX2 in prostate tumor cells upregulates expression of neuroendocrine genes, but does not reduce the inhibitory effects of enzalutamide. J Cell Physiol *235*, 3731-3740.

152. Modi, S., Stopeck, A. T., Gordon, M. S., Mendelson, D., Solit, D. B., Bagatell, R., Ma, W., Wheler, J., Rosen, N., Norton, L.*, et al.* (2007). Combination of trastuzumab and tanespimycin (17-AAG, KOS-953) is safe and active in trastuzumab-refractory HER-2 overexpressing breast cancer: a phase I dose-escalation study. J Clin Oncol *25*, 5410-5417.

153. Morales, M., Martín-Vasallo, P., and Ávila, J. (2022). Genetic Profiling of Glucocorticoid (NR3C1) and Mineralocorticoid (NR3C2) Receptor Polymorphisms before Starting Therapy with Androgen Receptor Inhibitors: A Study of a Patient Who Developed Toxic Myocarditis after Enzalutamide Treatment. Biomedicines *10*.

154. Morris, M. J., Heller, G., Hillman, D. W., Bobek, O., Ryan, C., Antonarakis, E. S., Bryce, A. H., Hahn, O., Beltran, H., Armstrong, A. J*., et al.* (2023). Randomized Phase III Study of Enzalutamide Compared With Enzalutamide Plus Abiraterone for Metastatic Castration-Resistant Prostate Cancer (Alliance A031201 Trial). J Clin Oncol *41*, 3352-3362.

155. Mourali, J., Bénard, A., Lourenço, F. C., Monnet, C., Greenland, C., Moog-Lutz, C., Racaud-Sultan, C., Gonzalez-Dunia, D., Vigny, M., Mehlen, P*., et al.* (2006). Anaplastic lymphoma kinase is a dependence receptor whose proapoptotic functions are activated by caspase cleavage. Mol Cell Biol *26*, 6209-6222.

156. Mu, P., Zhang, Z., Benelli, M., Karthaus, W. R., Hoover, E., Chen, C. C., Wongvipat, J., Ku, S. Y., Gao, D., Cao, Z*., et al.* (2017). SOX2 promotes lineage plasticity and antiandrogen resistance in TP53- and RB1-deficient prostate cancer. Science *355*, 84-88.

157. Murray, P. B., Lax, I., Reshetnyak, A., Ligon, G. F., Lillquist, J. S., Natoli, E. J., Jr., Shi, X., Folta-Stogniew, E., Gunel, M., Alvarado, D., and Schlessinger, J. (2015). Heparin is an activating ligand of the orphan receptor tyrosine kinase ALK. Sci Signal *8*, ra6.

158. Nakashima, J., Tachibana, M., Horiguchi, Y., Oya, M., Ohigashi, T., Asakura, H., and Murai, M. (2000). Serum interleukin 6 as a prognostic factor in patients with prostate cancer. Clin Cancer Res *6*, 2702-2706.

159. Nalla, A. K., Williams, T. F., Collins, C. P., Rae, D. T., and Trobridge, G. D. (2016). Lentiviral vector-mediated insertional mutagenesis screen identifies genes that influence androgen independent prostate cancer progression and predict clinical outcome. Mol Carcinog *55*, 1761-1771.

160. Nelson, K. N., Meyer, A. N., Siari, A., Campos, A. R., Motamedchaboki, K., and Donoghue, D. J. (2016). Oncogenic Gene Fusion FGFR3-TACC3 Is Regulated by Tyrosine Phosphorylation. Mol Cancer Res *14*, 458-469.

161. Nolan, K. D., Franco, O. E., Hance, M. W., Hayward, S. W., and Isaacs, J. S. (2015). Tumor-secreted Hsp90 subverts polycomb function to drive prostate tumor growth and invasion. J Biol Chem *290*, 8271-8282.

162. Ooi, L., and Wood, I. C. (2007). Chromatin crosstalk in development and disease: lessons from REST. Nat Rev Genet *8*, 544-554.

163. Pakneshan, P., Xing, R. H., and Rabbani, S. A. (2003). Methylation status of uPA promoter as a molecular mechanism regulating prostate cancer invasion and growth in vitro and in vivo. Faseb j *17*, 1081-1088.

164. Pan, Y., Deng, C., Qiu, Z., Cao, C., and Wu, F. (2021). The Resistance Mechanisms and Treatment Strategies for ALK-Rearranged Non-Small Cell Lung Cancer. Front Oncol *11*, 713530.

165. Parimi, V., Goyal, R., Poropatich, K., and Yang, X. J. (2014). Neuroendocrine differentiation of prostate cancer: a review. Am J Clin Exp Urol *2*, 273-285.

166. Paschalis, A., Welti, J., Neeb, A. J., Yuan, W., Figueiredo, I., Pereira, R., Ferreira, A., Riisnaes, R., Rodrigues, D. N., Jiménez-Vacas, J. M.*, et al.* (2021). JMJD6 Is a Druggable Oxygenase That Regulates AR-V7 Expression in Prostate Cancer. Cancer Res *81*, 1087-1100.

167. Pastorino, F., Capasso, M., Brignole, C., Lasorsa, V. A., Bensa, V., Perri, P., Cantalupo, S., Giglio, S., Provenzi, M., Rabusin, M.*, et al.* (2023). Therapeutic Targeting of ALK in

Neuroblastoma: Experience of Italian Precision Medicine in Pediatric Oncology. Cancers (Basel) *15*.

168. Patel, R. A., Coleman, I., Roudier, M. P., Konnick, E. Q., Hanratty, B., Dumpit, R., Lucas, J. M., Ang, L. S., Low, J. Y., Tretiakova, M. S*., et al.* (2022). Comprehensive assessment of anaplastic lymphoma kinase in localized and metastatic prostate cancer reveals targetable alterations. Cancer Res Commun *2*, 277-285.

169. Pavone-Macaluso, M., de Voogt, H. J., Viggiano, G., Barasolo, E., Lardennois, B., de Pauw, M., and Sylvester, R. (1986). Comparison of diethylstilbestrol, cyproterone acetate and medroxyprogesterone acetate in the treatment of advanced prostatic cancer: final analysis of a randomized phase III trial of the European Organization for Research on Treatment of Cancer Urological Group. J Urol *136*, 624-631.

170. Peng, S., Wang, Y., Peng, H., Chen, D., Shen, S., Peng, B., Chen, M., Lencioni, R., and Kuang, M. (2014). Autocrine vascular endothelial growth factor signaling promotes cell proliferation and modulates sorafenib treatment efficacy in hepatocellular carcinoma. Hepatology *60*, 1264-1277.

171. Rapisarda, A., and Melillo, G. (2012). Role of the VEGF/VEGFR axis in cancer biology and therapy. Adv Cancer Res *114*, 237-267.

172. Rehman, Y., and Rosenberg, J. E. (2012). Abiraterone acetate: oral androgen biosynthesis inhibitor for treatment of castration-resistant prostate cancer. Drug Des Devel Ther *6*, 13-18.

173. Reina-Campos, M., Linares, J. F., Duran, A., Cordes, T., L'Hermitte, A., Badur, M. G., Bhangoo, M. S., Thorson, P. K., Richards, A., Rooslid, T*., et al.* (2019). Increased Serine and

One-Carbon Pathway Metabolism by PKCλ/ι Deficiency Promotes Neuroendocrine Prostate Cancer. Cancer Cell *35*, 385-400.e389.

174. Richmond, E. J., and Rogol, A. D. (2007). Male pubertal development and the role of androgen therapy. Nat Clin Pract Endocrinol Metab *3*, 338-344.

175. Robinson, D., Van Allen, E. M., Wu, Y. M., Schultz, N., Lonigro, R. J., Mosquera, J. M., Montgomery, B., Taplin, M. E., Pritchard, C. C., Attard, G.*, et al.* (2015). Integrative clinical genomics of advanced prostate cancer. Cell *161*, 1215-1228.

176. Rodrigues, L. U., Rider, L., Nieto, C., Romero, L., Karimpour-Fard, A., Loda, M., Lucia, M. S., Wu, M., Shi, L., Cimic, A.*, et al.* (2015). Coordinate loss of MAP3K7 and CHD1 promotes aggressive prostate cancer. Cancer Res *75*, 1021-1034.

177. Rokhlin, O. W., Glover, R. B., Guseva, N. V., Taghiyev, A. F., Kohlgraf, K. G., and Cohen, M. B. (2006). Mechanisms of cell death induced by histone deacetylase inhibitors in androgen receptor-positive prostate cancer cells. Mol Cancer Res *4*, 113-123.

178. Romanel, A., Gasi Tandefelt, D., Conteduca, V., Jayaram, A., Casiraghi, N., Wetterskog, D., Salvi, S., Amadori, D., Zafeiriou, Z., Rescigno, P.*, et al.* (2015). Plasma AR and abiraterone-resistant prostate cancer. Sci Transl Med *7*, 312re310.

179. Roskoski, R., Jr. (2013). Anaplastic lymphoma kinase (ALK): structure, oncogenic activation, and pharmacological inhibition. Pharmacol Res *68*, 68-94.

180. Rotinen, M., You, S., Yang, J., Coetzee, S. G., Reis-Sobreiro, M., Huang, W. C., Huang, F., Pan, X., Yáñez, A., Hazelett, D. J.*, et al.* (2018). ONECUT2 is a targetable master regulator of lethal prostate cancer that suppresses the androgen axis. Nat Med *24*, 1887-1898.

181. Rudin, C. M., Durinck, S., Stawiski, E. W., Poirier, J. T., Modrusan, Z., Shames, D. S., Bergbower, E. A., Guan, Y., Shin, J., Guillory, J.*, et al.* (2012). Comprehensive genomic analysis identifies SOX2 as a frequently amplified gene in small-cell lung cancer. Nat Genet *44*, 1111-1116.

182. Ryan, C. J., Smith, M. R., Fizazi, K., Saad, F., Mulders, P. F., Sternberg, C. N., Miller, K., Logothetis, C. J., Shore, N. D., Small, E. J.*, et al.* (2015). Abiraterone acetate plus prednisone versus placebo plus prednisone in chemotherapy-naive men with metastatic castration-resistant prostate cancer (COU-AA-302): final overall survival analysis of a randomised, double-blind, placebo-controlled phase 3 study. Lancet Oncol *16*, 152-160.

183. Rybak, A. P., and Tang, D. (2013). SOX2 plays a critical role in EGFR-mediated self-renewal of human prostate cancer stem-like cells. Cell Signal *25*, 2734-2742.

184. Sakamoto, H., Tsukaguchi, T., Hiroshima, S., Kodama, T., Kobayashi, T., Fukami, T. A., Oikawa, N., Tsukuda, T., Ishii, N., and Aoki, Y. (2011). CH5424802, a selective ALK inhibitor capable of blocking the resistant gatekeeper mutant. Cancer Cell *19*, 679-690.

185. Sandow, J., Von Rechenberg, W., Jerzabek, G., and Stoll, W. (1978). Pituitary gonadotropin inhibition by a highly active analog of luteinizing hormone-releasing hormone. Fertil Steril *30*, 205-209.

186. Sartor, O., and de Bono, J. S. (2018). Metastatic Prostate Cancer. N Engl J Med *378*, 645-657.

187. Schally, A. V., Comaru-Schally, A. M., Plonowski, A., Nagy, A., Halmos, G., and Rekasi, Z. (2000). Peptide analogs in the therapy of prostate cancer. Prostate *45*, 158-166.

188. Scher, H. I., Fizazi, K., Saad, F., Taplin, M. E., Sternberg, C. N., Miller, K., de Wit, R., Mulders, P., Chi, K. N., Shore, N. D*., et al.* (2012). Increased survival with enzalutamide in prostate cancer after chemotherapy. N Engl J Med *367*, 1187-1197.

189. Scher, H. I., Graf, R. P., Schreiber, N. A., Jayaram, A., Winquist, E., McLaughlin, B., Lu, D., Fleisher, M., Orr, S., Lowes, L*., et al.* (2018). Assessment of the Validity of Nuclear-Localized Androgen Receptor Splice Variant 7 in Circulating Tumor Cells as a Predictive Biomarker for Castration-Resistant Prostate Cancer. JAMA Oncol *4*, 1179-1186.

190. Schmitt, B., Bennett, C., Seidenfeld, J., Samson, D., and Wilt, T. (2000). Maximal androgen blockade for advanced prostate cancer. Cochrane Database Syst Rev *1999*, Cd001526.

191. Seidenfeld, J., Samson, D. J., Hasselblad, V., Aronson, N., Albertsen, P. C., Bennett, C. L., and Wilt, T. J. (2000). Single-therapy androgen suppression in men with advanced prostate cancer: a systematic review and meta-analysis. Ann Intern Med *132*, 566-577.

192. Shan, L. X., Rodriguez, M. C., and Jänne, O. A. (1990). Regulation of androgen receptor protein and mRNA concentrations by androgens in rat ventral prostate and seminal vesicles and in human hepatoma cells. Mol Endocrinol *4*, 1636-1646.

193. Shang, Z., Cai, Q., Zhang, M., Zhu, S., Ma, Y., Sun, L., Jiang, N., Tian, J., Niu, X., Chen, J*., et al.* (2015). A switch from $CD44^+$ cell to EMT cell drives the metastasis of prostate cancer. Oncotarget *6*, 1202-1216.

194. Sharp, A., Porta, N., Lambros, M. B. K., Welti, J. C., Paschalis, A., Raj, G. V., Plymate, S. P., and de Bono, J. S. (2019). Dissecting Prognostic From Predictive Utility: Circulating AR-V7 Biomarker Testing for Advanced Prostate Cancer. J Clin Oncol *37*, 2182-2184.

195. Shigematsu, H., and Gazdar, A. F. (2006). Somatic mutations of epidermal growth factor receptor signaling pathway in lung cancers. Int J Cancer *118*, 257-262.

196. Shin, S., and Janknecht, R. (2007). Activation of androgen receptor by histone demethylases JMJD2A and JMJD2D. Biochem Biophys Res Commun *359*, 742-746.

197. Shiota, M., Fujimoto, J., Semba, T., Satoh, H., Yamamoto, T., and Mori, S. (1994). Hyperphosphorylation of a novel 80 kDa protein-tyrosine kinase similar to Ltk in a human Ki-1 lymphoma cell line, AMS3. Oncogene *9*, 1567-1574.

198. Shore, N. D., Saad, F., Cookson, M. S., George, D. J., Saltzstein, D. R., Tutrone, R., Akaza, H., Bossi, A., van Veenhuyzen, D. F., Selby, B.*, et al.* (2020). Oral Relugolix for Androgen-Deprivation Therapy in Advanced Prostate Cancer. N Engl J Med *382*, 2187-2196.

199. Siegel, R. L., Miller, K. D., and Jemal, A. (2020). Cancer statistics, 2020. CA Cancer J Clin *70*, 7-30.

200. Singh, D., Chan, J. M., Zoppoli, P., Niola, F., Sullivan, R., Castano, A., Liu, E. M., Reichel, J., Porrati, P., Pellegatta, S.*, et al.* (2012). Transforming fusions of FGFR and TACC genes in human glioblastoma. Science *337*, 1231-1235.

201. Small, E. J., Saad, F., Chowdhury, S., Oudard, S., Hadaschik, B. A., Graff, J. N., Olmos, D., Mainwaring, P. N., Lee, J. Y., Uemura, H.*, et al.* (2019). Apalutamide and overall survival in non-metastatic castration-resistant prostate cancer. Ann Oncol *30*, 1813-1820.

202. Smith, R., Liu, M., Liby, T., Bayani, N., Bucher, E., Chiotti, K., Derrick, D., Chauchereau, A., Heiser, L., Alumkal, J.*, et al.* (2020). Enzalutamide response in a panel of prostate cancer cell lines reveals a role for glucocorticoid receptor in enzalutamide resistant disease. Sci Rep *10*, 21750.

203. Soda, M., Choi, Y. L., Enomoto, M., Takada, S., Yamashita, Y., Ishikawa, S., Fujiwara, S., Watanabe, H., Kurashina, K., Hatanaka, H.*, et al.* (2007). Identification of the transforming EML4-ALK fusion gene in non-small-cell lung cancer. Nature *448*, 561-566.

204. Soh, P. X. Y., Mmekwa, N., Petersen, D. C., Gheybi, K., van Zyl, S., Jiang, J., Patrick, S. M., Campbell, R., Jaratlerdseri, W., Mutambirwa, S. B. A.*, et al.* (2023). Prostate cancer genetic risk and associated aggressive disease in men of African ancestry. Nat Commun *14*, 8037.

205. Stearns, M. E., Wang, M., Hu, Y., Kim, G., and Garcia, F. U. (2004). Expression of a flt-4 (VEGFR3) splicing variant in primary human prostate tumors. VEGF D and flt-4tΔ773–1081 overexpression is diagnostic for sentinel lymph node metastasis. Laboratory Investigation *84*, 785-795.

206. Steketee, K., Timmerman, L., Ziel-van der Made, A. C., Doesburg, P., Brinkmann, A. O., and Trapman, J. (2002). Broadened ligand responsiveness of androgen receptor mutants obtained by random amino acid substitution of H874 and mutation hot spot T877 in prostate cancer. Int J Cancer *100*, 309-317.

207. Stone, L. (2016). Prostate cancer: ROR-γ drives androgen receptor expression. Nat Rev Urol *13*, 237.

208. Stopa, N., Krebs, J. E., and Shechter, D. (2015). The PRMT5 arginine methyltransferase: many roles in development, cancer and beyond. Cell Mol Life Sci *72*, 2041-2059.

209. Su, J. L., Yang, P. C., Shih, J. Y., Yang, C. Y., Wei, L. H., Hsieh, C. Y., Chou, C. H., Jeng, Y. M., Wang, M. Y., Chang, K. J.*, et al.* (2006). The VEGF-C/Flt-4 axis promotes invasion and metastasis of cancer cells. Cancer Cell *9*, 209-223.

210. Sudhesh Dev, S., Zainal Abidin, S. A., Farghadani, R., Othman, I., and Naidu, R. (2021). Receptor Tyrosine Kinases and Their Signaling Pathways as Therapeutic Targets of Curcumin in Cancer. Front Pharmacol *12*, 772510.

211. Sun, G. G., Wang, Y. D., Cui, D. W., Cheng, Y. J., and Hu, W. N. (2014). EMP1 regulates caspase-9 and VEGFC expression and suppresses prostate cancer cell proliferation and invasion. Tumour Biol *35*, 3455-3462.

212. Sun, H., Li, T., Zhuang, R., Cai, W., and Zheng, Y. (2017). Do renin-angiotensin system inhibitors influence the recurrence, metastasis, and survival in cancer patients?: Evidence from a meta-analysis including 55 studies. Medicine (Baltimore) *96*, e6394.

213. Sun, M., Choueiri, T. K., Hamnvik, O. P., Preston, M. A., De Velasco, G., Jiang, W., Loeb, S., Nguyen, P. L., and Trinh, Q. D. (2016). Comparison of Gonadotropin-Releasing Hormone Agonists and Orchiectomy: Effects of Androgen-Deprivation Therapy. JAMA Oncol *2*, 500-507.

214. Suzuki, H., Ueda, T., Ichikawa, T., and Ito, H. (2003). Androgen receptor involvement in the progression of prostate cancer. Endocr Relat Cancer *10*, 209-216.

215. Tamae, D., Mostaghel, E., Montgomery, B., Nelson, P. S., Balk, S. P., Kantoff, P. W., Taplin, M. E., and Penning, T. M. (2015). The DHEA-sulfate depot following P450c17 inhibition supports the case for AKR1C3 inhibition in high risk localized and advanced castration resistant prostate cancer. Chem Biol Interact *234*, 332-338.

216. Tanaka, H., Kono, E., Tran, C. P., Miyazaki, H., Yamashiro, J., Shimomura, T., Fazli, L., Wada, R., Huang, J., Vessella, R. L.*, et al.* (2010). Monoclonal antibody targeting of N-cadherin

inhibits prostate cancer growth, metastasis and castration resistance. Nat Med *16*, 1414-1420.

217. Tanno, S., Ohsaki, Y., Nakanishi, K., Toyoshima, E., and Kikuchi, K. (2004). Human small cell lung cancer cells express functional VEGF receptors, VEGFR-2 and VEGFR-3. Lung Cancer *46*, 11-19.

218. Taylor, B. S., Schultz, N., Hieronymus, H., Gopalan, A., Xiao, Y., Carver, B. S., Arora, V. K., Kaushik, P., Cerami, E., Reva, B.*, et al.* (2010). Integrative genomic profiling of human prostate cancer. Cancer Cell *18*, 11-22.

219. Taylor, K. R., Barron, T., Hui, A., Spitzer, A., Yalçin, B., Ivec, A. E., Geraghty, A. C., Hartmann, G. G., Arzt, M., Gillespie, S. M.*, et al.* (2023). Glioma synapses recruit mechanisms of adaptive plasticity. Nature *623*, 366-374.

220. Titus, M. A., Schell, M. J., Lih, F. B., Tomer, K. B., and Mohler, J. L. (2005). Testosterone and dihydrotestosterone tissue levels in recurrent prostate cancer. Clin Cancer Res *11*, 4653-4657.

221. Tiwari, R., Manzar, N., Bhatia, V., Yadav, A., Nengroo, M. A., Datta, D., Carskadon, S., Gupta, N., Sigouros, M., Khani, F.*, et al.* (2020). Androgen deprivation upregulates SPINK1 expression and potentiates cellular plasticity in prostate cancer. Nat Commun *11*, 384.

222. Tossetta, G., Fantone, S., Gesuita, R., Goteri, G., Senzacqua, M., Marcheggiani, F., Tiano, L., Marzioni, D., and Mazzucchelli, R. (2022). Ciliary Neurotrophic Factor Modulates Multiple Downstream Signaling Pathways in Prostate Cancer Inhibiting Cell Invasiveness. Cancers (Basel) *14*.

223. Tran, C., Ouk, S., Clegg, N. J., Chen, Y., Watson, P. A., Arora, V., Wongvipat, J., Smith-Jones, P. M., Yoo, D., Kwon, A.*, et al.* (2009). Development of a second-generation antiandrogen for treatment of advanced prostate cancer. Science *324*, 787-790.

224. Unno, K., Chalmers, Z. R., Pamarthy, S., Vatapalli, R., Rodriguez, Y., Lysy, B., Mok, H., Sagar, V., Han, H., Yoo, Y. A.*, et al.* (2021). Activated ALK Cooperates with N-Myc via Wnt/beta-Catenin Signaling to Induce Neuroendocrine Prostate Cancer. Cancer Res *81*, 2157-2170.

225. Urbanucci, A., and Mills, I. G. (2018). Bromodomain-containing proteins in prostate cancer. Mol Cell Endocrinol *462*, 31-40.

226. van Poppel, H., and Nilsson, S. (2008). Testosterone surge: rationale for gonadotropin-releasing hormone blockers? Urology *71*, 1001-1006.

227. Velghe, A. I., Van Cauwenberghe, S., Polyansky, A. A., Chand, D., Montano-Almendras, C. P., Charni, S., Hallberg, B., Essaghir, A., and Demoulin, J. B. (2014). PDGFRA alterations in cancer: characterization of a gain-of-function V536E transmembrane mutant as well as loss-of-function and passenger mutations. Oncogene *33*, 2568-2576.

228. Vernersson, E., Khoo, N. K., Henriksson, M. L., Roos, G., Palmer, R. H., and Hallberg, B. (2006). Characterization of the expression of the ALK receptor tyrosine kinase in mice. Gene Expr Patterns *6*, 448-461.

229. Wallén, M. J., Linja, M., Kaartinen, K., Schleutker, J., and Visakorpi, T. (1999). Androgen receptor gene mutations in hormone-refractory prostate cancer. J Pathol *189*, 559-563.

230. Waltering, K. K., Helenius, M. A., Sahu, B., Manni, V., Linja, M. J., Jänne, O. A., and Visakorpi, T. (2009). Increased expression of androgen receptor sensitizes prostate cancer cells to low levels of androgens. Cancer Res *69*, 8141-8149.

231. Wang, B., Lo, U. G., Wu, K., Kapur, P., Liu, X., Huang, J., Chen, W., Hernandez, E., Santoyo, J., Ma, S. H.*, et al.* (2017). Developing new targeting strategy for androgen receptor variants in castration resistant prostate cancer. Int J Cancer *141*, 2121-2130.

232. Wang, J., Zou, J. X., Xue, X., Cai, D., Zhang, Y., Duan, Z., Xiang, Q., Yang, J. C., Louie, M. C., Borowsky, A. D.*, et al.* (2016a). ROR-γ drives androgen receptor expression and represents a therapeutic target in castration-resistant prostate cancer. Nat Med *22*, 488-496.

233. Wang, M., Ren, D., Guo, W., Huang, S., Wang, Z., Li, Q., Du, H., Song, L., and Peng, X. (2016b). N-cadherin promotes epithelial-mesenchymal transition and cancer stem cell-like traits via ErbB signaling in prostate cancer cells. Int J Oncol *48*, 595-606.

234. Wang, Q., Li, W., Liu, X. S., Carroll, J. S., Jänne, O. A., Keeton, E. K., Chinnaiyan, A. M., Pienta, K. J., and Brown, M. (2007). A hierarchical network of transcription factors governs androgen receptor-dependent prostate cancer growth. Mol Cell *27*, 380-392.

235. Wang, W., Wu, M., Liu, M., Yan, Z., Wang, G., Mao, D., and Wang, M. (2020). Hyperprogression to camrelizumab in a patient with esophageal squamous cell carcinoma harboring EGFR kinase domain duplication. J Immunother Cancer *8*.

236. Watson, P. A., Chen, Y. F., Balbas, M. D., Wongvipat, J., Socci, N. D., Viale, A., Kim, K., and Sawyers, C. L. (2010). Constitutively active androgen receptor splice variants expressed in castration-resistant prostate cancer require full-length androgen receptor. Proc Natl Acad Sci U S A *107*, 16759-16765.

237. Wehrman, T., He, X., Raab, B., Dukipatti, A., Blau, H., and Garcia, K. C. (2007). Structural and mechanistic insights into nerve growth factor interactions with the TrkA and p75 receptors. Neuron *53*, 25-38.

238. Wen, Y. C., Liu, C. L., Yeh, H. L., Chen, W. H., Jiang, K. C., Tram, V. T. N., Hsiao, M., Huang, J., Chen, W. Y., and Liu, Y. N. (2022). PCK1 regulates neuroendocrine differentiation in a positive feedback loop of LIF/ZBTB46 signalling in castration-resistant prostate cancer. Br J Cancer *126*, 778-790.

239. West, D. C., Pan, D., Tonsing-Carter, E. Y., Hernandez, K. M., Pierce, C. F., Styke, S. C., Bowie, K. R., Garcia, T. I., Kocherginsky, M., and Conzen, S. D. (2016). GR and ER Coactivation Alters the Expression of Differentiation Genes and Associates with Improved ER+ Breast Cancer Outcome. Mol Cancer Res *14*, 707-719.

240. White, J. W. (1893). II. The Present Position of the Surgery of the Hypertrophied Prostate. Ann Surg *18*, 152-188.

241. Wilding, G. (1992). The importance of steroid hormones in prostate cancer. Cancer Surv *14*, 113-130.

242. Wilson, S., Fan, L., Sahgal, N., Qi, J., and Filipp, F. V. (2017). The histone demethylase KDM3A regulates the transcriptional program of the androgen receptor in prostate cancer cells. Oncotarget *8*, 30328-30343.

243. Witek, B., El Wakil, A., Nord, C., Ahlgren, U., Eriksson, M., Vernersson-Lindahl, E., Helland, Å., Alexeyev, O. A., Hallberg, B., and Palmer, R. H. (2015). Targeted Disruption of ALK Reveals a Potential Role in Hypogonadotropic Hypogonadism. PLoS One *10*, e0123542.

244. Wong, O. G., Huo, Z., Siu, M. K., Zhang, H., Jiang, L., Wong, E. S., and Cheung, A. N. (2010). Hypermethylation of SOX2 Promoter in Endometrial Carcinogenesis. Obstet Gynecol Int *2010*.

245. Wyatt, A. W., Azad, A. A., Volik, S. V., Annala, M., Beja, K., McConeghy, B., Haegert, A., Warner, E. W., Mo, F., Brahmbhatt, S.*, et al.* (2016). Genomic Alterations in Cell-Free DNA and Enzalutamide Resistance in Castration-Resistant Prostate Cancer. JAMA Oncol *2*, 1598-1606.

246. Xiang, Y., Zhu, Z., Han, G., Lin, H., Xu, L., and Chen, C. D. (2007). JMJD3 is a histone H3K27 demethylase. Cell Res *17*, 850-857.

247. Xu, H., Xu, K., He, H. H., Zang, C., Chen, C. H., Chen, Y., Qin, Q., Wang, S., Wang, C., Hu, S.*, et al.* (2016). Integrative Analysis Reveals the Transcriptional Collaboration between EZH2 and E2F1 in the Regulation of Cancer-Related Gene Expression. Mol Cancer Res *14*, 163-172.

248. Yamada, Y., and Beltran, H. (2021). Clinical and Biological Features of Neuroendocrine Prostate Cancer. Curr Oncol Rep *23*, 15.

249. Yan, M., Wang, J., Wang, H., Zhou, J., Qi, H., Naji, Y., Zhao, L., Tang, Y., and Dai, Y. (2023). Knockdown of NR3C1 inhibits the proliferation and migration of clear cell renal cell carcinoma through activating endoplasmic reticulum stress-mitophagy. J Transl Med *21*, 701.

250. Yang, P., Guo, L., Duan, Z. J., Tepper, C. G., Xue, L., Chen, X., Kung, H. J., Gao, A. C., Zou, J. X., and Chen, H. W. (2012). Histone methyltransferase NSD2/MMSET mediates constitutive NF-κB signaling for cancer cell proliferation, survival, and tumor growth via a feed-forward loop. Mol Cell Biol *32*, 3121-3131.

251. Yasumizu, Y., Rajabi, H., Jin, C., Hata, T., Pitroda, S., Long, M. D., Hagiwara, M., Li, W., Hu, Q., Liu, S.*, et al.* (2020). MUC1-C regulates lineage plasticity driving progression to neuroendocrine prostate cancer. Nat Commun *11*, 338.

252. Yayon, A., Klagsbrun, M., Esko, J. D., Leder, P., and Ornitz, D. M. (1991). Cell surface, heparin-like molecules are required for binding of basic fibroblast growth factor to its high affinity receptor. Cell *64*, 841-848.

253. Yeh, Y. A., Yang, S., Constantinescu, M., Chaudoir, C., Tanner, A., Henry, M., Anderson, S., Saldivar, J. S., Serkin, F., Fazili, T.*, et al.* (2019). Prostatic adenocarcinoma with novel NTRK3 gene fusion: a case report. Am J Clin Exp Urol *7*, 341-345.

254. Yu, T., Wang, C., Yang, J., Guo, Y., Wu, Y., and Li, X. (2017). Metformin inhibits SUV39H1-mediated migration of prostate cancer cells. Oncogenesis *6*, e324-e324.

255. Yu, X., Wang, Y., DeGraff, D. J., Wills, M. L., and Matusik, R. J. (2011). Wnt/β-catenin activation promotes prostate tumor progression in a mouse model. Oncogene *30*, 1868-1879.

256. Zhang, S., Anjum, R., Squillace, R., Nadworny, S., Zhou, T., Keats, J., Ning, Y., Wardwell, S. D., Miller, D., Song, Y.*, et al.* (2016). The Potent ALK Inhibitor Brigatinib (AP26113) Overcomes Mechanisms of Resistance to First- and Second-Generation ALK Inhibitors in Preclinical Models. Clin Cancer Res *22*, 5527-5538.

257. Zhang, W., Liu, B., Wu, W., Li, L., Broom, B. M., Basourakos, S. P., Korentzelos, D., Luan, Y., Wang, J., Yang, G.*, et al.* (2018). Targeting the MYCN-PARP-DNA Damage Response Pathway in Neuroendocrine Prostate Cancer. Clin Cancer Res *24*, 696-707.

258. Zhang, X., Gureasko, J., Shen, K., Cole, P. A., and Kuriyan, J. (2006). An allosteric mechanism for activation of the kinase domain of epidermal growth factor receptor. Cell *125*, 1137-1149.

259. Zhao, J. C., Fong, K. W., Jin, H. J., Yang, Y. A., Kim, J., and Yu, J. (2016). FOXA1 acts upstream of GATA2 and AR in hormonal regulation of gene expression. Oncogene *35*, 4335-4344.

260. Zhu, Y. C., Wang, W. X., Li, X. L., Xu, C. W., Chen, G., Zhuang, W., Lv, T., and Song, Y. (2019). Identification of a Novel Icotinib-Sensitive EGFR-SEPTIN14 Fusion Variant in Lung Adenocarcinoma by Next-Generation Sequencing. J Thorac Oncol *14*, e181-e183.